



Maastricht University

universiteit
▶▶ hasselt

2015 | Faculty of Medicine and Life Sciences

DOCTORAL DISSERTATION

Aptamers as a tool to detect estrogens

Doctoral dissertation submitted to obtain the degree of
Doctor of Biomedical Science, to be defended by

Katrijn Vanschoenbeek

Promoter: Prof. Dr Luc Michiels

Co-promoter: Prof. Dr Marcel Ameloot

D/2015/2451/47

universiteit
▶▶ hasselt | BIOMED
BIOMEDISCH
ONDERZOEKSINSTITUUT

Proefschrift voorgelegd tot het behalen van de graad van
Doctor in de Biomedische Wetenschappen.

Chairman:

Prof. dr. Ivo Lambrichts

Promotor:

Prof. dr. Luc Michiels (UHasselt)

Co-promotor:

Prof. dr. Marcel Ameloot (UHasselt)

Members of the jury:

Prof. dr. Wilfried Langenaeker (UHasselt)

dr. Veronique Vermeeren (LRM)

dr. Reinhilde Weltens (VITO)

Prof. dr. Patrick Wagner (KU Leuven)

Prof. dr. Jeroen Lammertyn (KU Leuven)

Prof. dr. Bart van Grinsven (Maastricht University)

Since the groundbreaking double helix discovery in 1953 by Watson and Crick, DNA has long been ascribed one singular function: carrying genetic information, the blueprint of life. This idea was mind-boggling enough not to search for any other function for several years. Only after decades, when the molecular mechanisms of genetics were to some extent familiarized, attempts were made to search for additional functions. Finally, at the beginning of the 1990s, another important property of DNA was unraveled. Short DNA strands appeared to be able to bind other molecules, even if these molecules don't naturally interact with DNA. These strands were called aptamers. Using the principles of Darwinian evolution - variation, selection and replication - aptamers can easily be obtained. Well-defined and characterized aptamers promise a bounty of applications. For example, they emerged as auspicious and versatile building blocks in the construction of biosensors. A variety of aptasensors have already been designed and reported in literature. However, in real-life, they are conspicuous by their absence. Does this dearth of aptamers in everyday life mean that they are not ready for prime time?

Table of contents

List of abbreviations

List of Figures

List of tables

Samenvatting

Summary

1	General introduction and aims.....	1
1.1	Aptamers.....	2
1.1.1	Description.....	2
1.1.2	A little history	3
1.1.3	Advantages	4
1.2	Aptamer selection.....	6
1.2.1	Standard SELEX procedure	7
1.2.2	Adjustments standard SELEX procedure	9
1.3	Aptamer characterization	11
1.3.1	Affinity and kinetic analysis of binding interactions.....	12
1.3.2	Binding assays for affinity and kinetic analysis.....	13
1.4	Aptasensors	22
1.5	Aptasensor for the detection of estrogenic substances.....	25
1.6	Aims of the study	29

2	Selection of epitope specific 17β-estradiol aptamers	35
2.1	Introduction	36
2.2	Materials and Methods.....	41
2.2.1	Materials.....	41
2.2.2	DNA library construction, amplification and conditioning	42
2.2.3	Target.....	43
2.2.4	Selection design.....	44
2.2.5	Cloning and sequence/structure analysis of selected 17 β -estradiol aptamers	45
2.3	Results.....	46
2.3.1	DNA library construction, amplification and conditioning	46
2.3.2	Sequence/structure analysis of selected 17 β -estradiol aptamers.	48
2.4	Discussion	51
2.4.1	DNA library construction, amplification and conditioning	51
2.4.2	Optimized selection design	53
2.4.3	Sequence/structure analysis of selected 17 β -estradiol aptamers.	53
2.5	Conclusion and future perspectives	55
3	Monitoring aptamer selection	57
3.1	Introduction	58
3.2	Materials and Methods.....	62
3.2.1	Materials.....	62
3.2.2	Enrichment simulation in random starting libraries.....	62
3.2.3	Plate SELEX for C-Reactive Protein aptamers.....	63
3.2.4	Capillary electrophoresis SELEX for peptide X aptamers.....	64

3.2.5	Bead SELEX for 17 β -estradiol aptamers	65
3.3	Results.....	65
3.3.1	Remelting curve analysis of simulated enrichment	65
3.3.2	Remelting curve analysis of different SELEX procedures	68
3.3.3	Remelting curve analysis to identify contamination problems during SELEX	73
3.4	Discussion	73
3.4.1	Remelting curve analysis of simulated enrichment	74
3.4.2	Remelting curve analysis of different SELEX procedures	75
3.4.3	Remelting curve analysis to identify contamination problems during SELEX.....	79
3.5	Conclusion and future perspectives	80
4 Characterization of epitope specific 17β-estradiol aptamers 83		
4.1	Introduction	84
4.2	Materials and Methods.....	90
4.2.1	Materials.....	90
4.2.2	Enzyme-linked oligonucleotide assay	90
4.2.3	Quantitative real-time PCR binding assay	91
4.2.4	Competitive enzyme-linked oligonucleotide assay	92
4.2.5	Sensor set-up impedimetric and heat-transfer resistance measurements	93
4.2.6	Surface plasmon resonance measurement	96
4.3	Results.....	97
4.3.1	Enzyme-linked oligonucleotide assay	97
4.3.2	Quantitative real-time PCR binding assay	98
4.3.3	Competitive enzyme-linked oligonucleotide assay	98

4.3.4	Impedimetric and heat-transfer measurement	99
4.3.5	Surface plasmon resonance measurement	101
4.4	Discussion	106
4.5	Conclusion and future perspectives	111
5 Enhancement of signal generation via TISD		113
5.1	Introduction	114
5.2	Materials and Methods.....	117
5.2.1	Materials.....	117
5.2.2	Transition of dsDNA to ssDNA via thermal denaturation in an R_{th} set-up	117
5.2.3	Transition of dsDNA to ssDNA via chemical denaturation in an SPR set-up	118
5.2.4	Transition of dsDNA to ssDNA via target induced strand displacement in an SPR set-up.....	119
5.3	Results.....	121
5.3.1	Transition of dsDNA to ssDNA via thermal denaturation in an R_{th} set-up	121
5.3.2	Transition of dsDNA to ssDNA via chemical denaturation in an SPR set-up	121
5.3.3	Transition of dsDNA to ssDNA via target induced strand displacement.....	122
5.4	Discussion	127
5.5	Conclusion.....	132

6 General discussion, conclusion and future perspectives133

6.1	General discussion	134
6.2	Concluding remarks and future perspectives	139

Appendix160

Curriculum Vitae

Dankwoord

List of abbreviations

3D	three-dimensional
AFM	atomic force microscopy
AP	alkaline phosphatase
AptaBiD	aptamer-facilitated biomarker discovery
(β)E2	17 β -estradiol
bp	base pairs
BSA	bovine serum albumin
CE	capillary electrophoresis
CRP	C-reactive protein
dHPLC	denaturing high-performance liquid chromatography
DiStRO	diversity standard of random oligonucleotides
ds	double stranded
EDC	1-Ethyl-3-[3-dimethylaminopropyl]carbodiimide hydrochloride
EDTA	ethylenediaminetetraacetic acid
ELISA	enzyme-linked immunosorbent assay
ELONA	enzyme-linked oligonucleotide assay
ER	estrogen receptor
FA	fluorescence anisotropy
FC	flow cell
FCS	fluorescence correlation spectroscopy
FDA	food and drug administration
FRET	fluorescence resonance energy transfer
FP	forward primer
GC-MS	gas chromatography-mass spectrometry

List of abbreviations

GE	gel electrophoresis
HAPIscreen	high throughput aptamer identification screen
HRP	horseradish peroxidase
K_D	affinity constant
k_{on}	association rate constant
k_{off}	dissociation rate constant
LC-MS	liquid chromatography-mass spectrometry
MCA	melting curve analysis
mM	millimolar
μ M	micromolar
MES	2-(N-morpholino)ethanesulfonic acid
MIP	molecular imprinted polymer
MW	molecular weight
MS	mass spectrometry
NCD	nanocrystalline diamond
NECEEM	non-equilibrium capillary electrophoresis of equilibrium mixtures
NHS	<i>N</i> -Hydroxysuccinimide
nM	nanomolar
NMR	nuclear magnetic resonance
nt	nucleotides
PBS	phosphate buffered saline
PCR	polymerase chain reaction
pI	isoelectric point
pM	picomolar
PNA	peptide nucleic acid
QCM	quartz crystal microbalance

List of abbreviations

qRT-PCR	quantitative real-time PCR
RCA	rolling circle amplification
rMCA	remelting curve analysis
RP	reverse primer
RT	room temperature
R_{th}	heat-transfer resistance
RT-PCR	reverse transcriptase polymerase chain reaction
RU	response units
SA	streptavidin
SAM	self-assembled monolayer
SDS	sodium dodecyl sulfate
SELEX	systematic evolution of ligand by exponential enrichment
SOMAmer	slow off-rate modified aptamer
SPR	surface plasmon resonance
ss	single stranded
SSC	saline-sodium citrate
TBS	tris buffered saline
TGK	tris glycine potassium phosphate
TISD	target induced strand displacement
T_m	melting temperature

List of figures

Figure 1:

Schematic representation of aptamer–target interaction.

Figure 2:

Schematic illustration of a standard SELEX process.

Figure 3:

Typical ranges for biological interactions.

Figure 4:

Schematic illustration of different aptamer beacon formats.

Figure 5:

Schematic illustration of the principle of FA and FCS.

Figure 6:

Schematic illustration of potential ELONA set-ups.

Figure 7:

DNA-based amplification after aptamer–target interaction.

Figure 8:

Basics of SPR technology.

Figure 9:

Electrochemical assays to characterize aptamer functionality.

Figure 10:

General scheme of a biosensor.

Figure 11:

Chemical structure of cholesterol and E2.

Figure 12:

Visual display of target identification by means of a cross-reactive aptasensor.

Figure 13:

Schematic overview showing the relationship of the main goal, the three sub goals and the different chapters of this dissertation.

Figure 14:

Schematic illustration of two independently performed SELEX procedures to generate epitope specific aptamers.

Figure 15:

Methods of epitope specific aptamer selection.

Figure 16:

Sepharose® 6B affinity chromatography beads used for positive selections (functionalized with E2) and counter selections (functionalized with dexamethasone for SELEX A and with nortestosterone for SELEX B) used in two independent SELEX procedures.

Figure 17:

Analysis of the impact of PCR cycle number on the formation of by-products by means of agarose GE.

Figure 18:

Genescan view for asymmetric PCR product.

Figure 19:

An illustration of a secondary structure containing a three-way junction as predicted by Mfold.

Figure 20:

Schematic overview of the PCR protocol applied for rMCA.

Figure 21:

Amplification and rMCA data of three enrichment simulations.

Figure 22:

rMCA data of simulated D17.4 enrichment in random library after different reannealing times.

Figure 23:

rMCA data of simulated D17.4 enrichment in random library after different reannealing temperatures.

Figure 24:

rMCA data after ten rounds of CRP aptamer selection.

Figure 25:

rMCA data of the third elution fraction of consecutive SELEX rounds for CRP.

Figure 26:

Amplification and rMCA data of four elution fractions after 16 rounds of CRP aptamer selection.

Figure 27:

rMCA data of consecutive SELEX rounds for peptide X on two devices.

Figure 28:

rMCA data of consecutive CE SELEX rounds for peptide X after 1 min reannealing at 75°C.

Figure 29:

rMCA data of consecutive SELEX rounds for E2 (SELEX A).

Figure 30:

rMCA data of consecutive SELEX rounds for E2 (SELEX B).

Figure 31:

rMCA data of consecutive SELEX rounds for E2 (SELEX trial).

Figure 32:

Examples of different DNA immobilization procedures.

Figure 33:

Schematic overview of an ELONA set-up with SA-HRP detection.

Figure 34:

Schematic overview of a two-step competitive ELONA.

Figure 35:

Schematic lay-out of a sensor cell allowing for thermal, impedimetric and optical monitoring.

Figure 36:

Chemical structure of steroid hormones used for testing epitope specificity of E2 aptamers by means of SPR.

Figure 37:

Competitive ELONA.

Figure 38:

Impedimetric profile of Apta 5A-E2 interaction.

Figure 39:

Heat-transfer profile of Apta 5A-E2 interaction.

Figure 40:

Double referenced sensorgram obtained by SPR methodology showing a fast association and dissociation of Apta 1B interacting with different concentrations of E2.

Figure 41:

Kinetics and affinity results obtained by SPR methodology for Apta 1B.

Figure 42:

Binding responses of selected E2 aptamers of SELEX A towards several steroid hormones determined by SPR methodology.

Figure 43:

Binding responses of selected E2 aptamers of SELEX B towards several steroid hormones determined by SPR methodology.

Figure 44:

Schematic illustration of the chemical structure of E2 with the most crucial epitopes for binding of Apta 6A and Apta 1B / Apta 19B.

Figure 45:

Overview of SPR chips used to test TISD.

Figure 46:

Schematic representation of a TISD experiment in an SPR set-up in combination with results which can be expected.

Figure 47:

R_{th} in function of temperature T_1 during thermal denaturation of dsDNA compared to ssDNA.

Figure 48:

SPR sensorgrams of DNA immobilization, hybridization and chemical denaturation.

Figure 49:

A TISD experiment in solution.

Figure 50:

Visual display of target identification by means of a cross-reactive aptasensor.

List of tables

Table 1:

Variations of the standard SELEX procedure, their method characteristics and possible applications.

Table 2:

ssDNA libraries and primer sets applied during SELEX A and B.

Table 3:

Homo- and heterodimerization, hairpin formation and T_m of optimized primersets of SELEX A and B.

Table 4:

Sequences, ΔG values and G-scores of selected E2 aptamers.

Table 5:

ssDNA library and primer set applied during plate SELEX for CRP aptamers.

Table 6:

ssDNA library and primer set applied during CE-SELEX for peptide X aptamers.

Table 7:

ELONA assay with SA-HRP detection.

Table 8:

qRT-PCR binding assay.

Table 9:

K_D values of selected E2 aptamers as determined by SPR methodology, linked to χ^2 and R_{max} of a 1:1 model fit.

Table 10:

Probe and target DNA used for thermal denaturation in an R_{th} set-up.

Table 11:

Probe and target DNA used for chemical denaturation in an SPR set-up.

Table 12:

Applied buffers and target concentrations for TISD experiments.

Table 13:

Hetero-dimer analysis of Apta 13A/complementary strand hybrids.

Table 14:

Immobilization of complementary DNA, hybridization with Apta 13A and TISD in an SPR set-up.

Table 15:

Sequences described in literature proven to be useful for TISD.

Table 16:

Aptamer/complementary strand duplex described in literature proven to be useful for TISD + adaptations to the complementary strand.

Samenvatting

Biosensoren vormen een verlengde van de menselijke kijk op de wereld. Mensen zijn uiterst gevoelig voor de fysische omgeving en zijn in staat veranderingen in bijvoorbeeld licht, temperatuur en vochtigheid waar te nemen. De gevoeligheid van mensen voor de chemische en biologische omgeving is daarentegen veel beperkter. Levenskwaliteit is echter sterk afhankelijk van geschikte chemische of biologische composities. Afwijkingen in het menselijke lichaam (bv. betreffende metabolieten, metaalionen, hormonen en eiwitten) kunnen iemands gezondheid negatief beïnvloeden. Afwijkingen in de omgeving (bv. betreffende zware metalen, explosieven en hormonen) zijn nadelig voor de volksgezondheid. Daarom staat de ontwikkeling van uiterst sensitieve en specifieke sensoren voor analytherkenning centraal in tal van onderzoeksgebieden, waaronder omgevingsmonitoring, industriële kwaliteitscontrole en medische diagnostiek. Sensoren genereren detecteerbare en tevens kwantificeerbare signalen als reactie op fysische, chemische of biologische stimuli.

Biosensoren zijn het resultaat van een sterke samenwerking tussen verschillende wetenschappelijke disciplines. Zij combineren een biologisch herkenningselement (moleculaire biologie) met een *transducer* (fysica en chemie). Biochemische of biofysische gebeurtenissen worden vervolgens vertaald in kwantificeerbare waarden (ingenieurswetenschappen). Biosensoren kunnen onder andere geïnclassificeerd worden volgens het soort herkenningselement, bv. antilichamen, *molecular imprinted polymers* (MIPs) en aptameren. In dit onderzoek ligt de focus op aptameren als onderdeel van een biosensor.

Het hoofddoel van dit onderzoek omvat het nemen van de eerste stappen richting de ontwikkeling van een cross-reactieve aptasensor voor de detectie en identificatie van 17β -estradiol (E2) en zijn analogen in omgevingsstalen. Deze moleculen kunnen in de omgeving terecht komen en ageren als endocrien-verstorende chemicaliën (EDCs). Omwille van potentieel negatieve gezondheidseffecten is efficiënte monitoring aangewezen.

In Hoofdstuk 2 ligt de focus op aptameerselectie door middel van de *in vitro systematic evolution of ligands by exponential enrichment* (SELEX) procedure. Aangezien een SELEX procedure sterk targetafhankelijk is, werden bij aanvang van het onderzoek verschillende aspecten van het selectieproces geoptimaliseerd. Vervolgens werden, onafhankelijk van elkaar, twee SELEX procedures uitgevoerd. Beide SELEX procedures maakten gebruik van E2 als target gedurende positieve selectiestappen. De gebruikte moleculen gedurende counter selectiestappen verschilden echter van elkaar; dexamethasone voor SELEX A en nortestosteron voor SELEX B. Door gebruik te maken van verschillende counter moleculen tijdens beide procedures, werden twee reeksen aptameren geselecteerd met de verwachting dat beide reeksen gericht zijn tegen verschillende epitopen van E2. Klonering en sequentiebepaling van de twee reeksen aptameren brachten aanrijking aan het licht. Sequenties met éénzelfde motief waren talrijker aanwezig na SELEX A. SELEX B, daarentegen, leidde tot de aanrijking van twee volledige sequenties.

Optimalisatie en uitvoering van een SELEX procedure is vaak een proces van vallen en opstaan. In Hoofdstuk 3 wordt een interessante, nieuw ontwikkelde, methode voorgesteld voor het monitoren van de selectieprocedure. Door middel van *remelting curve analysis* (rMCA) werden drie verschillende SELEX designs (*bead* SELEX, plaat SELEX en CE-SELEX) voor drie verschillende targets (E2, CRP en peptide X) opgevolgd. Hierbij werd de universele toepasbaarheid van deze methode bewezen. Deze is onafhankelijk van het SELEX design en van targetkarakteristieken. Wanneer men de methode toepast zoals hier beschreven, kan een SELEX procedure geoptimaliseerd en uitgevoerd worden op een efficiëntere wijze dan wanneer deze blind wordt uitgevoerd. Deze methode biedt ook de mogelijkheid eventuele contaminaties in een vroeg stadium aan het licht te brengen.

Verschiedende bindingsstudies (Hoofdstuk 4) werden getest om te weten te komen welke test het meeste potentieel heeft voor de karakterisatie van de geselecteerde E2 aptameren betreffende affiniteit en epitoopspecificiteit. Bindingsstudies varieerden van een relatief eenvoudige *immunosorbent-like assay* tot hoogtechnologische technieken zoals *surface plasmon resonance* (SPR) analyse. SPR analyse bracht goede affiniteiten (laag μM bereik) aan het licht

voor alle geteste E2 aptameren. SPR analyse toonde ook epitopspecificiteit aan. Beide reeksen geselecteerde aptameren waren gericht tegen verschillende epitopen van E2, zoals de bedoeling was. Hiermee werd het succes van beide SELEX procedures aangetoond.

Aangezien het genereren van signalen na directe detectie van de interactie tussen aptameren en kleine moleculen beperkt is, wordt een alternatieve strategie bestudeerd in Hoofdstuk 5. Deze strategie, *target induced strand displacement* (TISD), detecteert aptameerbinding onafhankelijk van targetkarakteristieken hetgeen zou moeten leiden tot een verhoogde signalering. Niettegenstaande de eenvoudige theorie achter deze strategie en de beschikbaarheid van twee uitleesplaatvormen (SPR en *heat-transfer resistance*) die uitermate geschikt zijn voor de monitoring van deze strategie, waren we niet in staat TISD in de praktijk toe te passen. Noch één van onze eigen aptameren, noch verschillende aptameren uit de literatuur waarvan verwacht werd dat ze geschikt waren voor deze strategie, konden geïntegreerd worden in een TISD gebaseerde set-up. Verder onderzoek is vereist alvorens deze strategie kan worden geïmplementeerd.

De eerste stappen richting de ontwikkeling van een cross-reactieve aptasensor werden genomen. Deze stappen worden kritisch geëvalueerd in Hoofdstuk 6. In dit hoofdstuk werpen we ook een blik op de toekomst. We beschrijven een gedeelte van het werk dat nog moet gedaan worden alvorens het ultieme onderzoeksdoel te bereiken: de ontwikkeling van een cross-reactieve aptasensor voor de detectie van E2 en zijn analogen.

Summary

Biosensors are a critical extension of human perception of the world. Humans are extremely sensitive for the physical environment and are able to detect changes in for example light, temperature and humidity. The sensitivity of humans to the chemical and biological environment, on the other hand, is more limited. However, the quality of life is highly dependent on suitable chemical or biological compositions. Deviations in molecule and ion concentration inside a human body (e.g. metabolites, metal ions, hormones and proteins) can negatively affect a person's health. Disturbances in the environment (e.g. heavy metals, explosives and hormones) can negatively affect human health. Therefore, the development of highly sensitive and specific sensors for analyte recognition is a focus in a myriad of research areas, including environmental monitoring, industrial quality control and medical diagnostics. Sensors generate detectable and quantifiable signals in response to physical, chemical or biological stimuli.

Biosensors are the result of a strong collaboration between various scientific disciplines. They combine a biological recognition element (molecular biology) with a transducer (physics and chemistry). Biochemical or biophysical events are subsequently translated into quantifiable values (engineering). Biosensors can a.o. be classified according to the type of recognition element like antibodies, molecular imprinted polymers (MIPs) and aptamers. In this research, we focus on aptamers as part of a biosensor.

The main research goal presented in this dissertation is taking the first steps towards the development of a cross-reactive aptasensor for the detection and identification of 17 β -estradiol (E2) and its analogues in environmental samples. These molecules can end up in the environment, acting as endocrine disrupting chemicals (EDCs). Because of potential negative health effects, efficient monitoring is recommended.

In Chapter 2, the focus is put on aptamer selection by means of the *in vitro* systematic evolution of ligands by exponential enrichment (SELEX) procedure. Since a SELEX procedure is highly target dependent, several aspects of the selection process were optimized at the start. Subsequently, two independent SELEX procedures were performed. Both SELEX procedures used E2 as a target during positive selection steps. The difference lied in the applied molecule during counter selection steps; dexamethasone for SELEX A and nortestosterone for SELEX B. By using different counter molecules for both procedures, two series of aptamers - both expected to be directed towards different epitopes of E2 - were selected. Cloning and sequencing the two pools after the selection processes revealed the enrichment of motif containing sequences after SELEX A and the enrichment of two complete sequences after SELEX B.

Optimizing and performing a SELEX procedure is often characterized by trial and error. In Chapter 3, an interesting newly developed tool for monitoring the selection process is described. By means of remelting curve analysis (rMCA), three different SELEX set-ups (bead SELEX, plate SELEX and CE-SELEX) for three different targets (E2, CRP and peptide X) were monitored. This has proven the universal applicability of this tool, independent of SELEX design or target characteristics. By applying the monitoring tool as described here, a SELEX procedure can be optimized and performed in a more efficient way than when performed blindfolded. Also, contamination problems can be identified in a premature stage by using this tool.

Several binding assays (Chapter 4) were tested in order to explore which one has the most potential for characterization of the selected E2 binding aptamers in terms of affinity and epitope specificity. Binding assays varied from a relatively simple immunosorbent-like assay to high-end techniques such as surface plasmon resonance (SPR) analysis. SPR analysis showed good affinities (low μM range) of all tested E2 aptamers. SPR analysis also proved epitope specificity. Both series of selected aptamers turned out to be directed towards different epitopes of E2, as was intended. This proofed the success of both performed SELEX procedures.

Since signal generation after direct detection of aptamer-small molecule interaction is limited, an alternative strategy is explored in Chapter 5. This strategy, target induced strand displacement (TISD), detects aptamer binding independent of target characteristics and is expected to enhance signal generation. Notwithstanding the simple theory behind this strategy and the availability of two read-out platforms (SPR and heat-transfer resistance) which are extremely suitable to monitor this strategy, we were not able to apply this strategy. Nor one of our own aptamers, nor several aptamers out of literature which are supposed to be suitable for this strategy could be integrated in a TISD based set-up. Further investigation is required to implement this strategy.

The first steps towards the development of a cross-reactive aptasensor are taken. These steps are critically evaluated in Chapter 6. In this Chapter, we also take a glimpse into the future and summarize some work that still needs to be done to really achieve our ultimate research goal, the development of a cross-reactive aptasensor for the detection of E2 and its analogues.

1

General introduction and aims

In this chapter, some general information about aptamers will be highlighted. After giving a description of aptamers, the focus is a.o. put on their advantages, their selection process, the way they can be characterized in terms of affinity and specificity and their potential applications (e.g. for the detection of endocrine disrupting hormones such as estrogens). To end this introduction, the aims of our study will be explained.

1.1 Aptamers

1.1.1 Description

The term aptamer is derived from the Latin word *aptus* meaning 'to fit' and the Greek word *meros* meaning 'particle', referring to a lock-and-key relationship between an aptamer and its target [1]. Aptamers are short synthetic single stranded (ss) DNA or RNA oligonucleotides or a combination of one of these with non-natural nucleotides (nt), capable of adopting a specific three-dimensional (3D) structure. This 3D structure enables aptamers to bind with high specificity and sensitivity to a certain target [2], varying from a small molecule [3, 4] to a peptide or a protein [5, 6] and even a whole cell [7, 8] (Figure 1). Driving forces for aptamer–target binding are structure compatibility, stacking of aromatic rings, electrostatic and van der Waals interactions and hydrogen bonds, or a combination of these effects [9].

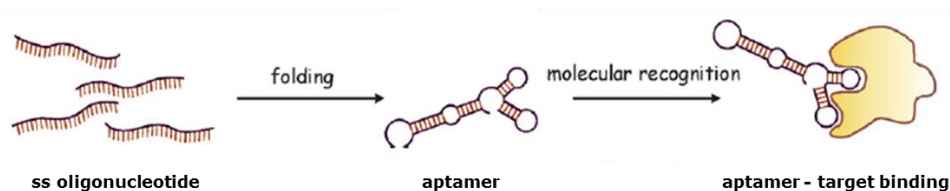


Figure 1: Schematic representation of aptamer-target interaction [10]. Ss oligonucleotides fold into a 3D structure and interact with their target via various driving forces.

The first studies on aptamers mainly comprised RNA oligonucleotides because of the assumption that RNA is more flexible and is able to form more diverse 3D structures than DNA. This was believed to be beneficial in terms of forming specific binding sites and establishing a higher affinity for the target. The selection of RNA aptamers, however, is more complicated than selecting DNA aptamers, a.o. because additional *in vitro* transcription steps are needed before and after each PCR amplification. Additionally, RNA oligonucleotides are more prone to enzymatic degradation. When currently comparing the affinity of either type of aptamers, no clear difference in affinity can be found [11]. Beside oligonucleotide aptamers, peptide aptamers are also described in literature. However, peptide aptamers have a distinct structure and they are selected by a different procedure than used for oligonucleotide aptamers [12, 13]. Therefore, peptide aptamers will not be discussed in this dissertation.

1.1.2 A little history

This year marks the 25th anniversary of the publication of two pioneering papers describing aptamers and their selection process. In 1990, the term aptamer was introduced in a Nature article by Ellington and Szostak. These researchers used randomized RNA libraries as a starting point for the affinity selection of RNA oligomers that specifically bind to several organic dye molecules like cibacron blue and reactive blue 4 [1]. Around the same time, Tuerk and Gold introduced a general method for aptamer selection which they called systematic evolution of ligands by exponential enrichment (SELEX). By means of this *in vitro* method, Tuerk and Gold selected RNA aptamers against bacteriophage T4 DNA polymerase [14].

Only 8 years later, in 1998, the first aptamer was integrated in a biosensor set-up. As a proof-of-concept, an anti-thrombin aptamer labeled with a fluorescent tag was covalently attached to a glass support matrix. Subsequently, thrombin was detected by following changes in the evanescent-wave-induced fluorescence anisotropy (FA) of the immobilized aptamer after thrombin binding [15].

A milestone was reached in 2004 when the food and drug administration (FDA) approved the first aptamer-based drug Macugen (or Pegaptanib). This drug is able to selectively block VEGF₁₆₅, an isoform of VEGF responsible for pathological neovascularization in age-related macular degeneration and diabetic macular edema [16]. Currently, a number of other aptamers are available in clinical and preclinical trials for the treatment of cancer and other diseases [17].

In 2008, AptaBiD (aptamer-facilitated biomarker discovery) was described as a promising technology for biomarker discovery. This technology comprises three successive steps: (1) selection of aptamers for biomarkers expressed on target cells being in their native state and conformation; (2) aptamer-based isolation of biomarkers present on target cells; and (3) mass spectrometric (MS) identification of isolated biomarkers. The crucial feature of this technology is that it generates synthetic affinity molecules simultaneously with biomarker discovery [18].

Currently, within 25 years, a large number of aptamer-related articles have been published (searching PubMed with the term 'aptamers' yields 5416 hits and 'DNA aptamers' yields 4428 hits) [19]. The original aptamers, pure DNA or RNA oligonucleotides, are in the meantime expanded with modified ones. SomaLogic's breakthrough SOMAmers (slow off-rate modified aptamers) comprise a short DNA sequence, incorporating several bases which have been modified to include protein-like side chains and a 5'-fluorescent linker for later detection purposes. Until now, they developed SOMAmer reagents to a broad array of more than 1000 different protein targets related to normal and disease biology [20].

1.1.3 Advantages

Aptamers are widely known as substitutes for antibodies since they overcome several of their weaknesses.

Their *in vitro* selection, independent of animals or cell lines, can be highlighted as one of their most important strengths. Selection parameters such as temperature, ionic strength and pH can be adjusted to future applications (whereas antibodies normally only work under specific physiologic conditions) and after sequence identification, aptamers can conveniently be prepared with high reproducibility and purity and little or no batch-to-batch variation. Moreover, aptamer selection can be employed where antibody selection fails, such as targeting pathogenic and toxic molecules or molecules which do not elicit an adequate immune response such as several small molecules [2, 10, 21].

Affinities of available aptamers are often similar to those defined for monoclonal antibodies. Most aptamers selected against protein targets reveal affinity values in the pico- to nanomolar (pM to nM) range. Most aptamers targeting small molecules show affinities in the micro- to millimolar (μ M to mM) range, although there are some aptamers directed towards small molecules with affinities in the nM range [10]. In addition to their substantial affinities, most aptamers have extremely high specificities. This enables them to discriminate between molecules with limited structural differences. This feature is illustrated by an RNA aptamer that binds theophylline with 10 000 fold greater affinity than caffeine, which differs from the target molecule by only one CH₃ group [22]. Some aptamers have even shown chiral specificity. An outstanding example is an RNA aptamer discriminating 12 000 fold between the D- and L-enantiomer of arginine [23].

Finally, conjugation chemistries can easily be applied during aptamer synthesis. Functional groups can be attached to aid immobilization and dyes or other labels can be tagged to offer signaling properties. Both are useful when introducing aptamers as recognition elements in a biosensor set-up. Nuclease resistance can be achieved by incorporating chemical modifications into the sugars or internucleotide phosphodiester linkages of the aptamers [24]. Once integrated in a biosensor, aptamers are also reusable as receptor molecule since introducing denaturing conditions easily disrupts aptamer-target interactions after which the native conformation of the aptamer is restored and complete functionality is reassured [10].

1.2 Aptamer selection

Like most of the groundbreaking ideas, the theory of a standard SELEX procedure is very simple, relying on Darwinian evolution at a molecular level. It is an iterative *in vitro* process consisting of a few recurrent basic positive selection steps: binding, selection (partitioning and elution), amplification and conditioning (Figure 2).

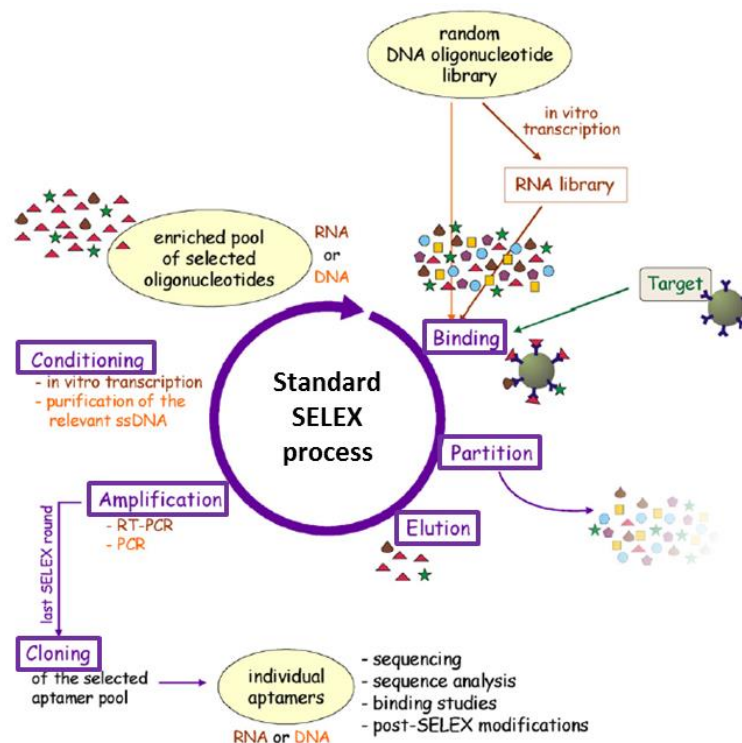


Figure 2: Schematic illustration of a standard SELEX process (adapted from [10]). Starting point is a synthetic oligonucleotide library enclosing a multitude of random ssDNA fragments. This library is used directly for the selection of DNA aptamers, but is transferred into an RNA library for the selection of RNA aptamers. Exposure of the library to the target of interest enables some oligonucleotides from the library to bind to the target. Unbound and weakly bound oligonucleotides get partitioned and discarded. Bound oligonucleotides are eluted and subsequently amplified by polymerase chain reaction (PCR) or reverse transcriptase (RT)-PCR. At last, the amplified oligonucleotides undergo a conditioning step. In the case of DNA SELEX, they are made ss. For RNA SELEX, the conditioning comprises *in vitro* transcription. The selected oligonucleotide pool is then ready for the next selection round. After the last selection round, the enriched aptamer pool is cloned and several individual aptamers are characterized.

1.2.1 Standard SELEX procedure

Step 1: Binding of oligonucleotides to the target of interest

The starting material of a SELEX is a random DNA oligonucleotide library consisting of about 10^{13} to 10^{15} different sequences. Each sequence comprises an inner random part of 20 to 80 nt flanked by two fixed primer binding regions of 18 to 21 nt each. For the selection of DNA aptamers, this library can be used as such. Conversion into an RNA library is necessary when the goal is to select RNA aptamers [10, 17, 25].

In order to allow potential aptamers to bind, the randomized RNA or DNA pool is incubated with the target of interest in a selective binding buffer [10, 17, 25]. The choice of binding conditions is very important since oligonucleotide structures, which are responsible for aptamer-target recognition, are greatly influenced by factors such as temperature, pH and ionic strength of the surrounding medium. Binding conditions during SELEX should mimic binding conditions of the eventual aptamer application as close as possible [26].

Step 2: Selection of bound oligonucleotides

After incubation of library and target, unbound and weakly bound oligonucleotides have to be discarded by several stringent washing steps and specifically bound oligonucleotides have to be separated from the target via one or more elution steps [10, 17, 25]. Efficient partitioning between bound and unbound strands forms a crucial step which is highly dependent on the way the target is implemented, immobilized on a surface or free in solution.

Immobilization of target on a particular matrix makes the separation of bound and unbound oligonucleotides rather easy. Unbound and weakly bound oligonucleotides are discarded during washing steps. Subsequent use of denaturing conditions such as high temperature and/or low ion concentration results in the elution of bound oligonucleotides [10]. Commonly used matrix materials are beads [27, 28] and chromatography columns [29]. Making use of immobilized target during SELEX has, however, some drawbacks.

Oligonucleotides can aspecifically bind to the support matrix or a combination of support matrix and target. Besides, certain functional groups on immobilized target are not available anymore as potential epitopes for aptamer binding. The latter is especially important when selecting aptamers for small molecules only bearing few functional groups. This problem can be circumvented by making use of oriented immobilization of the target so that the desired epitope is still available for aptamer generation [17].

Selection methodologies which do not require target immobilization are a.o. ultrafiltration by use of nitrocellulose filters with distinct molecular weight (MW) cut-offs [30], centrifugation [31] and capillary electrophoresis (CE) [32]. Here, separation mainly occurs based on a weight difference between complex and free aptamer/target. When the weight difference is limited, e.g. because of the low MW of the target, efficient separation is hard to achieve.

Step 3: Amplification of selected oligonucleotides

The third recurrent step of a standard SELEX procedure is amplification of eluted sequences by means of PCR (DNA SELEX) or RT-PCR (RNA SELEX). Due to the high complexity of the initial oligonucleotide library, it can be expected that few oligonucleotides bind to the target of interest during the first selection rounds. These rare oligonucleotides need to be amplified to yield enough sample to continue the SELEX process [10, 17, 25].

Step 4: Conditioning of oligonucleotides before the next selection round

In the last step, the amplified oligonucleotide pool is prepared for the next selection round. After PCR amplification, the enriched pool is present as dsDNA. In case of RNA aptamers, a transcription with T7 RNA polymerase occurs to render ssRNA oligonucleotides. In case of DNA aptamers, single strand separation has to be carried out [10]. Several methods exist to generate ssDNA, including asymmetric PCR [33], removal of biotin tagged anti-sense strands by using streptavidin(SA)-coated beads [34] and enzymatic digestion of anti-sense strands [35].

Finally, the new pool of selected oligonucleotides is reintroduced as template into a next selection round. By iteratively performing binding, selection, amplification and conditioning steps, the originally random oligonucleotide pool will gradually transform into a more enriched pool [10, 17, 25] .

The number of SELEX rounds needed to obtain enrichment is different for each SELEX procedure since it is dependent on many parameters such as target features and applied selection conditions. A general SELEX procedure comprises 6 to 20 SELEX rounds [10]. Several methods exist to follow-up the arising enrichment during SELEX. However, the decision when to stop the SELEX procedure is often made blindly [36].

The last SELEX round is stopped after the third step, amplification of relevant oligonucleotides. Subsequently, the dsPCR product is cloned into a bacterial vector in order to obtain individual aptamer clones from the selected pool. These aptamer clones are sequenced and the sequences are analysed. Sequence alignments are useful to assess the complexity of the selected aptamer pool and to identify clones with identical sequences or motifs [10, 17, 25].

1.2.2 Adjustments standard SELEX procedure

Notwithstanding the simple theory behind a standard SELEX procedure, implementation of aptamer selection is much more complex. Over the years, the standard SELEX procedure underwent numerous adjustments to improve its selection efficiency.

Besides the above described positive selection steps, additional steps can be included in the SELEX process in order to improve aptamer specificity [10]. When target is immobilized during the SELEX process, negative selection steps are recommended to remove oligonucleotides which bind to the immobilization matrix or to cross-linkers used for immobilization purposes [27]. Both when target is immobilized and when it is free in solution, counter selection steps can be useful to eliminate oligonucleotides that show affinity for structurally related molecules or to select oligonucleotides that specifically bind to a particular,

predefined epitope of the target. Functional groups which are present on the target applied during positive selection steps, but which are absent on the molecule used during counter selection, act as a predefined epitope [37].

To improve aptamer sensitivity, the stringency of the selection conditions can progressively be increased during the SELEX procedure. This is a.o. possible by gradually decreasing the target concentration, reducing the incubation time or increasing the amount of washing steps during the SELEX procedure. The ultimate goal is that only the best binders 'survive' [11].

Special libraries can be used as starting material for the SELEX procedure. These libraries may contain particularly designed flanking sequences to direct the aptamers to form a specific structure [38] or they may include modified nt. The latter expands the genetic alphabet on which selection takes place and also influences aptamer properties, such as *in vivo* stability and nuclease resistance [39]. For influencing aptamer properties, modifications to nt can also be introduced post-SELEX [24].

Besides the above mentioned adjustments, numerous other variations of the standard SELEX procedure are described in literature. A partial overview is given in Table 1.

Table 1: Variations of the standard SELEX procedure, their method characteristics and possible applications (modified from [10, 25, 40]).

SELEX method	Method characteristics	Applications
Tailored SELEX	Ligation and cleavage of primer sites before and after amplification	Selection of shorter aptamers
Toggle SELEX	SELEX with two different target molecules	Selection of bispecific aptamers
Mirror-image SELEX	Counter selections using a particular enantiomer of the target	Selection of aptamers specific for a predefined enantiomer of the target
Genomic SELEX	Use of libraries based on genomic sequences	Selection of natural genomic sequences acting as aptamers
Cell SELEX	Use of whole cells as selection target	Selection of aptamers for unknown cellular markers
Non-SELEX	Several selection rounds without amplification in between	Avoidance of PCR errors
Deconvolution SELEX	Use of complex mixtures as selection target. Post-SELEX: defining which aptamers bind to which components	Selection of aptamers for complex targets

1.3 Aptamer characterization

Although the success of aptamers in their final application is highly dependent on their selection process, also aptamer characterization in terms of affinity, kinetics and specificity plays a crucial role. Most selection processes result in a large number of aptamer candidates. Ideally, all these candidates need to be evaluated in terms of their target binding properties to designate those candidates which are most auspicious. However, characterization (*in silico* and via binding assays) of all candidates is expensive and time-consuming [11].

In silico characterization of aptamers depends on oligonucleotide sequence information. All oligonucleotides share a universal force of structure formation: the stacking of hydrogen-bonded base pairs (bp). This force enables folding of sequences into secondary structures characterized by a.o. stems and loops. Combination of secondary structures results in the formation of tertiary

structures such as quadruplexes, playing a meaningful role in target interaction [2, 41].

Base pairing turns structure prediction into a problem of discrete mathematics since two nt do or do not form a base pair. Computational prediction of secondary structures is possible by means of software programs such as Mfold. Based on minimal free energy algorithms, secondary structure formation is predicted under defined conditions like temperature and ionic strength of the used buffer [42]. G-quadruplexes, characterizing tertiary structures of several G-rich aptamers, can be predicted by using the software program QGRS mapper [43].

Secondary structure analysis may reveal both relevant structures for target binding and sequence motifs responsible for stabilization of these structures. This information can a.o. be useful when, in a later stage, aptamers need to be truncated to shorter sequences for certain applications. However, important to consider is that all predictions are made for oligonucleotides in the absence of target. Target interaction potentially induces adaptive conformational changes [10]. The ultimate 3D structure of the aptamer-target complex can be predicted via methods such as nuclear magnetic resonance (NMR) spectroscopy, X-ray structure analysis and crystallization [44, 45].

Binding assays are very diverse and come in different shapes and complexities, but also in different costs. The outcomes of these assays range from a binding or no-binding answer to highly detailed answers about binding characteristics. When analyzing many samples, it can be useful to start with simple, high-throughput and relatively cheap assays as a kind of pre-selection step. Afterwards, one can continue to more expensive and specialized techniques.

1.3.1 Affinity and kinetic analysis of binding interactions

Aptamer binding strength (affinity) can be described via an affinity constant (K_D), referring to the proportion of complex and free interactants (aptamer and

target) at equilibrium. Time dependent interaction of aptamer with its target (kinetics) can be described via an association and dissociation rate constant (k_a and k_d), indicating whether a complex forms or dissociates within a given time span. Figure 3 shows typical ranges of k_a , k_d and K_D for biological interactions.

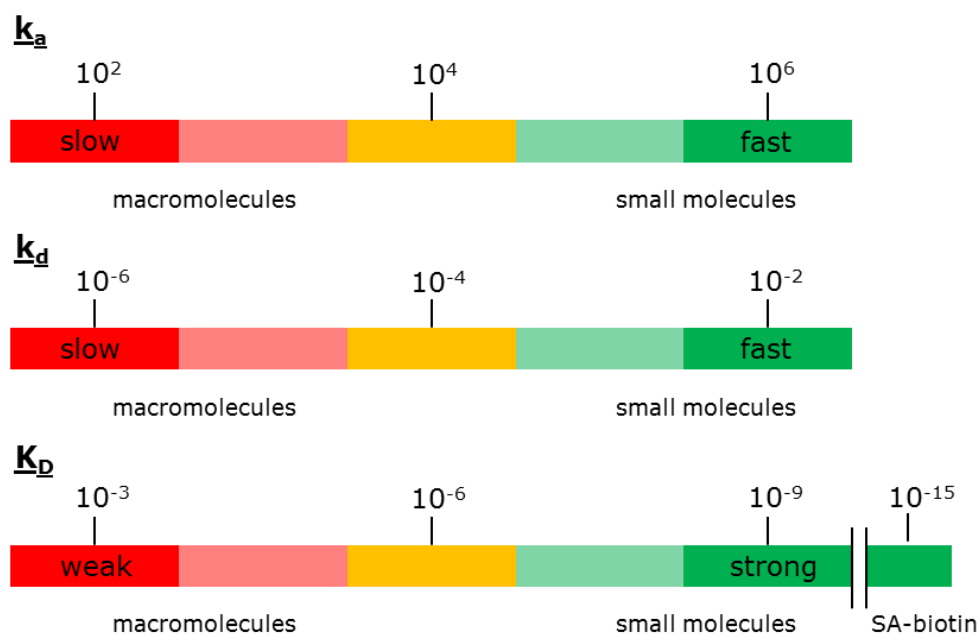


Figure 3: Typical ranges for biological interactions [46].

1.3.2 Binding assays for affinity and kinetic analysis

Basically, binding assays can be divided into homogeneous and heterogeneous assays. Homogeneous assays are solely using a liquid phase, whereby both aptamer and target stay in solution. Heterogeneous assays rely on immobilization of aptamers or target on a solid support matrix [2].

Homogeneous assays

Conformational changes of a signaling aptamer upon binding can be measured as a change in fluorescence signal. Since oligonucleotides do not have intrinsic fluorescence, fluorophore molecules have to be introduced in the detection system [2]. A well-known example is the molecular beacon. In many molecular beacons, one end of the aptamer is linked with a fluorophore while the other end is linked with a quencher. Dependent on the structure of the aptamer before and after target recognition, the fluorescence signal is turned from an 'on' to an 'off' state or *vice versa* [47]. Such aptamer beacons were a.o. constructed for the detection of cocaine [48] (Figure 4a) and ssDNA binding protein (SSB) (Figure 4b) [49]. Numerous other beacon formats have been described, such as a fluorophore-labeled aptamer in duplex with a quencher-labeled complementary strand. The complementary strand gets displaced from the aptamer by analyte binding, switching the 'off' state to an 'on' state [50] (Figure 4c).

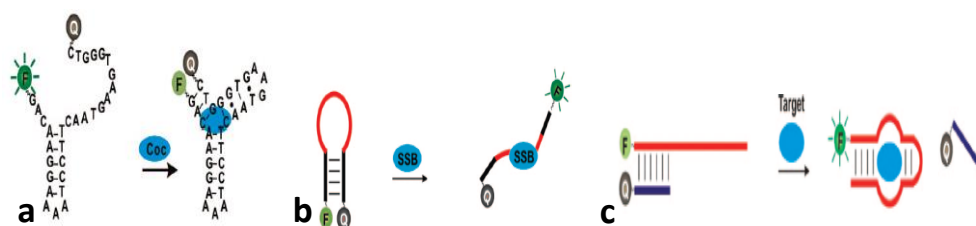


Figure 4: Schematic illustration of different aptamer beacon formats. (a) An aptamer beacon for cocaine (Coc), constructed by labeling the two ends with a fluorophore and a quencher. Target binding turns off the fluorescence signal [48]; (b) ssDNA binding protein (SSB) detected by means of an aptamer beacon labeled with a fluorophore and a quencher. After target binding, the fluorescence signal is turned on [49] and (c) A two strand beacon system consisting of a fluorophore-labeled aptamer and a quencher-labeled complementary strand. Target binding turns on the fluorescence signal [50].

Similarly, the fluorescence resonance energy transfer (FRET) phenomenon can be used when donor and acceptor molecules are applied instead of a fluorophore and a quencher. Target binding is then translated in a shift in emission wavelength. Nagatoishi *et al.* (2007) dual-labeled aptamers with a FAM and a TAMRA group at the 5' and 3' termini, respectively, in order to detect thrombin [51].

More advanced fluorescence spectroscopy techniques are FA and fluorescence correlation spectroscopy (FCS). FA is dependent on a fluorophore's ability to produce depolarized emission when excited by a polarized light source. Fluorophores linked to small compounds rotate relatively fast during their excited lifetimes. Therefore, they easily depolarize the excitation light and give a low anisotropy. When a fluorophore is linked to a larger compound, the motion of the fluorophore is lower which results in a higher anisotropy [52] (Figure 5a). Fang *et al.* (2001) labeled platelet-derived growth factor (PDGF) aptamers with fluorescein. Upon addition of PDGF, FA was significantly changed [53]. FA can also be applied in a heterogeneous assay set-up when fluorescently labeled aptamers are immobilized onto a surface, as was demonstrated by Potyrailo *et al.* (1998) (see section 1.1.2) [15]. FCS, on the other hand, monitors fluctuations in fluorescence intensity by the random in and out migration of fluorescently labeled molecules in a confocal area. Based on these fluctuations, information is generated about the diffusion rate of molecules and their concentration. An interaction between two compounds is detected as an increased diffusion time since small compounds diffuse more rapidly than larger ones [54] (Figure 5b). Book *et al.* (2011) fluorescently labeled aptamers oriented towards surface receptors of bacterial cells. By applying FCS, they were able to study receptor densities of bacterial cells [55].

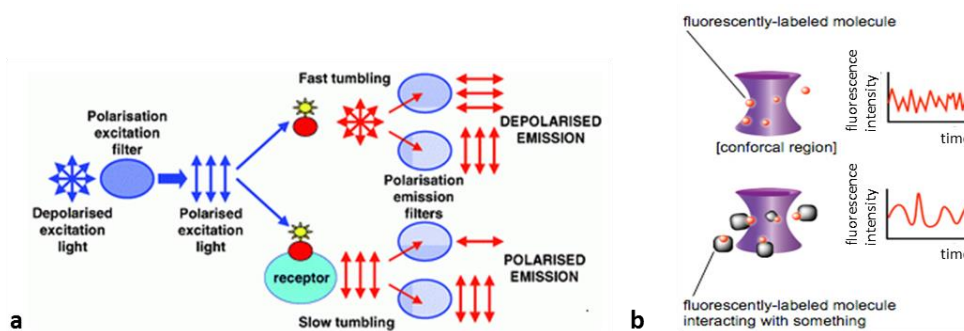


Figure 5: Schematic illustration of the principle of FA [56] and FCS [54]. (a) FA monitors polarization of emitted light. Fluorescently labeled compounds emit polarized light when excited by a polarized light source. However, when a compound is moving, it will tend to scramble the polarization of light, resulting in depolarized emission and (b) FCS detects fluctuations in fluorescence intensity caused by the random migration of fluorescently labeled compounds in and out a confocal area. Fluctuations are related to the size of the diffusing compounds and their sample concentration.

A way to create a homogeneous aptamer-analyte detection system without labeling of the aptamer itself relies on the use of DNA-intercalating dyes. The dye intercalates into free aptamer, but intercalation decreases when the aptamer interacts with its target [2]. This principle was applied to a thrombin-binding aptamer. A clear fluorescence signal was visible when the aptamer was mixed with crystal violet. In the presence of human thrombin, however, the fluorescence of crystal violet decreased [57].

The advantage of homogenous assays is that neither the aptamer, nor its target have to be immobilized so that it is more likely that they are both present in their original, native state. The use of fluorescent labels increases assay sensitivity, but also augments the cost price of these assays. Moreover, most homogenous binding assays are dependent on specific characteristics of the aptamers or their targets. Aptamer beacons often are dependent on conformation changes of the aptamers. Techniques such as FA and FCS, on the other hand, are dependent on the weight of the target. When the weight of the target is limited, complex formation will only generate a limited signal. Aptamer or target dependency makes general applicability of binding assays for different aptamers difficult.

Heterogeneous assays

The most basic binding assay with immobilized aptamers has been developed in analogy to the widely used enzyme-linked immunosorbent assay (ELISA) and is referred to as enzyme-linked oligonucleotide assay (ELONA). Since it is rather easy to label aptamers for immobilization or signaling purposes, aptamers are ideal candidates to use as capture and/or detection agents, alone or in combination with antibodies [2] (Figure 6). ELONAs are ideal as a first screening tool to characterize an initial batch of selected aptamers. They are sensitive and relatively cheap, but also prone to human errors because automation is often absent. Martin *et al.* (2013) used ELONA to analyse the affinity and specificity of aptamers to Leishmania histones. They coated histones onto the surface of a 96-well microtiter plate. Binding with digoxigenin-labeled aptamers was visualized by means of horseradish peroxidase (HRP)-labeled anti-digoxigen antibody [58].

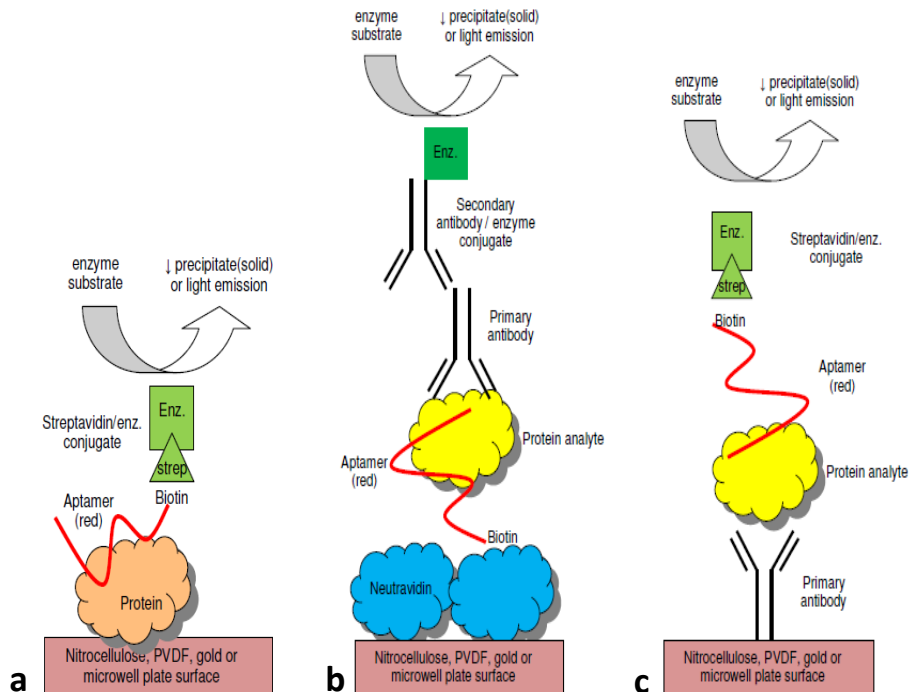


Figure 6: Schematic illustration of potential ELONA set-ups [59]. (a) ELONA by direct spotting of protein target onto a surface; (b) Indirect method 1 for a sandwich aptamer/antibody ELONA. In this method, aptamer is used as capture molecule and (c) Indirect method 2 for a sandwich aptamer/antibody ELONA. Here, antibody is used as detection molecule.

Signal amplification after target-aptamer interaction can also be obtained via DNA-based amplification techniques, analogous to what happens in immuno-PCR [37]. Fischer *et al.* (2008) identified aptamer-thrombin interaction by means of standard PCR or rolling circle amplification (RCA) (Figure 7a) [60]. Liao *et al.* (2010) detected aptamer-IgG interaction by means of qRT-PCR. Instead of direct amplification of the aptamer, they attached a PCR template to the aptamer which they amplified and used as signal enhancer (Figure 7b) [61].

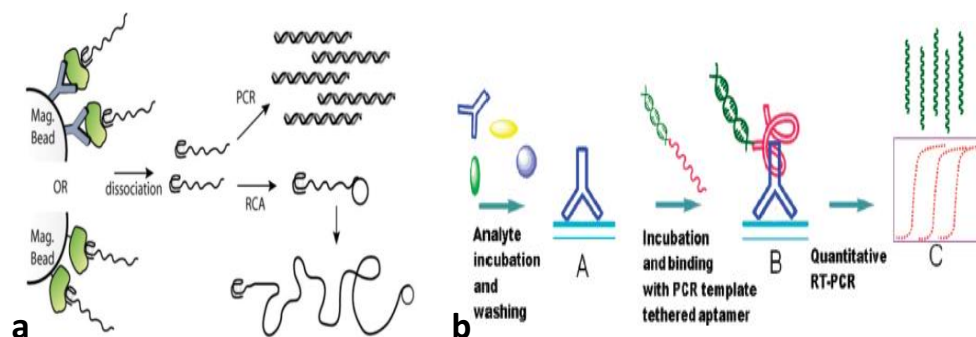


Figure 7: DNA-based amplification after aptamer–target interaction (modified from [60, 61]). (a) Anti-thrombin biotinylated antibody capturing thrombin or biotinylated thrombin were immobilized onto magnetic beads. After incubation with aptamers, unbound aptamers were removed. Bound aptamers were eluted and subsequently analysed via PCR or RCA and (b) Target molecules (IgG) were captured on a surface and subsequently incubated with dsDNA PCR-template tagged aptamers. Removal of unbound aptamers was followed by quantitative real-time PCR (qRT-PCR) to quantify the target molecule.

More advanced binding assays with immobilized aptamers are based on measuring the properties of thin films. Detection often relies on changes in optically or electrochemically measurable signals.

Surface plasmon resonance (SPR) is an optical phenomenon which occurs at the interface of a thin conducting metal coated prism. When plane-polarized light hits the back of the metal film under total internal reflection conditions, this results in an evanescent resonance plasmon wave. Moreover, the incident light is refracted under a certain resonance angle. When compounds bind to the metal surface, the resonance angle shifts because of changes in the refractive index of the dielectric medium at the interface. Changes in resonance angle are proportional to the mass of compounds bound to the back of the metal film and are translated in arbitrary response units (RU) [62] (Figure 8).

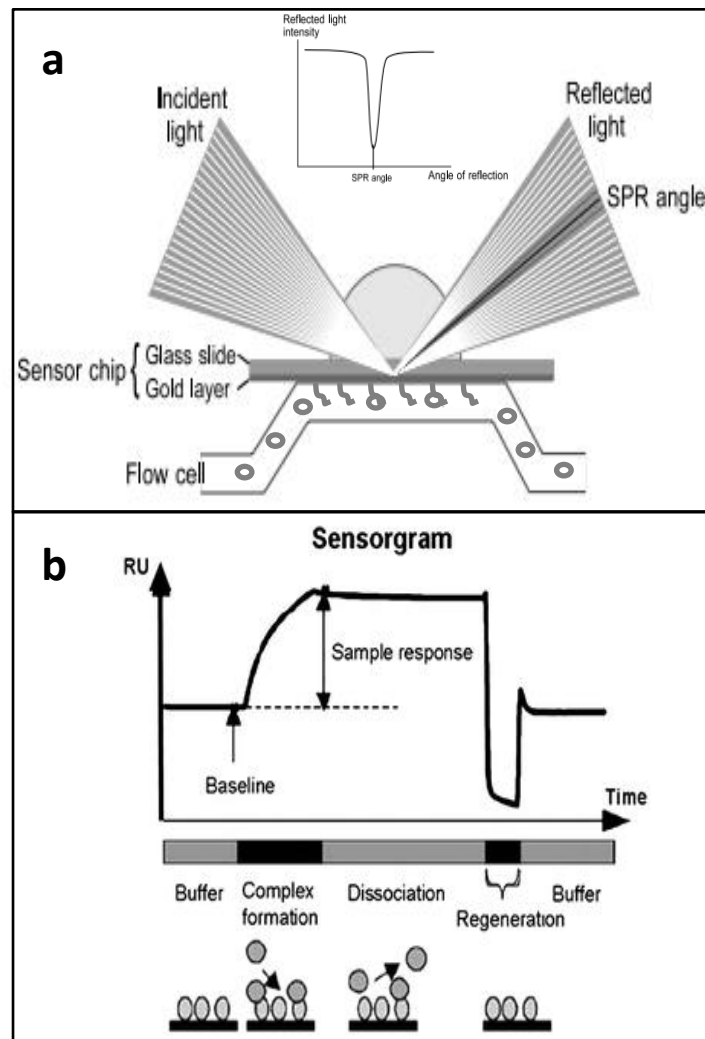


Figure 8: Basics of SPR technology (Adapted from [63]). (a) The SPR detection principle. Polarized light is applied to the surface of a sensor chip and subsequently becomes reflected. The intensity of the reflected light is reduced at a certain angle. Interacting compounds near the surface of the sensor chip increase the refractive index, which alters the SPR angle. An optical detection unit detects, in real-time, position changes of the intensity dips and translates these changes in arbitrary RU and (b) Schematic representation of an SPR sensorgram, shown as a response in function of time.

Ashley and Li (2013) reported the development of an SPR based assay to detect the presence of catalase in milk samples. They immobilized biotin tagged aptamers onto an SA-coated SPR sensor chip. Subsequently, they injected milk

samples spiked with different concentrations of catalase over the immobilized sensor chip [64].

Signals in electrochemical assays are generally generated through three mechanisms: (1) introducing catalytic labels to the electrodes, (2) altering the proximity of electrochemical labels to the electrodes and (3) switching the conductivity of immobilized DNA on the electrodes [65].

The introduction of catalytic labels to electrodes often requires a sandwich assay format. Sandwich based binding complexes bring catalytic labels to the electrode surface and then generate amperometric, voltammetric, impedimetric or gravimetric detection signals [65]. Mir *et al.* (2006) described a binding assay that used HRP as a catalytic label. Thrombin was 'sandwiched' between an immobilized capture aptamer and an HRP-labeled detection aptamer. The HRP label subsequently catalyzed the reduction of H_2O_2 and the resulting amperometric response was measured [66] (Figure 9a). To improve the sensitivity, several nanomaterials have been introduced as more efficient catalytic labels. Polsky *et al.* (2006) described the use of platinum nanoparticles to replace conventional enzymes as a catalytic label. These researchers developed a sandwich assay comprising immobilized thrombin aptamer (against epitope X), thrombin and platinum nanoparticle tagged thrombin aptamer (against epitope Y). The platinum nanoparticles enabled amperometric detection via electrocatalyzed reduction of H_2O_2 [67].

Structure-switching aptamers are most frequently used to alter the proximity between labels and electrodes upon target-binding [65]. For example, Xiao *et al.* (2005) developed an electrochemical thrombin aptasensor by attaching a redox-active methylene blue label to a thrombin aptamer that was immobilized onto an electrode. In the absence of its target, the aptamer showed a flexible conformation which ensured the close proximity between the methylene blue label and the electrode. A voltammetric response was generated. Upon target binding, however, the aptamer assembled into a G-quadruplex structure, distancing and shielding methylene blue from electron-transfer communication with the electrode [68] (Figure 9b).

Finally, electrochemical assays can also be constructed by directly measuring changes in the conductivity of DNA probes immobilized on electrodes. The molecular conductivity of DNA double helices has been shown to depend on their conformational state [65]. Huang *et al.* (2008) developed an electronic sensor by incorporating a thrombin aptamer into a double-helical conduction path. The conduction path was formed by a three-way junction structure and ferrocene served as an electrochemical label which was linked to the strand that encompassed the aptamer sequence. In the absence of thrombin, the conduction path was turned off since the three-way junction structure prevented conduction. Upon thrombin binding, the conformation of the three-way junction structure was changed and the conductivity of the conduction path was switched on, leading to an increase in the measured electrical signal [69] (Figure 9c).

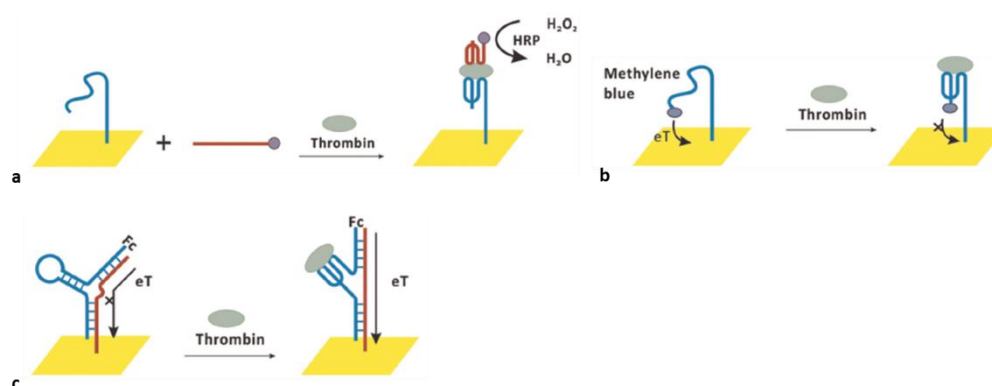


Figure 9: Electrochemical assays to characterize aptamer functionality (adapted from [65]). (a) HRP serves as a catalytic label for a sandwich-type thrombin detection; (b) Structure switching of aptamers upon target binding alters the distance between methylene blue and the electrode, resulting in an attenuation of an electrochemical signal and (c) Target binding alters the conformation of a three-way junction structure and subsequently switches on the conductivity of an adjacent helical conduction path resulting in an increased electrical signal.

Heterogeneous optical and electrochemical binding assays require specialized instrumentation, which is pricey, but this also often enables process automation. Generally spoken, these assays reach very good sensitivity and offer detailed information about binding characteristics. For example, SPR not only shows if

binding takes place, but it also gives information about the speed of binding association and dissociation.

1.4 Aptasensors

Biosensors are a critical extension of human perception of the world, producing detectable signals in response to physical or chemical stimuli. Appropriate chemical or biological compositions are tightly linked to the quality of life. For example, molecule and ion concentrations inside a human body (e.g. metabolites, metal ions, hormones and proteins) reflect a person's health. Chemicals in the environment (e.g. heavy metals, explosives and hormones) can negatively affect human health. Therefore, the development of highly sensitive and specific sensors for analyte recognition is a focus in many research areas, including environmental monitoring, industrial quality control and medical diagnostics [52].

In 1987, Turner *et al.* [70] were the first to describe a biosensor:

'A biosensor is a compact analytical device incorporating a biological or biologically derived sensing element with a physicochemical transducer. The usual aim of a biosensor is to produce either discrete or continuous digital electronic signals which are proportional to a single analyte or a related group of analytes.'

Thus, the key components of a biosensor are a sensing element and a transducer. The sensing element refers to a recognition element which is able to interact with a specific target. The transducer is responsible for converting target recognition into a measurable signal. The signal is subsequently processed by associated electronics or signal processors for displaying the results in a user-friendly way [52] (Figure 10).

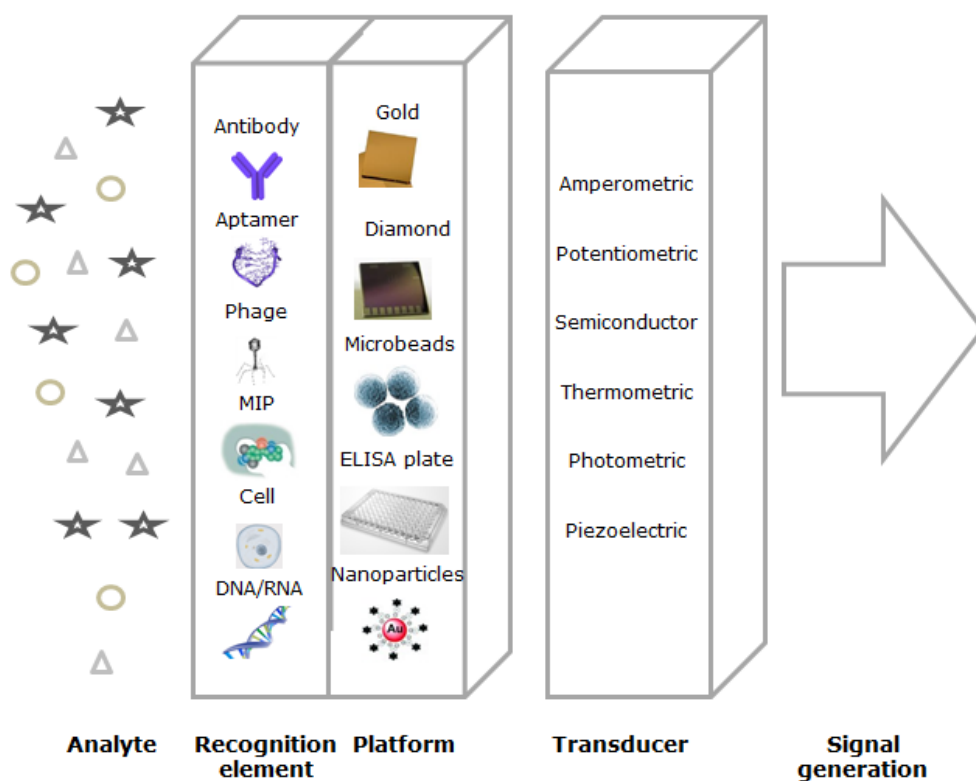


Figure 10: General scheme of a biosensor (based on [71]).

Sensors are often single-analyte sensors enabling the detection of one specific type of target. This type of approach, however, requires the synthesis of highly selective recognition elements for each analyte to be detected. Additionally, this kind of approach is not ideal when analyzing and classifying compositions of complex mixtures. A strategy complementary to single-analyte sensing involves the use of cross-reactive arrays. A minimal set of recognition elements, with every element responding to a number of different targets, enables the classification of samples into various groups, shortening the time required for differential detection [72, 73].

An ideal sensing element meets several criteria. Preferably, this element has a high affinity (low detection limit), a high specificity (low interference with other compounds or epitopes), a wide dynamic range, a fast response time, the

capacity to be re-used,... After reading the previous sections of this introductory chapter, it should be clear that aptamers fulfill these requirements. Therefore, a lot of efforts [52] have been made to fabricate aptamer-based sensors, also called aptasensors.

Disease diagnostics seems to be the most dynamic field in aptasensor research. [25]. Aptamers can detect low amounts of diseased or tumor cells for which they are selected. For example, anti-EGFR RNA aptamer immobilization on a chemically modified glass surface can determine the presence of glioblastoma tumor cells. EGFR is the most common oncogene in glioblastoma [74]. Newly developed CD30 aptamer, on the other hand, can be used for the diagnosis of CD30 expressing lymphomas in a flow-cytometry set-up [75]. Detection of microbial pathogens and virally infected cells is also possible by means of aptamers. Aptamers directed towards HIV-1 TAT protein immobilized on a gold surface of piezoelectric quartz crystals or SPR chips have proven their efficiency to identify HIV [5].

For environmental screening, aptasensors can be useful to detect contaminants in food, air and water such as small molecules (including hormones, antibiotics, toxins, pesticides and heavy metals) and pathogens. Zhang *et al.* (2010) developed a rapid electrochemical aptasensor using aptamers immobilized on glassy electrodes. By means of this aptasensor, they were able to detect the antibiotic tetracycline in spiked milk with a sensitivity limit of 2.2 nM [76]. Tang *et al.* (2009), on the other hand, developed a panel of aptamers capable of recognizing virus-infected cells in the nM range. These aptamers could be ideal candidates to integrate as recognition elements into a biosensor set-up to investigate potential virus treatment [77].

Contrary to what one might expect, commercial exploitation of aptasensors has lagged behind research discovery. The sensing and diagnostic market is still largely dominated by antibodies. There is no single good explanation for this discrepancy, but several factors clearly play a role [78].

The key limitation is probably associated with the specific nature of aptamer performance. Aptamers usually work under very specific conditions (e.g.

temperature, pH and ion concentration). Once one of these conditions changes, aptamer performance can seriously be affected and aptasensing becomes impossible. Before applying aptasensors to analyse 'real' samples, significant sample matrix effects need to be evaluated [52]. Baldrich *et al.* (2004) tested the effects of several parameters on the binding efficiency of a thrombin aptamer. Labeling the aptamer for immobilization purposes was observed to seriously hamper the formation of a G-quadruplex structure which is required for thrombin binding. They did not find any effect of buffer pH on thrombin binding. Incubation temperature, on the other hand, had a marked effect with better binding obtained at lower temperatures [79]. Secondly, aptamer research suffers from the so called 'thrombin problem'. This problem refers to the fact that (too?) many investigators focus their attention on studying thrombin binding aptamers as a proof-of-concept. To date, more than 900 papers have been published on thrombin aptamers. Other, maybe more relevant, aptamers and aptamer applications remain in the shadow of the thrombin aptamer [78]. Finally, the initial spread of aptamers was hampered by patent laws. Aptamers were first patented by Gold and Tuerk in 1990. During a 10 year period from 1990 to 2000, the original patents were expanded into a broad patent portfolio that consisted of approximately 140 issued US patents. The SELEX patent portfolio is generally regarded as one of the most dominant and comprehensive portfolios of all biotech portfolios. This problem is solved since the base patents on aptamer (selection) recently expired [78].

Further efforts are needed to push aptamer technology to make it a preferred option in biosensing technology.

1.5 Aptasensor for the detection of estrogenic substances

17 β -estradiol (β E2 or shortly E2) is one of four naturally occurring estrogens – next to 17 α -estradiol, estrone and estriol - belonging to the class of steroid hormones [80]. These hormones are all derived from the same precursor, cholesterol (Figure 11a). They share a basic skeleton (cyclopentanoperhydrophenanthrene ring system) possessing four fused rings:

three cyclohexane (A, B and C) and one cyclopentane (D) ring [81]. In most of the steroids, CH₃ groups are present at positions C10 and C13 and an alkyl chain (or substituted alkyl chain) at position C17. Functional groups like OH, CHO, CO or COOH are often attached to one or more rings and/or are present in the alkyl chain [82].

E2 (C₁₈H₂₄O₂) (Figure 11b) refers to the 17 β -isomer of estradiol, only differing from 17 α -estradiol by the stereochemistry of C-atom 17. It is an aromatized steroid consisting of 18 C atoms with a MW of 272.38 Da and it possesses two OH groups, one at position C3 and one at C17. Like most steroidal compounds, E2 is hydrophobic and has a neutral net charge [82].

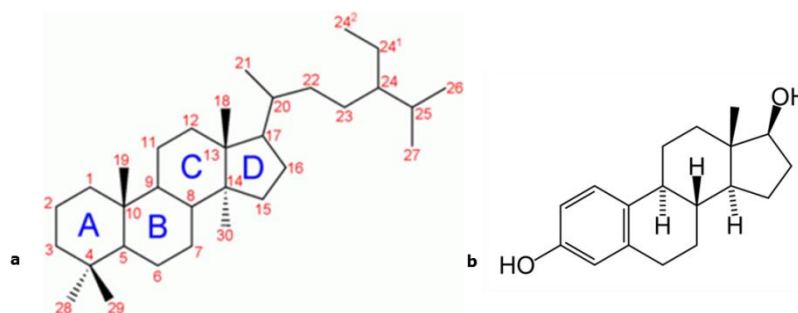


Figure 11: Chemical structure of (a) cholesterol and (b) E2.

E2 is the most potent type of endogenous estrogenic steroids. Circulating levels of this hormone in women vary strongly, with peak concentrations of more than 200 pg/ml. E2 is mainly produced by the ovaries and the placenta. At much lower concentrations, it is also produced by adipose tissue of men and postmenopausal women [82]. Cellular signaling of E2 is mediated through two estrogen receptors (ERs), ER α and ER β , both belonging to the nuclear receptor family of transcription factors [83]. Subsequent effects are very broad. E2 is well known for its growth promoting effects on diverse reproductive organs (e.g. mammary gland, uterus, ovary, testis and prostate). In addition, it has important beneficial effects on several non-reproductive tissues like bone, liver, cardiovascular organs and adipose tissue. E2 has a bone anabolic and calciotropic effect, it regulates the lipid profile by reducing low density

lipoproteins (LDL) and total cholesterol while increasing high density lipoproteins (HDL), it changes levels of blood clotting factors,... [82]

Several E2 analogues of natural or synthetic origin can mimic the normal function of E2, notwithstanding their (slightly) different chemical structures. These compounds can influence the hormonal system in different ways. Once bound to the ER, they can elicit a normal hormonal response, an abnormal hormonal response or no response at all because they block the receptor site and prevent natural hormones from binding. These mimickers can also bind to other receptors and elicit novel effects, interfere indirectly with normal hormonal actions or alter the production and/or breakdown of ERs or estrogens [80]. Many of these estrogen-mimicking compounds are of pharmaceutical or industrial origin. Examples are the semisynthetic estrogen 17 α -ethinylestradiol which is commonly used in birth control and hormonal replacement therapy and the synthetic estrogen diethylstilbestrol that can occur in meat and milk from animals that have consumed it as an additive in their food [84].

Via discharge of municipal waste water, industrial facility effluents, animal feeding operations, septic systems,... E2 and its analogues are released into the environment where they end up in natural water sources and waste water effluents [85, 86]. In domestic sewage effluents throughout Europe, Japan and the United States, detected concentrations range from < 1 to 48 ng/L for E2, from 1 to 76 ng/L for estrone and from 1 to 7 ng/L for 17 α -ethinylestradiol [87]. The ultimate fate and biological impact of these hormones is dependent on several physical (dilution, advection and dispersion), chemical (photolysis, sorption and volatilization) and biological (transformation and uptake) processes [85]. Sorption of E2 to sediments is substantial and acts as a major attenuation mechanism [85]. Attenuation by photolysis and volatilization is rather negligible. Photolysis is minimal since the absorption of light energy by E2 is weak in the visible spectrum [88]. Volatilization is limited due to its low vapor pressure [89]. Biotransformation of E2 to estrone has been observed to occur rapidly (< 1h) and prolongs the potential for downstream impacts. Complete degradation to CO₂ or CH₄ is not substantial [90].

Up till now, the potential risks of environmental E2 (analogues) are subject to considerable debate [91]. Different studies show that environmental estrogens in ng/L concentrations disrupt the endocrine system of fish and induce abnormalities of their reproductive tract [92, 93]. On the other hand, no 100% convincing evidence can be found about an impact of environmental estrogens on the human endocrine system. Some researchers postulate that chronic exposure of people to E2 causes drastic health effects like a decline in fertility [94]. Others state that a human health risk from exposure to low concentrations of environmental estrogens is an unproven and unlikely hypothesis [91]. However, grave concerns are warranted and in-field monitoring of environmental estrogenic substances is recommended.

In vitro bioassays can act as screening method to estimate total estrogenic activity in complex biological samples. Frequently applied are the transactivation assays which evaluate the ability of chemicals to stimulate the ER leading to the up-regulation of reporter gene expression. This expression level reflects the sum of all agonistic, antagonistic and cross-talk inducing molecules in the cell's environment [95]. A long test duration time of several days is one of the drawbacks of this technique. On the other hand, E2 and its analogues can uniquely be determined by means of gas or liquid chromatography coupled with mass spectrometry (GC-MS/LC-MS). However, because sample pre-treatment is required, analysis becomes laborious and time consuming. Moreover, special skills and instrumentation for analysis are required [96].

Nowadays, biosensors offer outstanding benefits for the detection of E2 and its analogues. Since molecular recognition forms the cornerstone of efficient sensing, the choice of the recognition element in a biosensor is crucial. It highly contributes to the final sensitivity and specificity of the sensing platform [97]. Human ERs, molecular imprinted polymers (MIPs) and antibodies are suggested to detect E2 (analogues). However, all these recognition elements have their drawbacks. ERs lack specificity and react in the same way to different E2 analogues [98]. MIPs also show high cross-reactivity [99] and moreover, chemical modification of these recognition elements for immobilization purposes is difficult [97]. Antibodies, on the other hand, suffer from functional limitations

including relative instability under harsh conditions and complex production and purification steps from animals or cell lines [100]. There is great need to establish a biosensor that incorporates receptor molecules which are able to overcome the aforementioned problems. In this context, aptamers have emerged as extremely promising recognition elements for the detection of both E2 and its analogues [101].

1.6 Aims of the study

E2 and its analogues are structurally related to each other. They often show the same cyclopentanoperhydrophenanthrene ring system possessing four fused rings, but they express a different combination of functional groups on that ring. This strong structural similarity makes identification and discrimination difficult. In this context, epitope specific aptamers can be very valuable, especially when they are integrated in a kind of cross-reactive array. Depending on which epitopes are present or absent in a certain analogue, the analogue will exhibit different binding responses towards the different aptamers. So each type of analogue will show its own characteristic binding pattern when analysed, making identification possible (Figure 12).

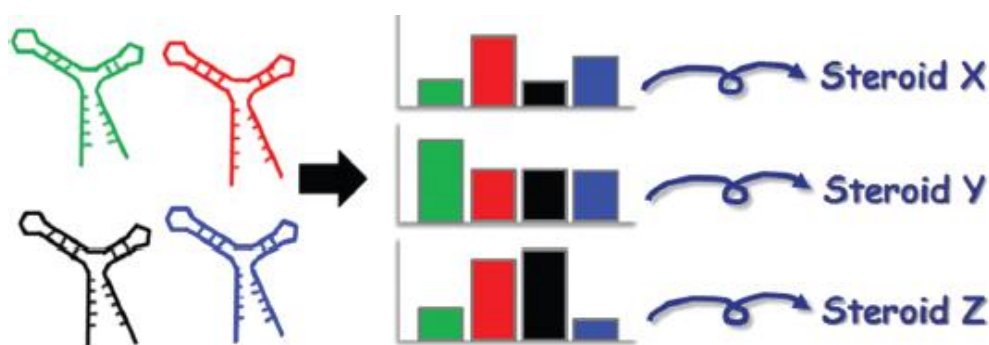


Figure 12: Visual display of target identification by means of a cross-reactive aptasensor. Various aptamers, all directed towards different epitopes of E2, are integrated in a cross-reactive sensor. Classification of individual analogues becomes possible since every analogue shows its own specific binding pattern towards the respective aptamers [38].

The ultimate goal of this dissertation is the development of a cross-reactive aptasensor suitable for the identification of E2 and its analogues present in environmental samples. Several aims, defining the outline of the different chapters of this thesis, will be addressed in order to systematically work towards this goal (Figure 13).

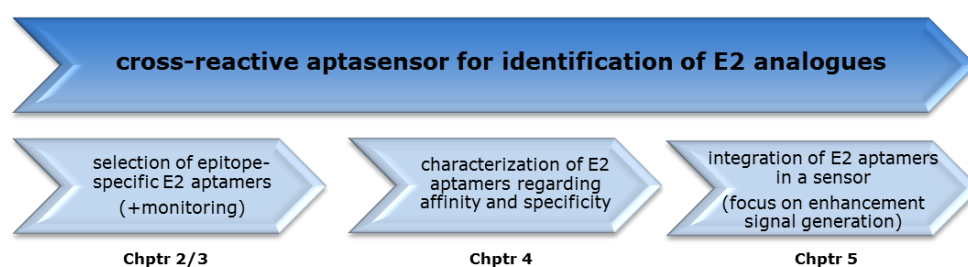


Figure 13: Schematic overview showing the relationship of the main goal, the three sub goals and the different chapters of this dissertation.

Aim 1: Selection of aptamers directed towards different epitopes of E2

At first, epitope specific aptamers need to be selected. General guidelines to set-up a SELEX process are described in literature. However, a standard SELEX process has to be optimized taking into account specific target characteristics and future application conditions. The intention to generate epitope specificity asks for some additional adjustments.

Aptamer optimization and selection often occur with limited control and knowledge on how the selection pool is evolving. This lack of transparency impedes the set-up and optimization of new SELEX procedures. Optimization steps are to a great extent documented trial and error. Only after various SELEX rounds, the selected oligonucleotide pool is sequenced and checked for enrichment. Monitoring selection progression, however, contributes to a successful SELEX since it allows early intervention and adjustment of selection conditions.

At first, SELEX optimization and implementation need to be established. This will be described in Chapter 2. During SELEX optimization, different components of the selection procedure will be tested. Topics regarding optimization that will be covered include design and amplification of the random library, transformation of dsDNA into ssDNA and the set-up of a SELEX design comprising both positive and counter selection steps. A balanced switching between positive and counter selection steps is essential to reach the desired epitope specificity. After optimization, two separate SELEX procedures will be applied. Both procedures will make use of E2 as a target during positive selection steps. In order to obtain epitope specificity, the difference will lie in the molecule applied during counter selection steps. For one SELEX, dexamethasone will be used as a counter molecule and for another SELEX, nortestosterone will be applied (Figure 14).

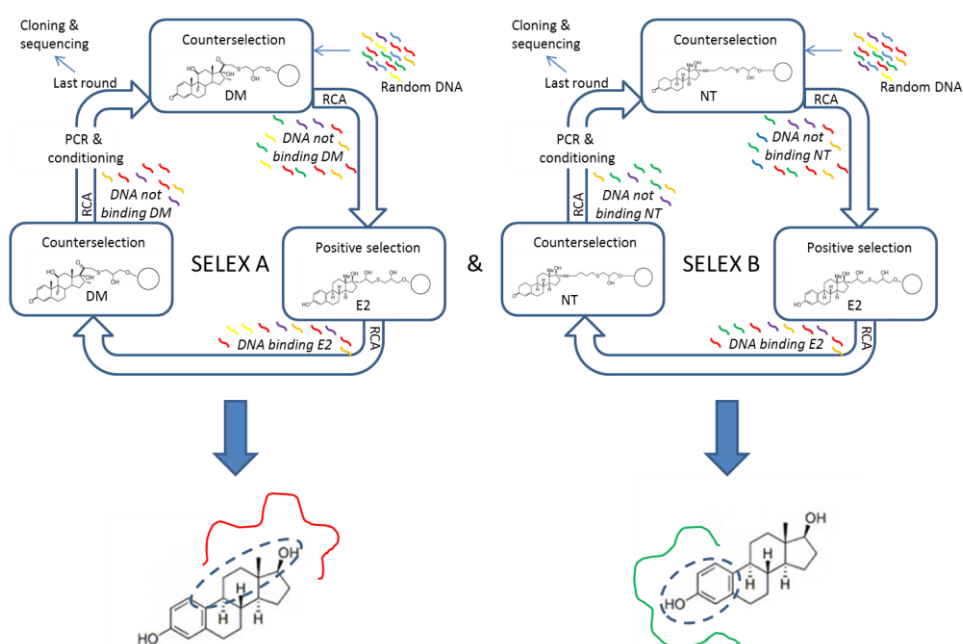


Figure 14: Schematic illustration of two independently performed SELEX procedures to generate epitope specific aptamers. Both SELEX procedures apply E2 as a target during positive selection steps. The difference lies in the used molecule during counter selection steps, which is dexamethasone for SELEX A and nortestosterone for SELEX B. This difference in used counter molecules is expected to generate epitope specific aptamers.

Secondly, a newly developed method - SELEX monitoring by remelting curve analysis (rMCA) - will be explored. Simulation experiments on libraries comprising different degrees of enrichment are planned. After simulation, the technique will be used to monitor several independent SELEX procedures, based on different designs (plate SELEX, bead SELEX and CE-SELEX) and different targets (C-reactive protein (CRP), E2 and peptide X). This topic is highlighted in Chapter 3.

Aim 2: Characterization of selected E2 aptamers regarding affinity and epitope specificity

Secondly, following aptamer selection, validation of the selected E2 aptamer candidates in terms of affinity and specificity is required. In-depth knowledge about aptamer characteristics is required for bringing aptamers from benchmark to final application. Several questions need to be answered.

- *Are the selected aptamers able to bind E2 free in solution?*
This is an important question to be answered since the aptamers are originally selected against E2 linked to sepharose beads. This way of selecting can negatively influence the binding capacity of aptamers for free, unmodified E2. We will start to test selected aptamer candidates via binding assays mimicking the selection design (binding of free aptamer to immobilized target), but in a next phase, we will switch to binding assays showing more resemblance to final applications (binding of free target to immobilized aptamer).
- *What is the affinity of the selected aptamers for E2?*
The most promising binding assay which is tested, will be used to characterize the E2-binding aptamers in terms of affinity. Therefore, the binding response of each aptamer towards a concentration range of E2 will be measured. The concentration leading to half the maximum response will be defined as the affinity constant K_D of the aptamer.
- *Is the intended epitope specificity of the selected aptamers achieved?*
Also to answer this question, the most promising binding assay tested earlier will be applied. The binding response of each aptamer towards

different E2 analogues will be examined. The binding pattern of an aptamer towards the different analogues will reveal its epitope specificity. Only E2 analogues expressing the epitope towards which the aptamer is directed, will be able to bind.

In Chapter 4, these questions will be addressed.

Aim 3: Integration of E2 aptamers as recognition element in a sensor set-up suitable for lab-on-chip screening

In order to integrate the selected E2 aptamers in a lab-on-chip sensor, different conditions have to be fulfilled. It requires a.o. others a compact and cost effective, array-type sensor set-up which accurately and reproducibly translates aptamer-target interaction in a clear and detectable signal.

During the final stage of this research, the focus is limited to the generation of a 'clear' signal. Due to the low MW of E2, signal generation after direct aptamer-target interaction as is described in Chapter 4 is restricted. This negatively affects the detection limit of the sensor set-up. Therefore, enhancement of signal generation by applying target induced strand displacement (TISD) will be explored in Chapter 5.

A TISD approach requires the formation of a hybrid complex between aptamer and (partially) complementary strand. Exposure of this complex to target induces disruption of the complex because of target-aptamer interaction. Measuring the break-down of the hybrid generates clear signals with the great advantage that these signals are independent of target characteristics such as MW or charge. Several read-out systems offer high potential to monitor this hybrid break-down and will in this context be tested. Also the influence of various parameters which characterize the complementary strand as part of the hybrid complex, such as length and number of mismatches, will be investigated.

2

Selection of epitope specific 17 β -estradiol aptamers

Partly based on:

Aptamers targeting different functional groups of 17 β -estradiol

Katrijn Vanschoenbeek, Jeroen Vanbrabant, Baharak Hosseinkhani, Veronique Vermeeren, Luc Michiels

J Steroid Biochem Mol Biol, 2014. 147c: p. 10-16

Part of paper: Performance of two independent SELEX procedures, sequencing and structure analysis of enriched libraries

Absent in paper: Optimization SELEX procedure

In this chapter, we will focus on the selection of E2-binding aptamers directed towards different functional groups on the cyclopentanoperhydrophenanthrene ring system of E2. During trial experiments, some aspects of the SELEX process were tested and optimized. Afterwards, two separate SELEX procedures were performed in order to select the desired aptamers. For both procedures, E2 was used as a target during positive selection steps. During counter selection steps, dexamethasone and nortestosterone were applied for SELEX A and B, respectively. The latter is important to direct aptamer selection towards different, predefined epitopes present on E2. In the future, these epitope specific E2-binding aptamers can be used to develop a cross-reactive array for in-field monitoring of E2 and analogues present in environmental samples.

2.1 Introduction

Multiple aptamers oriented towards E2 are described in literature [38, 102, 103]. Once integrated in a biosensing set-up, these aptamers proved their utility as sensitive receptor molecules with affinities in the low nM to intermediate μM range. However, no information is available about the epitopes towards which they are oriented, but it is known that they are highly specific for E2. Subsequently, these aptamers cannot be used to detect E2 analogues showing a comparable but (slightly) different chemical structure. In order to be able to detect E2 analogues, aptamers oriented towards specified epitopes of E2, instead of towards the entire E2 molecule, are more useful. These aptamers can be integrated in a cross-reactive array. Depending on which epitopes are present or absent in a certain analogue, the analogue will exhibit different binding responses towards the different aptamers of the sensor. So each type of analogue will show its own characteristic binding pattern in a cross-reactive array making identification possible.

In order to obtain aptamers to any particular epitope of a target, several methods can be applied, as described by Kulbachinskiy in 2007 [104]. One way of directed aptamer selection is via competitive elution and withdrawal of target-bound sequences by means of ligands which bind an identical target epitope. Aptamers binding other target epitopes are retained (Fig 15a). A second way is by introducing counter selection steps. Sequences interacting with the target but not with a structurally related molecule lacking the epitope of interest are selected (Figure 15b). A third approach comprises blended SELEX. A low-molecular-weight ligand with target affinity is joined to a random SELEX library. This leads sequences towards a specific site on the target and in this way results in aptamers showing affinity for a site near the binding site of the ligand (Figure 15c). A fourth method includes the use of only part of the target corresponding to the desired epitope during aptamer selection instead of the full target (Figure 15d). The efficiency of this approach can be improved by applying the whole target after several selection rounds against only part of it. Finally, selection of epitope specific aptamers for proteins can be obtained via the anti-idiotypic approach. In an initial step, antibodies are developed against a protein partner of the target protein. In a next step, these antibodies are used as target during SELEX and aptamers are selected. Because of complementarity of interaction sites of aptamers, antibodies, protein partner and protein target, the selected aptamers can bind the protein target (Figure 15e).

All aforementioned methods have their own advantages and drawbacks, mainly depending on the identity of the target of interest. For a small molecule like E2, the first and second method for epitope specific aptamer selection are the most feasible approaches. We decided to make use of the second approach, switching between positive and counter selection steps, to select epitope specific E2-binding aptamers. However, one has to keep in mind that it is not always possible to target the desired epitope owing to the dominance of certain epitopes [104].

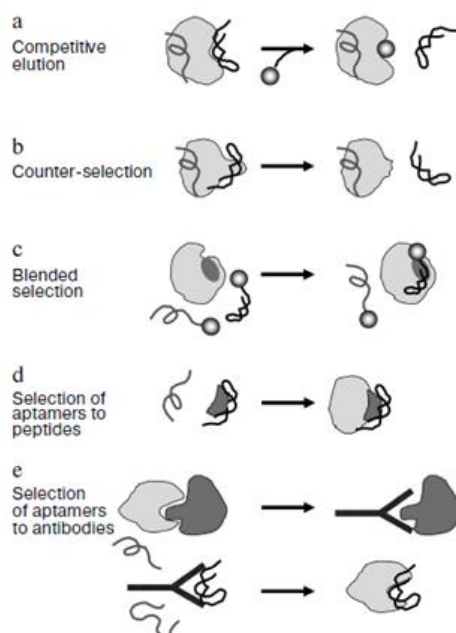


Figure 15: Methods of epitope specific aptamer selection. (a) Competitive elution of aptamers using ligands binding the same target epitope; (b) Counter selection steps to withdraw aptamers which bind target related molecules lacking the epitope of interest; (c) Blended SELEX. Sequences used during selection are blended with a ligand having affinity for the target; (d) Aptamer selection using only part of the target corresponding to the desired epitope and (e) Anti-idiotypic approach. After generation of antibodies specific for a protein partner, aptamers directed towards these antibodies are selected. These aptamers also recognize the protein target [104].

Besides a balanced SELEX design, comprising both positive and counter selection steps, we have to consider several other factors when setting up a SELEX procedure for the selection of epitope specific E2-binding aptamers. The success of the procedure relies on seemingly minor experimental factors [10].

The starting library is one of the critical factors of successful aptamer selection. Both the randomness and length of the inner region and the composition and length of the fixed primer binding regions are crucial. Once selected, a significant number of aptamers are truncated down to a minimal functional sequence. Aptamer truncation often occurs by using a trial-and-error process, but also rational truncation approaches guided by aptamer structure prediction and docking algorithms are possible [105, 106]. This suggests that a short

aptamer library with only few (<20) nt in the inner region is sufficient for aptamer selection. Besides, an advantage of short libraries is their cost-effectiveness in chemical synthesis [107]. On the other hand, increasing the length of the inner region augments the structural variation of the SELEX library, potentially increasing the likelihood of selecting the strange aptamers with desired properties out of an extensive oligonucleotide pool. However, chemical synthesis and downstream applications impede the use of libraries with random regions longer than 80 nt [108, 109]. Primer binding regions can hamper the amplification process of the SELEX library and lead to the generation of by-products via the formation of stable secondary structures through self-association (homodimerization), association with the opposing primer binding region (heterodimerization) and/or association with complementary nt within the random core region. Each of these structures can occur within one aptamer or between complementary regions of different aptamers of the library [110]. Homo- and heterodimerization can be avoided via efficient design of the primer binding regions and associated primers. Association with complementary nt within the random region is outside the researcher's control. Efforts have been made to come up with primer-free [111] and minimal-primer [112] selection protocols. Based on a bioinformatics study of 2000 aptamers directed towards 141 different targets in the aptamer database, it is clear that most fixed primer binding regions do not significantly contribute to the ultimate aptamer structure formation in their final application [113]. A second reason why the fixed primer binding regions are a cause of concern is the risk of cross-contamination between different SELEX procedures if they make use of libraries with identical primer binding regions [114]. As a preventive measure, switching between libraries with different constant regions for each selection is recommended [108].

The way target is employed, immobilized on a surface or free in solution, is a second key factor for successful aptamer selection. The main advantage of employing target free in solution is that all potential epitopes stay available for aptamer binding. However, from a practical point of view, immobilization of target offers a lot of advantages, such as easy and gentle elution and minimal requirement for specialized equipment. Moreover, the problem of epitope loss

can be circumvented by making use of oriented immobilization and inclusion of a linker in between target and immobilization matrix. Beads covalently modified with different kinds of steroid hormones, leaving all important functional groups free, are commercially available. However, library then gets exposed to chemically modified target instead of to the desired unmodified target. Moreover, it increases the likelihood of selecting sequences that display binding properties towards the matrix and/or the linker arm [97]. Despite negative and/or counter selection steps, carry-over of these sequences is difficult to avoid [115]. Consequently, selected aptamers have to be tested to check if they are capable of binding unmodified target present in its native state [97]. Any affinity derived from partial binding to the matrix or from chemical modification can hamper the functionality of the aptamers in the intended applications. For example, a published rhodamine aptamer displays a weaker binding to the target rhodamine when it is free in solution compared to when it is immobilized onto the surface which was used for its selection [116].

The binding conditions, including the applied binding buffer, incubation time and elution, are a third important factor for aptamer performance. The binding buffer should be as similar as possible to the ultimate environment of the target of interest. Moreover, inclusion of monovalent cations in the buffer reduces the risk of non-specific binding and for some targets, divalent cations are necessary to make the aptamer binding specific [117]. Incubation times ideally are long during initial selection rounds and then gradually decrease when the SELEX procedure continues [11, 117]. Methods for aptamer elution are numerous. Denaturing methods like heat treatment [118] and addition of chaotropic substances such as urea, sodium dodecyl sulfate (SDS) or ethylenediaminetetraacetic acid (EDTA) [30] belong to the possibilities. Other approaches are affinity elution using target [119] or elution with competitive binders [120].

The fourth and last factor which is important for an efficient SELEX procedure is the amplification process. Random ssDNA library is different from homogenous DNA in the behavior of PCR amplification. When target random dsDNA accumulates to a certain level, it rapidly converts to by-products [121]. In general, product formation of random library reaches its maximum after 20

cycles (20 to 50 nM) and then by-products start to appear. After 25 cycles, the desired product is completely converted to by-products even though free primers are still available in excess [122]. Shorter or longer sequences which are defined as by-products result from the presence of secondary structures that disturb polymerization reactions because of polymerase jumping or from product-product, primer-product or primer-primer annealing [123]. This phenomenon is characteristic for random DNA and is more pronounced if library length is increased and primer design is not optimized [122]. It can severely affect the selection process and eventually hamper aptamer selection [121]. A number of strategies are suggested to alleviate this problem such as amplification of individual aptamers in separate droplets via emulsion PCR (so that heterodimerization is avoided) or removal of undesired product after gel electrophoresis (GE) [124]. For the ultimate transformation of dsDNA into ssDNA different methods are available. Linear PCR and enzymatic digestion are routinely run after symmetric PCR [123]. Another approach makes use of the SA/biotin system and uses the arising size difference in GE to separate the two strands or lets one of the two strands bind to a SA surface via a biotin label and subsequently separates the strands after denaturation [125].

In the following sections, some optimization steps of the SELEX process are described, as well as the results of two optimized SELEX procedures for the selection of epitope specific E2-binding aptamers.

2.2 Materials and Methods

2.2.1 Materials

DNA was purchased from Integrated DNA Technologies (IDT, Leuven, Belgium). E2 Sepharose® 6B affinity chromatography beads, Dexamethasone Sepharose® 6B Novel Immobilized Steroid Beads and Nortestosterone Sepharose® 6B Novel Immobilized Steroid Beads were supplied by Polysciences Inc. (Eppelheim, Germany). Blocking solutions bovine serum albumin (BSA) and marvel, phenol,

chloroform, isoamylalcohol and sephadex® G-100 were obtained from Sigma Aldrich (Diegem, Belgium). Synthetic blocker NB3025 was purchased from NOF corporation (Tokyo, Japan). Sonicated salmon sperm ssDNA, TOPO® TA Cloning® Kit (including TOP 10 chemically competent *E. Coli* cells and pCR®2.1-TOPO vector system), Lennox L agar, ABI Prism® BigDye® Terminator v3.1 Cycle Sequencing Kit and an ABI PRISM® 310 Genetic Analyzer were received from Life Technologies (Carlsbad, US). 10x PCR buffer, Taq DNA polymerase and dNTPs were supplied by Roche (Merelbeke, Belgium). λ -exonuclease enzyme was bought from New England Biolabs (Frankfurt, Germany). Perfect match PCR enhancer was supplied by Agilent Technologies (Diegem, Belgium). All buffers were homemade.

2.2.2 DNA library construction, amplification and conditioning

Two analogue libraries (SELEX A and SELEX B), each consisting of 10^{15} molecules of ssDNA, were bought. These libraries were comprised of a central random region of 40 nt (40N) flanked on either side by a 20-nucleotide-long primer binding region necessary for amplification and cloning purposes. The composition of the primer binding regions was optimized in order to prevent homo- and heterodimerization and hairpin formation as well as to obtain similar primer melting temperatures (T_m). These characteristics were checked by means of Oligo v.7 Primer Analysis Software [126]. For both libraries, a specific primer set was available. During SELEX, a 5' phosphorylated reverse primer (RP) and unlabeled forward primer (FP) were applied. For cloning purposes, both FP and RP were unlabeled (Table 2).

Table 2: ssDNA libraries and primer sets applied during SELEX A and B.

SELEX A	5'-AGCAGCACAGAGGTCAGTTC-40N-CCTATGCGTGCTACCGTGAA-3'	
	FP:5'-AGCAGCACAGAGGTCAGTTC-3'	RP:5'-TTCACGGTAGCACGCATAGG-3'
SELEX B	5'-TGTGTGTGAGACTTCGTTCC-40N-CAGCAAGGCATCAGAGGTAT-3'	
	FP:5'-TGTGTGTGAGACTTCGTTCC-3'	RP: 5'-ATACCTCTGATGCCTTGCTG-3'

PCR conditions were optimized as 50 μ l reaction mixes containing 1x PCR buffer, 2.5 mM extra Mg^{2+} , 0.2 μ M of each primer, 0.5 units of Taq DNA polymerase and DNA template. A three-step PCR procedure of 20 cycles with an annealing temperature of 60°C (SELEX A) or 54°C (SELEX B) was performed.

Two methods were tested to avoid by-product formation after consecutive PCR amplifications during SELEX. The first method comprised addition of an additive, 'perfect match PCR enhancer'. This enhancer destabilizes many mismatched primer-template complexes that would otherwise lead to the generation of by-products. Per 100 ng of DNA template one unit of this additive was added to the PCR mix. The PCR procedure was conducted as described above. The second method comprised size separation on a high percentage agarose gel. The PCR product was loaded on a 4% agarose gel, together with a size ladder. After running the gel, the band of the desired length was cut out of the gel and immersed in crush and soak buffer (500 mM NH_4OAC , 0.1 % SDS and 0.1 mM EDTA pH 8). Overnight incubation at 4° C was followed by two centrifugation steps at high speed and collection and purification of the supernatant containing DNA of the desired length.

Additionally, two methods for transforming dsDNA into ssDNA were tested. The first method comprised an extra asymmetric amplification with 100x excess of FITC-labeled FP after conventional amplification. The yield of this asymmetric PCR was tested by performing fragment analysis using an ABI PRISM 310 and GeneScan Analysis Software. The second method encompassed digestion of the anti-sense by λ -exonuclease digestion according the instructions provided by the manufacturer. Therefore, an unlabeled FP was combined with a 5' phosphate labeled RP. The result of this technique was checked via a non-denaturing polyacrylamide gel.

2.2.3 Target

Commercially available E2 Sepharose® 6B affinity chromatography beads were used for positive selection in both SELEX A and B. Dexamethasone Sepharose®

6B Novel Immobilized Steroid Beads and Nortestosterone Sepharose® 6B Novel Immobilized Steroid Beads were used for counter selection in SELEX A and B, respectively (Figure 16). All beads were blocked using a blocking solution containing 1% BSA, 1% marvel, 4% synthetic blocker NB3025 and an excess of sonicated salmon sperm ssDNA. Blocking was necessary to reduce the risk of losing specific E2 binders by non-specific DNA adsorption during counter selection steps and of selecting non-specific binders during positive selection steps.

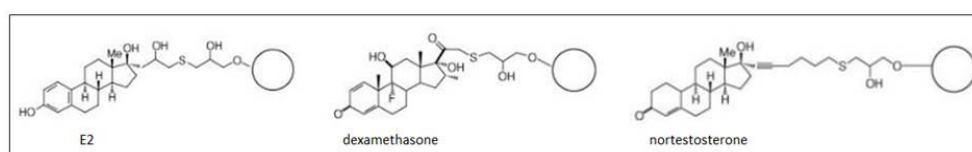


Figure 16: Sepharose® 6B affinity chromatography beads used for positive selections (functionalized with E2) and counter selections (functionalized with dexamethasone for SELEX A and with nortestosterone for SELEX B) used in two independent SELEX procedures.

2.2.4 Selection design

Optimization of the SELEX procedure was previously described by Vanbrabant *et al.* (2014) [127]. The focus was mainly put on the number of counter selection steps within the selection cycles as well as on the timing of amplification.

Each selection cycle of the optimized SELEX process consisted of a counter selection step, a positive selection step and another counter selection step prior to PCR amplification and conditioning. The first selection cycle is an exception to this rule and consisted of 4 counter selection steps, one positive selection step and 1 counter selection step. SELEX A and B were performed independent from each other.

For each positive selection step, a homogeneous suspension of target-linked and blocked beads was washed 3 times with 1x Phosphate Buffered Saline (PBS). The oligonucleotide pool was dissolved in binding buffer [10mM HEPES, pH 7.4 (SELEX A) or 1x PBS with 10% ethanol, pH 7.4 (SELEX B)], denatured at 90°C

for 5 min and cooled at ice for 5 min. Thereafter, the oligonucleotide pool was added to the target-linked beads and incubated at room temperature (RT) for 1 hour with rotation. The unbound oligonucleotides were removed by 5 washing steps using washing buffer [1x Tris Buffered Saline (TBS)]. The bound oligonucleotides were eluted from the target by incubating the target-DNA complex in elution buffer [Tris-EDTA (TE) buffer + 3M urea, pH 8] at 80°C for 5 min. Finally, the eluted oligonucleotides were purified by means of phenol-chloroform extraction (Phenol:Chloroform:Isoamylalcohol 25:24:1) and gel filtration (Sephadex[®] G-100) before using them for the next selection step.

For each counter selection step, countermolecule-linked and blocked beads were exposed to the oligonucleotide pool as described for positive selection steps. However, after the incubation period unbound oligonucleotides were collected and purified before further use.

The conditioning steps following PCR amplification included the removal of PCR by-products on agarose gel and the transformation of dsDNA into ssDNA via enzymatic digestion. After conditioning, the oligonucleotide pool was ready to start a new selection cycle.

During SELEX, the gradually arising enrichment was monitored by means of rMCA (see Chapter 3).

2.2.5 Cloning and sequence/structure analysis of selected 17 β -estradiol aptamers

The enriched oligonucleotide pools containing the collected dsDNA products of the 5th (SELEX A) and 10th (SELEX B) selection cycle were transformed into a pCR[®]2.1-TOPO vector system and cloned by means of a TOPO[®] TA Cloning[®] Kit for subcloning with TOP 10 chemically competent *E. Coli* cells in order to obtain individual aptamer clones from the selected pool [128]. *E. Coli* cells were grown overnight on Lennox L agar plates. DNA isolation and amplification of individual clones was followed by highly specific amplification and sequencing

using the ABI Prism® BigDye® Terminator v3.1 Cycle Sequencing Kit on an ABI PRISM® 310 Genetic Analyzer.

Secondary structure analysis of aptamers was performed by free energy minimization algorithms according to Zuker using Mfold software [42]. Predictions of G-quadruplex formations were done by means of the internet tool QGRS Mapper [43].

2.3 Results

2.3.1 DNA library construction, amplification and conditioning

Oligo v.7 analysis of both optimized primersets applied during SELEX A and B showed overall homodimer formation for all four primers, whereas only the FP of SELEX A potentially forms 3' homodimers. Both primersets have also the potential to form overall heterodimers, but 3' heterodimerization is absent. There is no risk of hairpin formation. Moreover, for each primer set, FP and RP have an identical calculated T_m (Table 3).

Table 3: Homo- and heterodimerization, hairpin formation and T_m of optimized primersets of SELEX A and B*.

		Most stable 3'homodimer (ΔG in kcal/mol)	Most stable homodimer overall (ΔG in kcal/mol)	Most stable 3'heterodimer (ΔG in kcal/mol)	Most stable heterodimer overall (ΔG in kcal/mol)	Hairpin	T_m ($^{\circ}C$)
SELEX A	FP	-0.3	-3.5	/	-0.7	/	62
	RP	/	-2.1	/	-0.7	/	62
SELEX B	FP	/	-0.8	/	-1.3	/	60
	RP	/	-1.5	/	-1.3	/	60

*Information about homo- and heterodimerization, hairpin formation and T_m of primersets applied during SELEX was obtained by Oligo v.7 Primer Analysis Software [126]. Absence of dimerization or hairpin formation is indicated by a slash. T_m was calculated according to the $[2(A + T)^{\circ} + 4(G + C)^{\circ}]$ method.

Pilot experiments performed prior to SELEX A and B revealed the importance of efficient amplification and conditioning of a random library. Agarose GE of amplified library showed the formation of by-products (dimerization; oligomerization) when increasing the number of PCR cycles (Figure 17).

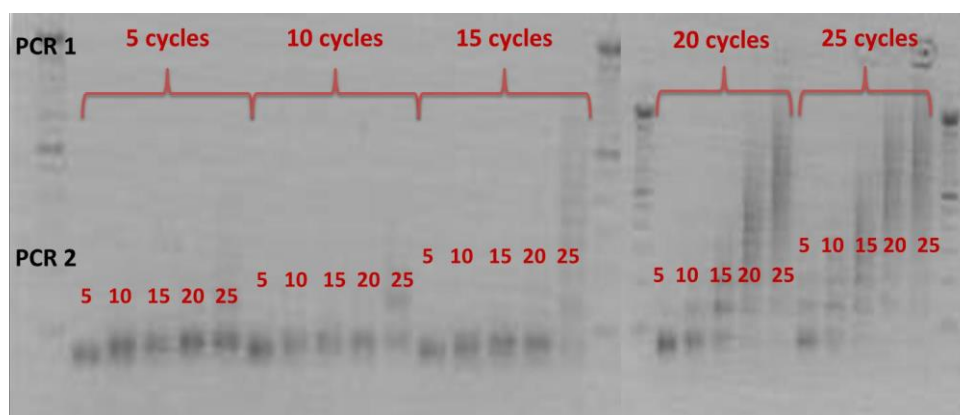


Figure 17: Analysis of the impact of PCR cycle number on the formation of by-products by means of agarose GE. In a first step, random ssDNA library was amplified 5, 10, 15, 20 or 25 cycles (indicated above). Consecutively, the amplified DNA library was Sephadex® purified, again amplified 5, 10, 15, 20 or 25 cycles and loaded on a 2% gel (indicated below). Dimerization and oligomerization are visible when the total number of PCR cycles increases.

This by-product formation became problematic when starting initial SELEX trials since already after a few (two to three) selection cycles by-product formation prevented continuation of the selection process (data not shown).

An initial attempt to solve the problem of by-product formation comprised addition of 'perfect match PCR enhancer' to the PCR mix. This enhancer claims to increase the specificity and yield of PCR amplification products. However, by-product formation still appeared after increasing the PCR cycle number (data not shown). A second attempt involved size separation of DNA on a 4% agarose gel. This method solved the problem of by-product formation and was therefore included in the ultimate SELEX design.

Both techniques tested to transform dsDNA into ssDNA - the asymmetric PCR and enzymatic digestion via λ exonuclease - turned out to be successful. For the asymmetric PCR, the number of cycles appeared to be important to improve the product / free primer ratio. After 10 cycles with FP in excess, a lot of primer was still present in the reaction mix. When increasing the number of cycles, free primer was decreasing gradually and most of the mixture was made out of ssDNA of the desired length. Up till 30 cycles, no by-product formation was visible (Figure 18). For enzymatic digestion of the anti-sense DNA strands, different incubation times of the λ -enzyme with the PCR product were tested, ranging from 30 min to 2 h. On the non-denaturing polyacrylamide gel it was seen that already after 30 min all dsDNA was transformed into ssDNA. Increasing the incubation time, did not alter this result (data not shown).

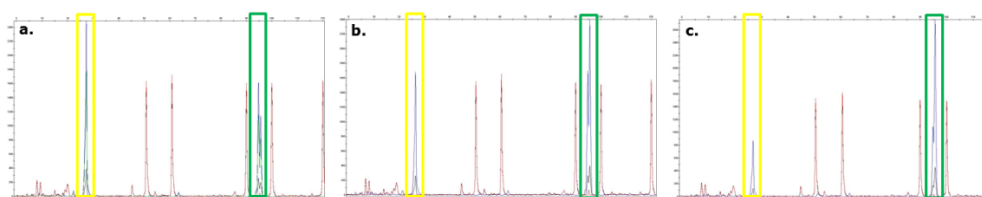


Figure 18: Genescan view: raw data for asymmetric PCR product after (a) 10, (b) 20 and (c) 30 amplification cycles with a 100x excess of FITC-labeled FP following conventional amplification. Free primer is indicated via a yellow box, PCR product with a green box. Other peaks originate from the internal size standard added to each sample. On the X-axis, the length of the DNA is depicted. On the Y-axis, the fluorescence signal is depicted.

2.3.2 Sequence/structure analysis of selected 17 β -estradiol aptamers

Following SELEX A, 19 clones were sequenced after 5 selection cycles. All clones showed a unique sequence, whereas 9 of them expressed a similar motif of 8 nt (CTCTGCAT). Following SELEX B, 24 clones were sequenced after 10 selection cycles. Results revealed a strong enrichment of 2 G-rich sequences in 18 and 5 clones, respectively. The remaining clone Apta 24B had the same nucleotide

composition as clones Apta 19B to Apta 23B except for a C to T transition at position 22 (Table 4).

Table 4: Sequences, ΔG values and G-scores of selected E2 aptamers*.

Clone ID (SELEX A)	Initially random sequence 5' → 3'	ΔG (kcal/mol)
Apta 1A	TCTGTATAGGTCATTCTATCGGCGATTCTCGAATAAATGT	-8,2
Apta 2A	CTCTGCAT TCGTGGCTGACTATCTTTGGGAATATCAAGCC	-8,3
Apta 3A	GTTGTATTTTGGTGCATTTCAATGTTTTGTTATATGGTGT	-4,7
Apta 4A	CTGATATATTTATTGTAGTGCTATATTTGCTACATGTGTT	-3,7
Apta 5A	GTCCATTATTCTGGTAGCGTTGAACAACATTCAACACGCC	-10
Apta 6A	GTCGAATCAGCAC CTCTGCAT AGGTTACGTTTATACTGCG	-9,9
Apta 7A	TCCTT ACTCTGCAT AGGATGCATACCCTGTCTTGCTAATG	-7,4
Apta 8A	AGCGTC CTCTGCAT AGTGATTACGCTATGTGTACAGTGC	-9,5
Apta 9A	CATGA CTCTGCAT AGGCTAATGAAACTAGTTCTTATTTA	-11
Apta 10A	CAGACTATACCCTCCACCGCTCCGATAAATAGGTGTTGGC	-6,4
Apta 11A	CAAGTCGTACGACACAGGGTAATCCTGTTTGGTAAAACGA	-9,9
Apta 12A	GGGACGTTCCGAACTGTAAT TCTGCAT AAGGTCTTTTCGAT	-5,9
Apta 13A	TTATGTCGAACTAAATTTGGCCTGACCAAGCCGAATTTGA	-11
Apta 14A	CTCTAATATTCAGTTAATATTGTGTTGCCAGGCCATT	-9,1
Apta 15A	GTAAGGACTGGTGCACATGGATGTAATAATAGTGCAGCGA	-9,8
Apta 16A	TGTTGTAAGTGGTCCAACGATTTATATGAGTTATGGGCCA	-5,5
Apta 17A	TCTACTCTATACCCCACTTTCTTACTTCAAC CTCTGCAT T	-5,7
Apta 18A	TCCGGCCCCGTATTTACTTTAATTATGTAC CTCTGCAT TA	-6,0
Apta 19A	ATTATCACCATGGAGTCGATTTGAAATC CTCTGCAT ATTA	-7,2
Clone ID (SELEX B)	Initially random sequence 5' → 3'	G-score
Apta 1 → 18B	GGCGAT GG GGTAGGG GG TGTGGAG GG GCCGGAC GG AGGGG	21
	(<i>TGTGTGTGAGACTTCGTTCCGGCGATGGGGTAGGGGTGTGGAGGGGC</i> CGGACGGAG GGGG CAGCAA GG CATCAGAG GG TAT)	(14)
Apta 19B → 23B	CCCGGTCGGTG GGG TAGG GGG CGTGGAGTCACC GGGGGGG	31
Apta 24B	CCCGGTCGGTG GGG TAGG GGG TGTGGAGTCACC GGGGGGG	31

* Sequences of clones obtained after 5 (SELEX A) and 10 (SELEX B) selection cycles. Fixed primer binding regions are omitted. SELEX A: A common motif is highlighted. ΔG values (kcal/mol) of predicted secondary structures were determined using Mfold. SELEX B: Nt involved in G-quadruplex formation are highlighted. G-scores, denoting the likelihood to form a stable G-quadruplex, were predicted by QGRS mapper. For Apta 1B, two potential G-quadruplexes were predicted. One of them includes a fixed primer binding region. Therefore, fixed primer binding regions for this sequences were indicated in Italic.

Secondary structures of the 19 selected sequences of SELEX A and their free energies were predicted using Mfold software. In 68% of all sequences, results revealed the presence of a three-way junction structure consisting of three double helical arms linked via a common cross-point. An example of a predicted secondary structure containing a three-way junction is given in Figure 19. An

overview of all predicted secondary structures can be found in the appendix (Appendix Figure 1). Predicted ΔG 's of the 19 aptamers varied from -10.8 to -3.7 kcal/mol (Table 4).

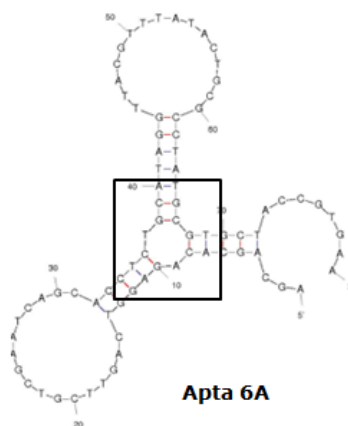


Figure 19: An illustration of a secondary structure containing a three-way junction as predicted by Mfold. The three-way junction is highlighted by a squared box.

QGRS mapper was used to predict the formation of G-quadruplexes by the G-rich aptamers of SELEX B. Two possible 4-plane G-quadruplexes were predicted for Apta 1B and 1 potential 4-plane G-quadruplex for Apta 19B and Apta 24B (Table 4). The suggested G-quadruplexes for Apta 19B and Apta 24B were composed of 3 G-repeats forming the G-tetrad planes, whereas the G-quadruplexes of Apta 1B were only composed of 2 G-repeats. This caused the potential quadruplexes of Apta 19B and Apta 24B to be more stable than those of Apta 1B, which is reflected in their higher G-scores.

Apta 5A, 6A, 8A, 9A, 11A, 13A, 1B and 19B were chosen for further characterization (see Chapter 4).

2.4 Discussion

In order to select aptamers which target different functional groups of E2, two independent SELEX procedures were performed using E2 as target molecule during positive selection steps and dexamethasone or nortestosterone during counter selection steps. E2 and dexamethasone exhibit several differences in functional groups on their cyclopentanoperhydrophenanthrene ring system. In contrast, the only structural difference between E2 and nortestosterone is the A ring of their cyclopentanoperhydrophenanthrene ring system. E2 contains an aromatized A ring with a hydroxyl group whereas nortestosterone shows a ketone group on its A ring [129]. Therefore, the selected aptamers in both procedures were foreseen to target different functional groups of E2. Aptamers are mainly targeting functional groups that are expressed on the molecule applied during positive selection steps which are not present on the molecule used during counter selection steps [130].

2.4.1 DNA library construction, amplification and conditioning

As mentioned earlier, both RNA and ssDNA libraries can be used as starting material for a SELEX procedure. Most studies show that DNA and RNA aptamers do not differ in affinity and specificity [104]. Because of the higher stability of DNA aptamers in a broad range of applications and the ease of handling [11, 128], we chose to make use of ssDNA libraries for this research.

Amplification of a random DNA library is crucial during SELEX, but also very tricky, often resulting in the formation of by-products [122]. Several factors had to be taken into account in order to prevent the generation of unwanted PCR products. Like for the amplification of all kinds of DNA, PCR conditions such as template amount, primer concentration, PCR protocol and cycle number had to be optimized. Additionally, the design of the random library was essential [10, 25]. For SELEX procedures A and B, two analogue libraries were constructed. On the one hand, both were comparable in length, having an inner random region

of 40 nt. An intermediate inner region length was chosen because that offered sufficient structural complexity, but was still manageable when handling. On the other hand, both libraries contained different fixed primer binding regions. This was important to avoid cross-contamination between the two SELEX procedures [114]. In previously performed SELEX trials, cross-contamination was an issue of great concern since DNA sequences selected in one SELEX emerged excessively in other SELEX procedures even though they could not have been selected in these procedures. Primer design constraints which we considered were the primer length, the primer length difference, the primer composition, the T_m and the T_m difference [131]. Furthermore, secondary structures such as dimers and hairpins were also taken into account [132]. We chose for a primer length of 20 nt for all four primers, which is the average recommended primer length for optimal amplification [131]. The GC content of the four primers was between 45 and 50% and per primer set, both FP and RP showed similar T_m 's. Also this is considered as ideal for DNA amplification [133]. Homo- and heterodimerization were kept to a minimum. The most stable dimers of all four primers showed a Gibbs free energy > -6 kcal/mol, which means that their stability is too low to disturb the amplification process. A 3' homodimer, posing a higher risk of amplification errors when compared to overall homo- and heterodimers, could only be formed by one primer. However, this homodimer showed a stability of only -0.3 kcal/mol which is above the recommended threshold and should therefore not cause any amplification problems. Based on the predictions, no hairpin formation was expected since the primers did not contain regions of internal complementary sequences [134].

However, even under optimal amplification conditions and after careful design of the random library, there is a high risk of by-product formation. The problem of by-product formation was successfully solved by GE and isolation of PCR-product with the desired length. Even after ten consecutive SELEX rounds, no by-products appeared anymore.

Since both techniques which were tested to transform dsDNA into ssDNA were successful, we chose for the least laborious and fastest method, the enzymatic digestion. Moreover, according to literature, asymmetric PCR products still comprise a lot of dsDNA. These dsDNA products have to be separated from the

ssDNA by a non-denaturing polyacrylamide gel and the ssDNA has to be eluted from the gel. Purification of small fragments from polyacrylamide gels is time-consuming and results in poor yields. The latter is not desirable during the first SELEX cycles because of the potential loss of target binding aptamers. The issue of dsDNA still present in the sample, is not existing when applying enzymatic digestion. Purification of the sample to remove the enzyme is needed after exonuclease digestion. This purification step is associated with a loss of ssDNA, but this loss is significantly lower than when performing asymmetric PCR [35].

2.4.2 Optimized selection design

For the selection of epitope specific E2-binding aptamers, switching between positive and counter selection steps was crucial. By means of counter selection steps, sequences which showed affinity for undesired epitopes of E2 or for the immobilization matrix and/or linker could get discarded [11]. In a crowded pool of oligonucleotides used to start SELEX, only few sequences were of interest. In order to remove all other sequences as fast as possible, the selection cycles of our optimized selection design existed of twice as much counter selection steps as positive selection steps. Moreover, in order to pre-filter the SELEX library, the first selection cycle consisted of additional counter selection steps. Additionally, the timing of PCR was a crucial aspect of the SELEX design. PCR amplification only took place after multiple selection steps, in order not to amplify unwanted sequences.

2.4.3 Sequence/structure analysis of selected 17 β -estradiol aptamers

Both SELEX procedures successfully resulted in the enrichment of originally random DNA pools (Table 4). All clones obtained by SELEX A displayed a unique sequence, but a common motif was detected in 47% of the clones. Formation of this motif is a clear indication of transition of a random library into an enriched library. However, also aptamers without this motif showed good binding affinity

for E2. Probably, this motif may only contribute to the formation of specific secondary structures. Several aptamers with and without this motif converged to three-way junction structures. Since random DNA oligonucleotides are able to form all kinds of secondary structures without preference for a specific structure, the increased presence of this three-way junction structure further supports the success of the SELEX selection. A three-way junction structure for DNA aptamers was previously described by Kato *et al.* (2000) [4]. The authors selected several cholic acid-binding aptamers which could all fold into three-way junction structures. In these structures, cholic acid was suggested to interact with a hydrophobic cavity formed by three stems linked to a common cross-point [4]. Later, Yang *et al.* (2011) [38] used a structurally biased DNA library to generate a series of four three-way junction aptamers that bind with varying affinity and selectivity to several steroids. In contrast with SELEX A, SELEX B resulted in the clear enrichment of two sequences. Both sequences tended to fold into G-quadruplexes, without the explicit need of their fixed primer binding regions [43]. G-quadruplex structures couple a common scaffold to varying loop motifs. The scaffold is supposed to form the architectural basis of the aptamer, whereas the nt in the loop motifs are important for target recognition [104, 135]. These structures are not only biologically relevant since they frequently occur in eukaryotic genomes [136], also a significant proportion of aptamers described in literature display this type of architecture [137-139]. For SELEX B, the aptamers were selected in 1x PBS with 10% ethanol containing K^+ and Na^+ ions. K^+ and Na^+ are known to thermodynamically and kinetically stabilize G-quadruplexes by fixing themselves into the assembled quadruplex structure [140]. The formation of these structures can thus be assumed for aptamers obtained by SELEX B. In SELEX A, on the other hand, a K^+ and Na^+ free HEPES buffer was used. Stabilization of potential G-quadruplexes could not occur here, resulting in the absence of this kind of structures for aptamers of SELEX A. Besides, the difference in library design between the two SELEX procedures could have an important impact on the final structures of the selected aptamers.

As expected, stronger enrichment appeared after SELEX B in comparison with SELEX A. Since E2 and dexamethasone are structurally different, aptamers obtained by SELEX A cannot be directed against one particular epitope. This

caused a heterogeneous population of DNA strands to bind to E2. On the other hand, E2 and nortestosterone are structurally more similar. Hence, this caused SELEX B to be a more stringent selection procedure than SELEX A. Aptamers obtained by SELEX B can be directed against one particular functional group of E2. This way, few different DNA strands were able to bind. However, selecting these few different strands in SELEX B required more cycles than selecting a heterogeneous pool of aptamers in SELEX A. The heterogeneity in functionally active aptamers also clearly illustrates that molecular recognition of E2 can be achieved by different kinds of ssDNA sequences.

2.5 Conclusion and future perspectives

The aim of this chapter was twofold. First of all, we aimed to optimize the SELEX process for the selection of E2-binding aptamers. Therefore, we focused a.o. on the composition of the random ssDNA library, the prevention of by-product formation after PCR amplification, the transformation of ds into ssDNA and the balance between positive and counter selection steps making up the SELEX process. Secondly, after optimization, two independent SELEX procedures were performed according to the optimized SELEX protocol. For both SELEX procedures, E2 was used as target during positive selection steps. On the other hand, during counter selection steps, dexamethasone was used for SELEX A and nortestosterone for SELEX B. The differential use of counter molecules was important to direct both aptamer sets towards different functional groups of E2. Aptamers directed towards different epitopes of E2 can in a later stage be used to integrate as receptor molecules in a cross-reactive array making identification of several E2 analogues possible.

The design of a random ssDNA library to start a SELEX process is crucial. Out of this crowded pool of oligonucleotides only few highly sensitive and specific aptamers will be selected. Amplification of random library however turned out to be tricky. Even carefully designed fixed primer binding regions and an optimized amplification protocol were not sufficient to avoid by-product formation after consecutive PCR cycles. By-products are a phenomenon typically appearing after

multiple amplifications of random DNA strands. Prevention of this by-product formation from the start of the SELEX is recommended and turned out to be possible via size separation on gel.

Next to an efficiently designed random ssDNA library, target is the other essential component of the SELEX process. One of the main advantages of the used beads during this research is the oriented immobilization of E2 (or one of its analogues) leaving potential epitopes available for aptamer binding. By using this kind of commercially available beads, the ease of target handling was combined with fully available target.

Monitoring the effect of several factors involved during SELEX on the ultimate selection process provides useful information needed for efficient aptamer selection. Monitoring should not only include the measurement of DNA quantities, but also the follow-up of changes in randomness/diversity of selected ssDNA. This monitoring is addressed in Chapter 3. In that chapter, a new tool for following-up gradually arising enrichment during SELEX will be highlighted.

Once selected, aptamers have to be analysed carefully. The most abundant oligonucleotides in the final selection pool are not always the aptamers with the highest sensitivity and specificity for the target of interest. One of the main reasons is that aptamer selection can be distorted by intrinsic differences in amplification efficiency of oligonucleotides [141]. Another important reason is that even if counter selection steps make up most of the selection steps, selection of aspecific binding oligonucleotides cannot be 100% prevented. In order to end up with the best aptamers for final applications, the selected ones have to be analysed in terms of sensitivity and specificity. Characterization of the selected E2-binding aptamers will be described in Chapter 4.

3

Monitoring aptamer selection

Based on:

reMelting Curve Analysis as a tool for enrichment monitoring in the SELEX process

Jeroen Vanbrabant, Karen Leirs, [Katrijn Vanschoenbeek](#), Jeroen Lammertyn and Luc Michiels

Analyst, 2014. 139(3): p. 589-595

Own contribution: Set-up and validation remelting curve analysis during E2 aptamer selection, monitoring contamination during SELEX, co-author of publication

Current aptamer selection procedures enable limited control and transparency on how the DNA selection pool is evolving. Affinity tests and binding analysis are not always as informative. In this chapter, we show that qRT-PCR provides a valuable tool for the follow-up of aptamer selection. Limited time, work and amount of amplified ssDNA make this an interesting instrument to set up a SELEX design and monitor the enrichment of oligonucleotides. rMCA after reannealing at stringent conditions provides information about enrichment, compared to a random library. Monitoring the SELEX process and optimizing conditions by means of the proposed methods can increase the selection efficiency in a controlled way. rMCA was applied in enrichment simulations and three different selection procedures. Our results imply that rMCA can be used for different SELEX designs and different targets. SELEX pool diversity analysis by rMCA is proven to be a useful, reproducible tool to detect and evaluate enrichment of specific binding aptamers while the selection procedure is performed.

3.1 Introduction

Although selection conditions during SELEX are critical, they are to a great extent documented trial and error. Often, only after a number of SELEX rounds, the selected DNA pool is sequenced and checked for enrichment of target-specific oligonucleotides [10]. Assessing the effect of separate selections under different binding and washing conditions on the DNA pool provides valuable information to increase selection efficiency. Monitoring of the progression is critical for the success of an *in vitro* selection experiment and the characteristics of the selected aptamers. This allows early intervention and adjustment of the selection stringency to achieve the desired activities of the selected aptamers [142]. To date, both direct measurement of SELEX progression, in terms of affinity of the ssDNA pool for the target, and indirect measurements have been addressed.

Measuring the amount of target-binding oligonucleotides in selection pools offers a way of monitoring enrichment directly by assessing average affinity of the SELEX pool for the target. For example, ELISA-like assays enable comparison of different consecutive ssDNA selection pools. A fraction is labeled with a fluorophore or enzyme and incubated on a target-coated substrate. Binding is then visualized and quantified by fluorescence or chemiluminescence, for example on a membrane by blotting [143] or on magnetic beads to perform flow cytometry for fluorescence acquisition [144, 145]. Other studies use radiolabeling to visualize and quantify bound DNA [146]. Non-equilibrium capillary electrophoresis of equilibrium mixtures (NECEEM) has proven to be a good way to control and compare SELEX fractions for target binding and even determine K_D of the SELEX pools [147]. Another way of direct screening for affinity is the HAPIScreen (high throughput aptamer identification screen) methodology [148]. Target and candidate fractions are both coated onto beads, which results in chemiluminescence when the two types of beads come in proximity *i.e.* when there is interaction between them. As such, an arbitrary score for affinity is determined and only fractions with a high score are further evaluated.

These described assays suffer from several limitations and drawbacks. They are time- and material-consuming and do not always offer the required resolution or sensitivity for concise SELEX monitoring. One needs a very sensitive and good assay to see the difference in binding capacity of consecutive SELEX pools, especially in the onset of selection, when there are still a lot of random, non-specific oligonucleotides present in the eluted fractions. These assays are also target dependent and not applicable for all SELEX targets. For example, small molecules often lack functional groups that are needed for attachment of the target to the carriers needed in these assays. When they have a functional group, there is the risk of using the functional group the aptamer recognizes for binding. NECEEM measures in solution, yet suffers from other limitations. Not all targets are suited for analysis by CE. For example, when a small target has a low isoelectric point (pI) and the charge to size ratio of the target is highly similar to that of the ssDNA, it is difficult to distinguish the complex peak from the peak with free ssDNA [32, 149]. Moreover, these assays all involve labeling

the ssDNA oligonucleotides with fluorophores, biotin or other functional groups. This labeling can change the characteristics, structure and hence binding properties of the ssDNA pools and decreases the power of these assays to assess enrichment and evolution in the selection process in a concise way. As stated by Rowe *et al.* (2009) [150], complications may arise with the use of labels, either by altering the protein chemistry or from interactions between tags and the target aptamers, which can lead to either high background noise or a decrease in aptamer specificity. Since direct monitoring of affinity is often limited by the need for labels, signal enhancers or other functional groups, monitoring of progression needs to be done in other ways. As label-free and radiolabeled affinity assessments need specialized instrumentations, methods that indirectly measure selection progression in the SELEX pools are developed.

Monitoring the *in vitro* selection process can be performed in terms of ssDNA quantities that are eluted during different SELEX rounds. Niazi *et al.* (2008) [151] performed seven selection rounds until the ssDNA quantity (measured by spectrophotometry) in the eluted pools was 90% of the ssDNA quantity that was added to the target. A more straightforward way of monitoring is assessing sequence diversity of the pools and the most informative but elaborate technique to do this is sequencing individual clones. However, this is expensive and one does not know how many clones to sequence. Furthermore, it is not applicable to the more random stages of the procedure since the sensitivity of this approach is not high enough for the follow-up of premature arising enrichment. Müller *et al.* (2008) [142] proposed a method based on sequence diversity that enables monitoring of a SELEX procedure by employing denaturing high-performance liquid chromatography (dHPLC). The technique is useful for both analysis of the selection progression and separation of distinct sequences. Charlton and Smith (1999) [152] reasoned that the sequence complexity of a ssDNA pool can be quantified by observing the renaturation rate of its dsPCR product by performing a C_0t analysis. A sample with a highly-repetitive sequence will renature more rapidly, while complex sequences will renature more slowly. Instead of simply measuring the percentage of dsDNA versus time, the amount of renaturation is measured relative to a C_0t value. The C_0t value is the product of C_0 (the initial concentration of DNA), t (time in seconds) and a constant that

depends on the buffer composition. Repetitive DNA will renature at low C_0t values, while complex and unique DNA sequences will renature at high C_0t values. C_0t analysis was initially developed to measure the oligonucleotide complexity of genomes [153]. In a later stage, C_0t analysis was applied to PCR products [154]. However, this analysis appears impossible for libraries with diversities higher than 10^6 different oligonucleotides. Remelting curves following an annealing step are observed to be a better characteristic indicator for the analysed diversity [155]. On an increase of diversity, a decrease in remelting temperature was detected, denoting the amount of imperfectly formed heteroduplexes. The applied annealing temperature determines the resolution in a given diversity range. Using DiStRO (diversity standard of random oligonucleotides), population dynamics of an aptamer selection against daunomycin were analysed and quantified.

Various attempts have been made to monitor the selection progress of target-specific ligands. Direct measurements of SELEX pool affinities for the target are prone to several limitations and need a target-specific approach. Therefore, indirect monitoring applies the characteristics of the DNA pool as such, ideally without the need for labeling and independent of the target characteristics. Diversity analysis of the recovered DNA pools is the most straightforward way to achieve this. In this study, rMCA after a short reannealing step is proven to be a useful tool for diversity analysis of a given SELEX pool and hence for enrichment monitoring, independent of extra DNA modifications, the SELEX target and design. The principle of rMCA monitoring was shown using an enrichment simulation procedure. Furthermore, rMCA was applied to different SELEX strategies (plate based, CE based and bead based SELEX) using targets of ranging physical properties (CRP, peptide X and E2) to demonstrate the general applicability of the rMCA as a monitoring tool. The selection on peptide X was analysed with the proposed method on a different qRT-PCR platform. Monitoring different approaches in different labs demonstrates the robustness, reproducibility and ease of use of this method. This proves complexity analysis of SELEX pools by rMCA to be very useful to increase selection efficiency by hands-on evaluation of the selection process steps and making the right decisions.

3.2 Materials and Methods

3.2.1 Materials

DNA was purchased from IDT. A lightcycler® 1.5 carousel and 1x SYBR mix were derived from Roche. CRP was obtained from BBI Solutions (Cardiff, UK). NucleoLink™ Plates and salmon sperm ssDNA were received from Life Technologies. Peptide X was synthesized by Eurogentec (Seraing, Belgium). A P/ACE-MDQ CE system was supplied by Beckman Coulter (Fullerton, USA). AccuMelt™ HRM SuperMix was obtained from Quanta Biosciences (Gaithersburg, USA). A Rotor-Gene Q was derived from Qiagen (Venlo, the Netherlands). All buffers were homemade.

3.2.2 Enrichment simulation in random starting libraries

Two different starting libraries were spiked with increasing concentrations of aptamer sequence, from 0% enrichment to 100% enrichment. A random library earlier used for CE SELEX was spiked with increasing amounts of IgE aptamer, D17.4 [156]. A random library earlier used for plate SELEX was gradually enriched with either one single oligonucleotide or a homogeneous mix of ten different oligonucleotides. Oligonucleotides were extended with the primer binding sites of the corresponding applied random libraries to allow amplification. The analysis was performed on a Lightcycler® 1.5 carousel with 20 µL reaction mixes containing 1x SYBR Mastermix, 100 nM of each primer, 2 mM extra Mg²⁺ and 100 pM (for one oligonucleotide or the mix of ten) or 10 pM (for IgE aptamer) enriched library. The PCR protocol consisted of 5 min of denaturation, followed by 35 cycles of 5 s at 95°C, 3 s at primer annealing temperature and 4 s at 72°C for elongation. After amplification, a first melting curve analysis (MCA) was performed after the final elongation at 72°C plus a rMCA after a short reannealing phase (Figure 20). Different reannealing

temperatures and times were tested for rMCA. Reannealing was tested for 30 s, 1 and 2 min at 65°C, 70°C and 75°C. The remelting rate was set at 0.1°C/s.

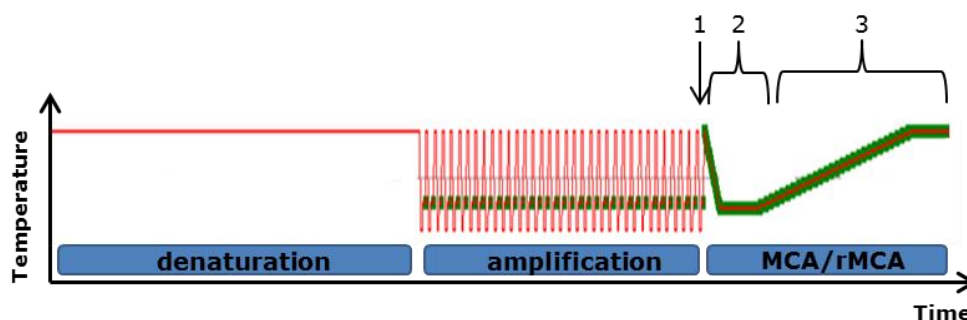


Figure 20: Schematic overview of the PCR protocol applied for rMCA. The protocol contained a denaturation, amplification and analysis (MCA/rMCA) step. The analysis step can further be divided in a first melting (1), renaturation (2) and second melting (3) step. During the second melting step, rMCA was performed.

3.2.3 Plate SELEX for C-Reactive Protein aptamers

A random 40nt library was constructed, flanked by 18nt primer binding regions (Table 5).

Table 5: ssDNA library and primer set applied during plate SELEX for CRP aptamers.

SELEX CRP	5'-GCACCAGCATATTCGATT-40N-GGCTAGTAGGTGCATCAG-3'	
	FP:5'-GCACCAGCATATTCGATT-3'	RP:5'-CTGATGCACCTACTAGCC-3'

CRP was covalently coupled to NucleoLink™ Plates by the instructions provided by the manufacturer. These plates were deactivated with 100 mM ethanolamine. Plates with only ethanolamine were also used, since negative selections are as important as positive ones. Each selection cycle consisted of a negative selection step, a positive selection step and another negative selection step prior to PCR amplification, to avoid amplification of non-specific binders. By-product formation by excessive PCR amplifications was avoided by performing only 15 amplification cycles per round and by PCR-product clean-up via 4% agarose GE

separation and extraction of the band with the desired length of 76 bp (40 bp of the random region and 2 x 18 bp from the fixed primer binding regions). During positive selections, elution was performed in four separate fractions. Buffer for incubation was 10 mM HEPES + 5mM CaCl₂, pH 7.4; washing buffer was 1x PBS, pH 7.4 and elution buffer was 1xTE buffer + 3 M urea, pH 8 at 80°C. Before negative selection steps, sonicated salmon sperm ssDNA was added in a 50x excess to avoid losing CRP binding oligonucleotides by non-specific DNA absorption in negative selections.

After each selection step, a fraction of the elutions was analysed separately by qRT-PCR on the Lightcycler® for quantitative analysis, but also to assess oligonucleotide diversity of the pool by means of rMCA. PCR mix and amplification protocol were the same as mentioned for the enrichment simulation, with a primer annealing temperature of 58°C. Reannealing was set at 1 min at 70°C.

3.2.4 Capillary electrophoresis SELEX for peptide X aptamers

A random 40nt library was constructed, flanked by 20nt primer binding regions (Table 6).

Table 6: ssDNA library and primer set applied during CE-SELEX for peptide X aptamers.

SELEX peptide X	5'-TCGCACATTCCGCTTCTACC-40N-CGTAAGTCCGTGTGTGCGAA-3'	
	FP:5'-TCGCACATTCCGCTTCTACC-3'	RP:5'-TTCGCACACACGGACTTACG-3'

Selection was performed using a P/ACE-MDQ CE system with an uncoated fused silica capillary (length: 40.2 cm, outer diameter: 375 µm, inner diameter: 50 µm). The 488 nm line of a 3 mW Argon-ion laser was used for excitation of the fluorescently labeled DNA. The emission was measured using a 520 ± 10 nm band pass filter. Running buffer was tris glycine potassium phosphate (TGK) buffer (25 mM tris(hydroxyamino)methane, 192 mM glycine and 5 mM K₂HPO₄,

pH 8.4). Samples were incubated in tris magnesium buffer solution (10 mM tris(hydroxyamino)methane and 1 mM MgCl₂, pH 7.2). Separation was performed at 15 kV under normal polarity. Free DNA sequences move slower through the column so only complex was collected to use for the following SELEX round.

After each selection step, a fraction of the pool was amplified by qRT-PCR and subsequently analysed by rMCA on a Rotor-Gene Q. A 30 µl reaction mix was prepared containing 1x AccuMelt™ HRM SuperMix, 67 nM of each primer and a fraction of the SELEX pool. Before amplification, a denaturation step at 95°C was performed for 10 min. This was followed by a two-step amplification process (5 s at 95°C and 30 s at 60°C) of 35 cycles. The amplification products were melted from 60°C to 95°C by increasing the temperature. Reannealing was allowed at 70°C for 1 min followed by a second melting analysis from 70°C till 95 °C at 0.5 °C/s.

3.2.5 Bead SELEX for 17β-estradiol aptamers

Two random 40nt libraries were designed as explained in section 2.2.2. Two SELEX procedures (SELEX A and B, described in section 2.2.4) for the selection of E2-binding aptamers were analysed according to the protocol described in 3.2.3, with primer annealing temperatures of 60°C (SELEX A) or 54°C (SELEX B). Reannealing was set at 1 min at 72°C.

3.3 Results

3.3.1 Remelting curve analysis of simulated enrichment

As shown in Figure 21, all three simulations showed a similar trend in both amplification (Figure 21, up) and remelting (Figure 21, low) data. Where 100% enriched fractions showed normal exponential amplification curves, 100%

random libraries showed a drop in fluorescence after reaching a maximum. The amplification curves changed along with increasing enrichment of spiked oligonucleotide(s). When diversity decreased, the drop in fluorescence was less pronounced and eventually disappeared in more enriched conditions.

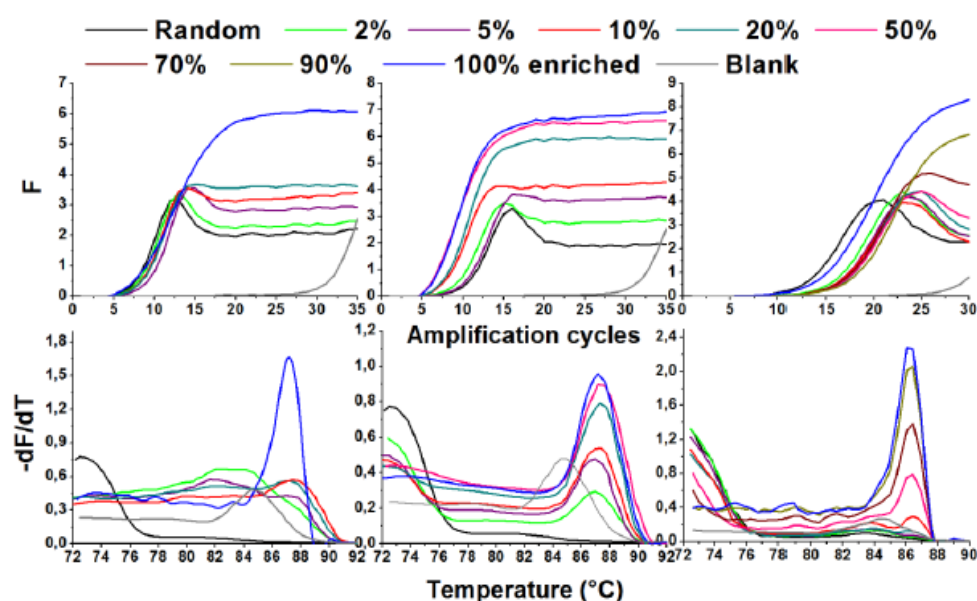


Figure 21: Amplification (up) and rMCA (down) data of three enrichment simulations. (Left) Random library earlier used for plate SELEX spiked with increasing concentrations of a singular oligonucleotide (CRP aptamer 2-20), from 0% enrichment to 100% enrichment; (Middle) Random library earlier used for plate SELEX spiked with a homogenous mix of ten different oligonucleotides. The total mix made up 0% to 100% of the sample; (Right) Random library earlier used for CE SELEX spiked with increasing concentrations of a singular oligonucleotide (IgE aptamer D17.4), from 0% enrichment to 100% enrichment. (F = fluorescence, generated by SYBR Green. $-dF/dT$ = first negative derivative of F , denoting the decrease in fluorescence or dsDNA melting with increasing temperature T)

Remelting data showed an evolution from a gradual melting behavior of 100% random library (broad melting zone around 70-75°C) to a melting peak at the expected melting temperature of the spiked oligonucleotide or the average melting temperature of the oligonucleotide mix, which was reflected in a broader melting peak. The speed and form of this shift in melting behavior differed. 2% enrichment of random library used for plate SELEX with singular oligonucleotide 2-20 (Figure 21, left) induced a clear shift in remelting behavior of the DNA

pool. On the other hand, 2% enrichment of random library used for CE SELEX with singular oligonucleotide D17.4 (Figure 21, right) had almost no effect on the remelting behavior of the DNA pool. Nevertheless, there was a clear general effect of higher remelting temperatures as the diversity decreased, with an enrichment of 10% clearly distinguishable from the random DNA pool in the three cases. Blank amplifications showed a rise in fluorescence after 30 amplification cycles and a remelting peak which correlates with the formation and disruption of primer dimers after iterative heating and cooling of the mix.

Simulation also showed that reannealing goes very fast: reannealing 30 s gave comparable empirical results as reannealing 2 min (Figure 22). Remelting occurred at the same temperature independent of the reannealing temperature, but longer reannealing resulted in sharper melting peaks.

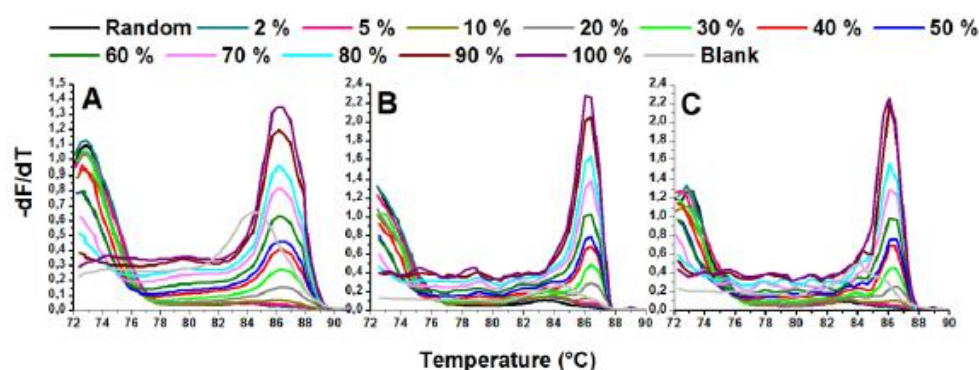


Figure 22: rMCA data of simulated D17.4 enrichment in random library after different reannealing times. rMCA was compared after reannealing at 70°C for (A) 30 s; (B) 1 min and (C) 2 min.

Changing the reannealing temperature changed the window and resolution of rMCA. Reannealing at 70°C (Figure 23, left) resulted in a broad melting zone starting from this reannealing point in random or poorly enriched conditions. In more enriched conditions, this broad melting zone disappeared and a more narrow melting zone appeared at a higher temperature. When reannealing at 75°C, the melting zone of random library at 72-74°C was not formed and remelting started at 75°C. This allowed to zoom in on more enriched libraries.

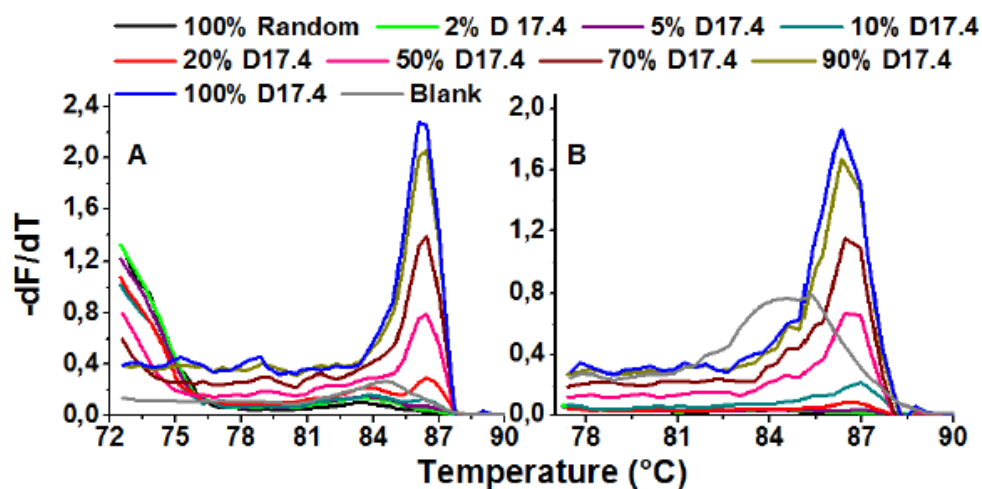


Figure 23: rMCA data of simulated D17.4 enrichment in random library after different reannealing temperatures. rMCA was compared after 1 min reannealing at (A) 70°C and (B) 75°C.

3.3.2 Remelting curve analysis of different SELEX procedures

Plate SELEX for C-reactive protein aptamers

In the plate SELEX protocol for CRP, four elution fractions were collected after each positive selection step. These fractions were separately analysed by rMCA. Until round 10, all four fractions showed similar melting peaks. Hence, the four elution fractions were each time combined to continue the next SELEX round. After round 10, there was a clear difference in DNA composition of the separate fractions, indicated by different remelting peaks (Figure 24). At this point, the selection procedure was continued in parallel with these four elution fractions separately.

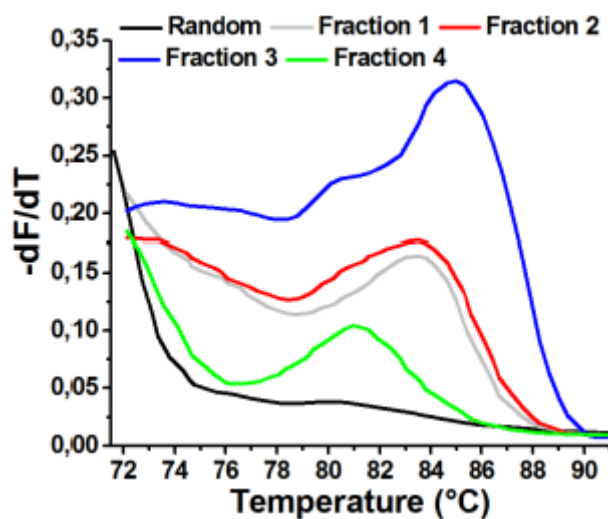


Figure 24: rMCA data after ten rounds of CRP aptamer selection. A clear difference was seen in remelting behavior of different elution fractions.

Figure 25 shows rMCA data of elution fraction 3 throughout the CRP SELEX procedure and illustrates clear evolution from a random DNA pool with a remelting temperature of 72°C (Figure 25A) to a more enriched one with a higher average remelting temperature of 84°C (Figure 25H). rMCA data of the other elution fractions also indicated gradually arising enrichment reflected by a shift in remelting behavior (data not shown).

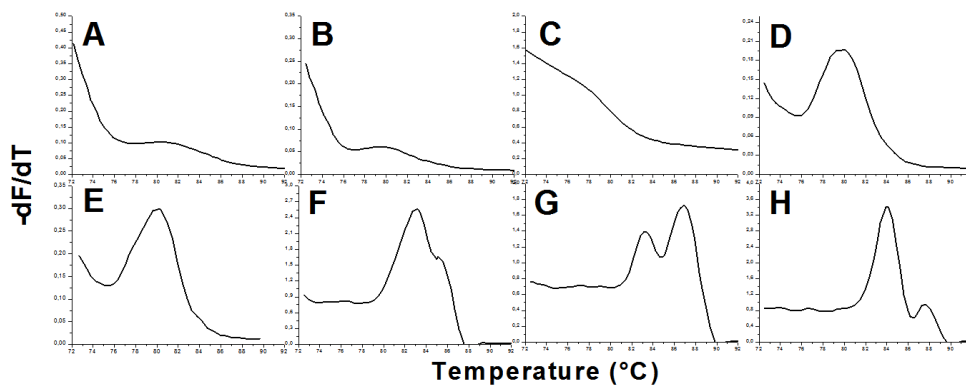


Figure 25: rMCA data of the third elution fraction of consecutive SELEX rounds for CRP. (A) random library; (B) round 1; (C) round 3; (D) round 7; (E) round 9; (F) round 12; (G) round 15 and (H) round 16. (Temperature on X-axis is ranging from 72° to 92°C)

Even after 16 selection rounds, the four elution fractions differed from each other, demonstrated by both the amplification curves and rMCA data (Figure 26). The remelting peaks (Figure 26B) shifted from 72°C to higher temperatures in all of them. The position and form of these peaks differed for each fraction. Fraction 3 formed a clearly distinct peak at 84°C and a small peak at 88°C, whereas fraction 1 and 2 formed broader peaks from 80 to 86°C. The difference was reflected in the amplification curves as well (Figure 26A), with a drop in fluorescence after 4 amplification cycles for fraction 1 and 2 and absence of this drop for fraction 3. Fraction 4 demonstrated an intermediate enrichment and an intermediate drop.

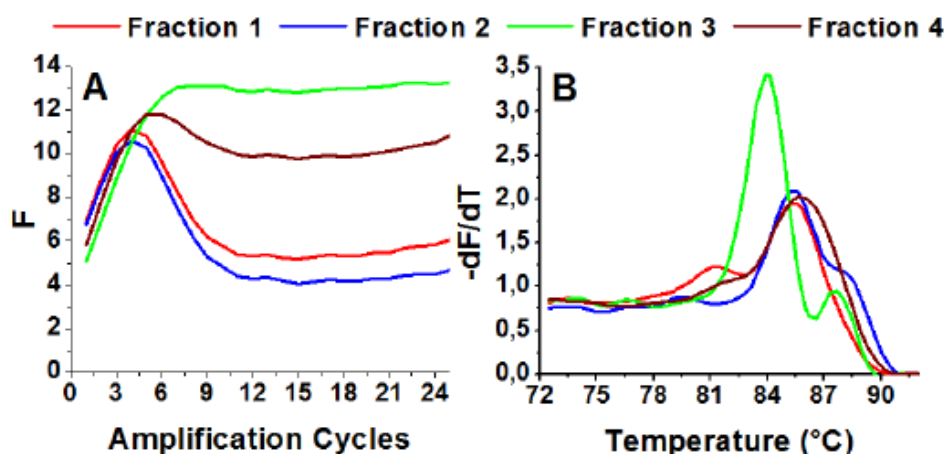


Figure 26: Amplification (A) and rMCA (B) data of four elution fractions after 16 rounds of CRP aptamer selection.

Capillary electrophoresis SELEX for peptide X aptamers

rMCA of peptide X CE SELEX was performed on two devices, a Rotor Gene-Q (Figure 27; up) and a Lightcycler® (Figure 27, down). Both analyses showed a broad melting zone at a 'low' temperature of 70-74°C which remained present throughout the whole selection procedure. This indicates that even after 11 selection rounds, a large fraction of random DNA was present.

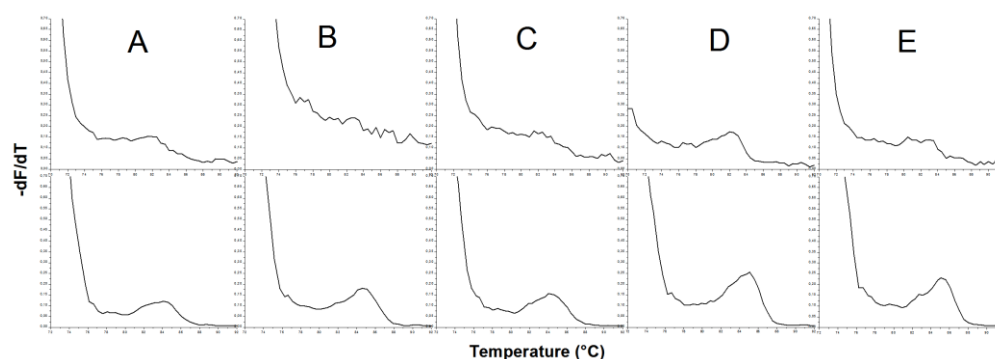


Figure 27: rMCA data of consecutive SELEX rounds for peptide X on two devices. (Up) Analysis on a Rotor Gene-Q; (Down) Analysis on a Lightcycler®. (A) round 1; (B) round 4; (C) round 6; (D) round 9 and (E) round 11. (Temperature on X-axis is ranging from 72° to 92°C)

rMCA with a higher reannealing temperature of 75°C instead of 70°C (Figure 28), changing the rMCA window, elucidated changes in the DNA pool better and indicates that enrichment was occurring yet at a slow rate. In the onset of the procedure, rMCA only resulted in a broad melting zone. When the procedure continued, after round 4, there was a growing remelting peak appearing at higher temperatures.

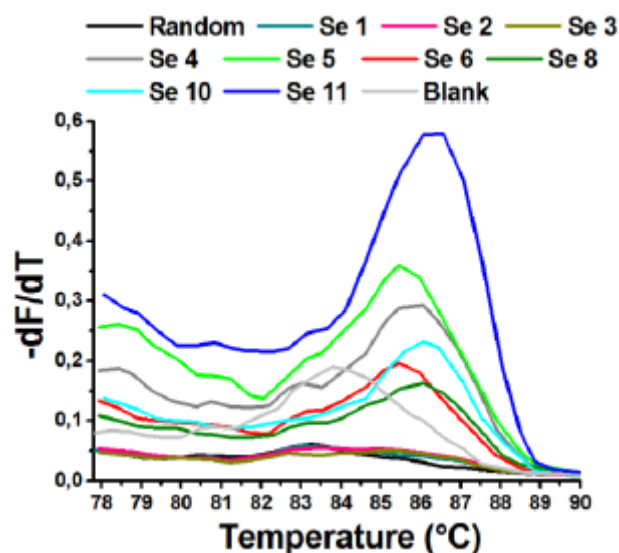


Figure 28: rMCA data of consecutive CE SELEX rounds for peptide X after 1 min reannealing at 75°C.

Bead SELEX for 17 β -estradiol aptamers

rMCA was executed during two in parallel performed procedures for the selection of E2 aptamers (SELEX A and B; see Chapter 2).

SELEX A comprised only 5 selection rounds. At a relatively low temperature of 73°C, a clear remelting peak was present and this peak stayed visible until round 5. At a higher temperature of 86°C, a melting zone gradually arised throughout the SELEX procedure. However, remelting at this temperature stayed much lower when compared to the remelting at 73°C (Figure 29).

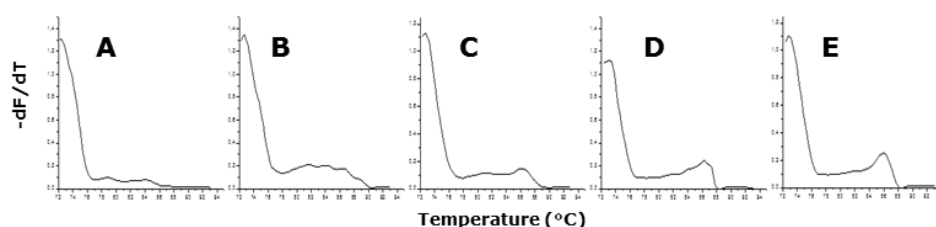


Figure 29: rMCA data of consecutive SELEX rounds for E2 (SELEX A). (A) round 1; (B) round 2; (C) round 3; (D) round 4 and (E) round 5. (Temperature on X-axis is ranging from 72° to 94°C)

For SELEX B, after ten rounds, the melting peak of the DNA pool was evolved from a broad random peak at 73°C (Figure 30A) to two specific peaks at 84 and 87°C (Figure 30H) and a low random part.

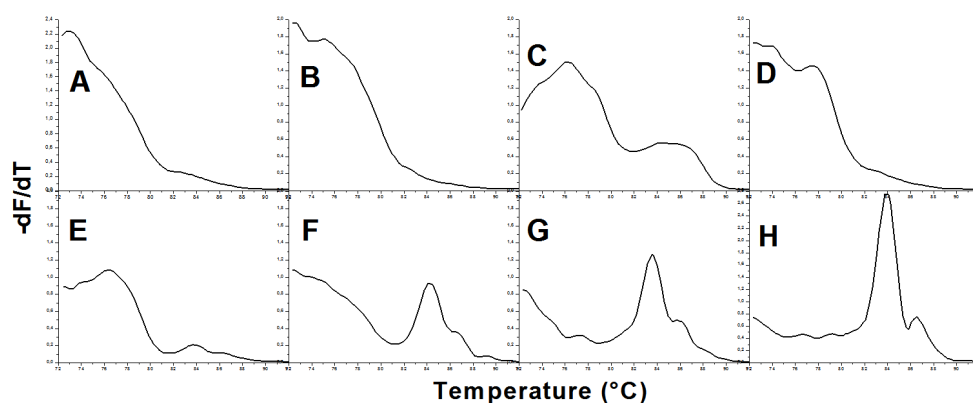


Figure 30: rMCA data of consecutive SELEX rounds for E2 (SELEX B). (A) round 1; (B) round 3; (C) round 5; (D) round 6; (E) round 7; (F) round 8; (G) round 9 and (H) round 10. (Temperature on X-axis is ranging from 72° to 92°C)

3.3.3 Remelting curve analysis to identify contamination problems during SELEX

rMCA was performed during a trial SELEX for E2 aptamer selection which was performed for optimization purposes (Figure 31). A suddenly arising enrichment, not present before, was visible after the first counter selection step of round 2 in the form of a narrow remelting peak at a temperature of 86.5 °C (Figure 31A). This enrichment became less pronounced after the positive selection step (Figure 31B) and second counter selection step (Figure 31C) of the same round, with again a high degree of random DNA as visualized by a remelting peak around 72 °C. The narrow remelting peak at 86.5 °C started to reappear again after the first counter selection step of round 3 (Figure 31D).

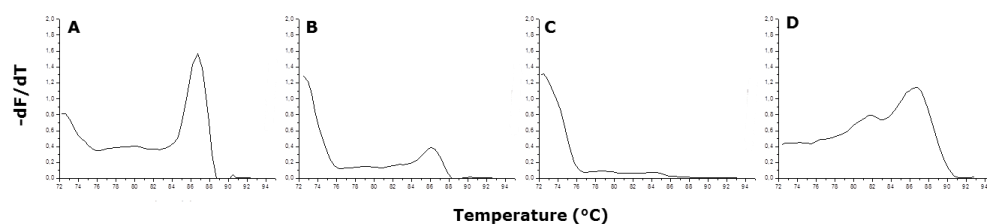


Figure 31: rMCA data of consecutive SELEX rounds for E2 (SELEX trial). (A) 1st counter selection step round 2; (B) positive selection step round 2; (C) 2nd counter selection step round 2 and (D) 1st counter selection step round 3. (Temperature on X-axis is ranging from 72° to 94°C)

3.4 Discussion

Annealing and melting kinetics of DNA are extensively studied since C_0t analysis [153], from gene analysis [156] and genome sequencing [157] to analysis of selection libraries. Schütze *et al.* (2010) [155] created the diversity calibration standard DiStRO for the evaluation of DNA pools by analysing remelting curves after an annealing step of 180 min. In this dissertation, remelting analysis was applied and optimized for monitoring diversity changes during the SELEX procedure, regardless of design and target properties.

In a standard MCA, all high-copy pools are slowly denatured directly after the last elongation phase of amplification, containing in theory mostly homoduplexes. In this way, MCA analyses melting temperatures in terms of internal structures and stability of the homoduplexes. In rMCA, a short reannealing step at a relatively high temperature is introduced after total denaturation. In this stringent reannealing phase, both hetero- and homoduplexes are formed and their proportions completely depend on the sequence diversity. rMCA is then performed and analyses remelting temperatures in terms of hetero- versus homoduplexes. As the diversity of SELEX pools decreases due to enrichment of target-binding ssDNA species, more homoduplexes will be formed in the reannealing phase and one can expect a shift in the obtained remelting temperatures. Consequently, rMCA will provide crucial information on enrichment in terms of diversity.

3.4.1 Remelting curve analysis of simulated enrichment

Simulation of enrichment in different libraries was performed to demonstrate the broad applicability of rMCA, studying amplification and remelting behavior of complex DNA pools with different diversities. The simulation experiments revealed that both amplification and remelting data offer useful information about the diversity of a DNA pool.

Regarding DNA amplification, a clear difference between random and enriched pools was seen. A 100% random pool showed a drop in fluorescence after reaching a maximum. When diversity decreased, the drop in fluorescence got less pronounced. This fluorescence drop eventually disappeared in the more enriched conditions which showed a standard exponential amplification curve. This phenomenon can be explained by the same principle as rMCA. At this drop, there is no amplification anymore (because of limitation of primers or dNTP) and fluorescence acquisition at 72°C is performed after a short reannealing phase instead of an elongation phase. Random pools contain more unstable heteroduplexes at this temperature and fluorescence drops.

The fluorescence drop in the amplification curves of highly diverse SELEX pools indicates there is already heteroduplex formation before the amplification cycles are finished. This means that the first MCA is not performed after final elongation, but after a short reannealing step at primer annealing temperature and elongation temperature. Comparison between MCA and rMCA results indeed showed similarities but the rMCA data after reannealing at 70°C displayed the increasing enrichment more accurately.

Regarding DNA remelting, a shift from a lower, broad remelting peak to a more distinct, higher remelting temperature was seen as diversity decreased and enrichment occurred. Remelting peaks at 72°C due to heteroduplex formation gradually disappeared and evolved to the (average) remelting temperature of the more stable homoduplexes of the enriched oligonucleotide(s). The speed and form of this shift differed, which makes the sensitivity of this method dependent on the library and enriched oligonucleotide(s).

Since these are simulated enrichment experiments, all pools endured the same amount of controlled amplification cycles. The effect of changing remelting temperatures of the DNA pools can only be attributed to the simulated changed composition of the DNA pools and not to PCR artifacts and by-product formation due to excessive PCR cycling. This shows the rMCA method to be specific for changing DNA pool compositions and diversities.

3.4.2 Remelting curve analysis of different SELEX procedures

rMCA was successfully applied in three different selection procedures for different targets. It was demonstrated to be applicable for different SELEX designs (plate based, CE SELEX and bead based) and targets of various physical properties, a macroprotein (CRP, 115 kDa, pI 5.3-7.4) [158], a peptide (X, 1.6 kDa, pI 11) and a steroid (*E2*, 272 Da, pKa 10.7) [159].

Plate SELEX for C-reactive protein aptamers

The CRP SELEX comprised 16 selection rounds, with four elution fractions collected after each positive selection step. All elutions were analysed separately, allowing to monitor the whole CRP SELEX procedure in detail from round 1 to 16.

Eluted fractions appeared to contain only low amounts of DNA. When performing the rMCA immediately after standard amplification of the low-copy number samples, the remelting data showed a peak at the same position as the blank sample, indicating that primer dimers were melted here. When analysing the same samples with an extra pre-amplification step, the remelting data changed and remelting behavior of homo- and heteroduplexes of the DNA pool became visible. Therefore, an extra pre-amplification step was included when analysing results of the plate SELEX for CRP aptamers. This extra pre-amplification step was not required, and thus omitted, for analysing the CE SELEX for peptide X aptamers and the bead SELEX for E2 aptamers. Higher amounts of DNA were eluted during positive selection steps of these SELEXes, probably because more target was presented to the DNA pools.

Before CRP SELEX round 10, the four elution fractions were each time combined to continue the next SELEX round, since no clear difference could be seen between the remelting behaviors of the four fractions. After CRP SELEX round 10, the selection procedure was continued in parallel with these four DNA fractions separately, because rMCA illustrated different DNA compositions. These differences can be explained by selection stringency differences: the oligonucleotides that were eluted in fraction 4 had survived the three previous elutions. After 16 rounds of selection, both amplification and remelting data indicated enrichment in the four fractions. However, these fractions still differed from each other, demonstrated by both the amplification curves and rMCA data.

The presence of oligonucleotide enrichment after 16 rounds was post-SELEX supported via sequence analysis which showed enrichment in all fractions. The observed rMCA differences between the four elution fractions were reflected by

the sequencing results. One aptamer was highly enriched in fraction 3, which can be related to the clear peak at 84°C. The smaller peak at 88°C cannot be explained based on the sequencing results. The other fractions contained enrichment of multiple sequences, which can be related to the broader peaks these fractions showed during rMCA. Kinetic analysis of selected aptamers by means of SPR was performed by multi-cycle kinetic analysis on CRP coated sensor chips and showed affinities in the nM range.

Capillary electrophoresis SELEX for peptide X aptamers

CE SELEX on peptide X was challenging because of the lack of a ssDNA-peptide X complex peak in the CE separation. Therefore, the collection window was chosen to be sufficiently broad, reducing separation efficiency of specific and non-specific oligonucleotides. This challenging selection process was reflected in the obtained remelting data. Even after 11 selection rounds, still a large amount of random DNA appeared present as illustrated by the large melting zone at a relatively low temperature after 1 min reannealing at 70°C. Nevertheless, library evolution and changes in DNA composition became clear when focusing on higher temperatures, correlating with enriched oligonucleotides. rMCA with a higher reannealing temperature of 75°C, changing the rMCA window, elucidated changes in the DNA pool better and indicated that enrichment was occurring yet at a very slow rate.

The absence of clear enrichment after 11 selection rounds was supported by the sequence analysis data, which showed that the DNA pool was still very heterogeneous. Because of this high degree of heterogeneity, no kinetic analysis on selected oligonucleotides took place.

rMCA for CE SELEX for peptide X aptamers was performed on a different qRT-PCR device, the Rotor-Gene Q (Qiagen) to test the general applicability of this diversity analysis method. Analysis on this device was compared with analysis on the Lightcycler®, which was the only device used for monitoring the CRP and E2 SELEX. Although rMCA on the Rotor-Gene Q and the Lightcycler® gave the same empirical results, the Lightcycler® and the SYBR Mix appeared more

sensitive in fluorescence acquisition in the remelting phase. In the Rotor Gene Q, the temperature transition rate needed to be increased from 0.1°C/s to 0.5°C/s to produce conclusive data.

Bead SELEX for E2 aptamers

For the selection of E2 aptamers, two SELEX procedures were performed, independent from each other. Both SELEX procedures used E2 as target during positive selection steps. The difference between the two procedure laid in the molecule used during counter selection steps. Therefore, the selected aptamers in both procedures were expected to target different functional groups of E2.

In order to allow a heterogeneous population of DNA strands to bind to several functional groups of E2, SELEX A was comprised of only 5 selection rounds. As can be expected, after 5 selection rounds, still a large amount of random DNA was present in the DNA pool as reflected by a clear remelting peak at a relatively low temperature. However, some enrichment was gradually arising during the selection procedure since a melting zone at a higher temperature became visible after few selection rounds. This heterogeneity as predicted by rMCA was supported by the sequence analysis data. These data revealed that all oligonucleotides were still unique after 5 selection rounds. The melting zone at higher temperature was possibly due to the presence of a common motif in 47% of the oligonucleotides of the pool. Affinity analysis of few selected aptamers was performed by means of SPR (see section 4.3.5) and showed affinities in the μM range.

SELEX B was comprised of 10 selection rounds. This SELEX procedure was expected to be a more stringent selection procedure than SELEX A because of the nature of the countermolecule. Few sequences are capable to bind E2 under these conditions, thus more selection rounds were required. After 10 rounds, the remelting peak of the DNA pool was evolved from a broad random peak at a low temperature to two specific peaks at higher temperatures and a low random part. Sequencing of the pool after selection round 10 revealed enrichment of two

oligonucleotides. These two oligonucleotides showed affinities in the low μM range as was measured via SPR (see section 4.3.5).

As indicated by the previous sections, rMCA enables monitoring of the SELEX progress regardless of target properties. When direct monitoring of affinity of the SELEX pools for the target is not possible, rMCA provides an interesting tool for arbitrary detection of enrichment in the analysed DNA pools. As it is clear from the enrichment simulation and three SELEX analyses, the observed shifts in remelting temperature of the pools are different since they are dependent on the random library and enriched oligonucleotides. Although this method is not generally quantifiable for enrichment, it allows real-time monitoring of the ssDNA pool diversity while the selection is performed and it helps to decide when to stop a SELEX procedure.

For the CRP SELEX, the random remelting peak completely disappeared when analysing elution fraction 3 and only one sequence was highly enriched as visualized by means of sequence analysis. A same correlation between remelting at a high temperature and clear enrichment of two oligonucleotides could be seen for the E2 SELEX B. For E2 SELEX A and peptide X SELEX, much less enrichment could be detected by means of rMCA, but also this was in accordance with sequence analysis data.

3.4.3 Remelting curve analysis to identify contamination problems during SELEX

In the onset of selection, rMCA is also useful to indicate possible contaminations. A contamination of the SELEX library with one singular sequence can be easily detected since it appears as a suddenly arising large, narrow melting peak in an otherwise broad melting zone. During a SELEX trial for E2 aptamer selection, a narrow remelting peak at a relatively high temperature already showed up in the second selection cycle. This remelting peak resembled a remelting peak for a highly enriched library. Since strong enrichment was not yet expected at this time of the SELEX, this was a first indication that there was contamination. An additional sign was that the narrow remelting peak was visible after the first

counter selection step of the second cycle, but became less pronounced after the positive and second counter selection step of this cycle. The narrow remelting peak reappeared however after the first counter selection step of the third selection cycle. Contaminating sequences have a big chance to survive counter selection steps since they will not tend to bind the counter molecule applied during counter selection steps. However, when performing a positive selection step, most contaminating sequences will get discarded since they are not able to bind to the target. The few contaminating sequences that stay present in the SELEX library will get amplified after a selection cycle is finished and in this way the remelting peak symbolizing contamination is appearing again after the first counter selection step of a next selection cycle. The presence of a contaminating sequence during this SELEX trial was later proven when sequencing the library pool. The contaminating sequence appeared to be a commercially purchased aptamer oriented towards CRP, bearing the same fixed flanking sequences as were present in the applied selection library.

3.5 Conclusion and future perspectives

rMCA enables monitoring of the SELEX progress while the selection is going on, regardless of target properties and SELEX design. When direct monitoring of affinity of the selection pools for the target is not possible, rMCA provides an interesting monitoring tool. The method can be used to detect and judge enrichment for target-binding sequences during the SELEX process, but can also be used in decision making to optimize selection conditions. rMCA does not require a lot of input material, no supplementary target is needed and no extra labeling and incubation steps are involved. Real-time SELEX monitoring by rMCA makes use of the characteristics of the selected ssDNA as such in terms of amplification and denaturation kinetics and is therefore independent of SELEX approach, properties of target and different qRT-PCR devices, as demonstrated in this work.

Expansion on the repertoire of rMCA will further demonstrate the power of this remelting method for assessing enrichment in various SELEX designs, on

different qRT-PCR platforms and for different targets and starting libraries. Effects of the primer binding regions are to be determined. As these regions are equal for all sequences in the pool, they may reduce rMCA resolution capacity. Studying the effect of primer removal on the outcomes and resolution of diversity analysis by rMCA can result in more sensitive analysis or more insight in the role of these identical regions. Assessment of SELEX pool affinities for the target in the CE SELEX has interesting potential for rMCA validation. When a higher SELEX pool remelting temperature can be correlated with a higher overall SELEX pool affinity for the target, this clearly indicates lost diversity and enrichment of oligonucleotides in the pool that have higher affinities for their selection target than other sequences.

After selecting two series of epitope specific E2 binding aptamers (Chapter 2) - whereby the selection processes were monitored by rMCA to follow-up the arising enrichment (Chapter 3) - the selected aptamers will be characterized in terms of affinity and specificity (Chapter 4).

4

Characterization of epitope specific 17 β -estradiol aptamers

Partly based on:

Aptamers targeting different functional groups of 17 β -estradiol

Katrijn Vanschoenbeek, Jeroen Vanbrabant, Baharak Hosseinkhani, Veronique Vermeeren, Luc Michiels

J Steroid Biochem Mol Biol, 2014. 147c: p. 10-16

Part of paper: SPR binding assays regarding affinity and epitope specificity

Absent in paper: suitability testing of different types of binding assays

A major bottleneck in aptamer development and application for small molecules occurs at the point of aptamer characterization regarding affinity and specificity. Approaches for characterization which are applicable to aptamers oriented towards large targets often cannot be used for characterization of small molecule binding aptamers. In this chapter, we will focus on the characterization of our selected E2 aptamers. At first, several binding assays were tested to unravel which one is the most appropriate assay to apply. Subsequently, the most promising binding assay was used to define affinity and epitope specificity. A good characterization of aptamers is essential before successful implementation in a sensor set-up becomes possible.

4.1 Introduction

Although the eventual success of aptamers is to a great extent dependent on the planning, implementation and monitoring of their selection process [160], there is still another aspect which defines aptamer applicability. Feasible aptamer applications depend on the exact establishment of their affinity and specificity under defined conditions [10]. What ultimately matters, is how well and how selectively aptamers bind to their target [11]. Therefore, binding assays are a crucial post-SELEX step in aptamer research.

Characterization of aptamers in terms of affinity and specificity is one of the most costly and time-consuming tasks of aptamer production. Developed methods vary from low-cost, simple approaches such as ELONA [161, 162] to more complex methodologies requiring dedicated instrumentation such as interaction analysis based on SPR technology [163, 164]. It has to be kept in mind that all these methods have different sensitivities, so that K_D values obtained via different methods can be rather divergent [165, 166]. Moreover, measurements can be further complicated since post-SELEX labeling or immobilization of aptamers may significantly affect binding properties altering the K_D of the native aptamer. Because of these hindrances, it is suggested to characterize aptamers via different methods. Moreover, the ultimate value of

aptamers cannot be revealed without their evaluation in the eventual application [11].

In some binding assays, selection conditions are mimicked. Immobilized target gets incubated with aptamer instead of with random library. Subsequently, the amount of binding aptamer has to be quantified and compared with negative control conditions.

ELONA based on immobilized target requires direct labeling of aptamers with signal generating and amplifying enzymes such as alkaline phosphatase (AP) or HRP [167]. Alternatively, aptamers can be labeled with a tag that is recognized by an enzyme-linked detector. For example, conjugation of aptamers with a biotin tag enables visualization via HRP-conjugated SA or HRP-labeled antibodies against biotin [161, 168]. Non-specific binding is one of the most encountered problems when performing ELONA. This problem can largely be tackled by proper blocking techniques [169] and disruption of weak interactions [170] combined with the choice of a suitable enzyme-linked detector. Nevertheless, negative control conditions stay of crucial importance to correct for remaining non-specific binding. On the other hand, a clear advantage of ELONA is that it is a rather cheap and easy to perform technique without the requirement of specialized instrumentation [79].

Aptamers themselves can serve as signal amplifier. Then, signal generation and amplification occur via direct real-time amplification of the aptamer or indirect via real-time amplification of an additional PCR template attached to the aptamer [61]. This technique is rather easy to perform and combines high sensitivity and specificity. The high sensitivity of this technique is both an advantage and a drawback. Even slight amounts of bound DNA can be detected. However, this means that also minor amounts of non-specifically bound or adsorbed DNA are made visible. For this reason, the same actions have to be taken as for performing ELONA; reducing non-specific binding as much as possible and implementation of proper negative control conditions. The absence of labels and the fact that the qRT-PCR protocol of ssDNA is already optimized during the SELEX process are great advantages of this technique [61].

Other binding assays don't mimic selection conditions, but use aptamers as recognition element immobilized onto a solid support matrix, showing more resemblance with most aptasensors. Different support matrices can be applied (e.g. an ELISA well plate, a boron-doped nanocrystalline diamond (NCD) chip and a gold chip) in combination with different read-out systems (e.g. enzymatic signal generation, impedance, heat-transfer resistance (R_{th}) and SPR) in order to detect the interaction between immobilized aptamer and target free in solution.

In this kind of set-up, the creation of a nicely oriented layer of immobilized aptamers is crucial. Several immobilization methods exist (Figure 32), dependent on the chemical composition of the solid support matrix, the availability of suitable linkers and the employed attachment chemistries [171]. Direct attachment to a gold surface is possible via conjugation of a thiol-alkane to the aptamers so that they form a self-assembled monolayer (SAM) [172]. Alternatively, aptamers can covalently be immobilized onto a functionally modified surface via different routes. Biotin-labeled aptamers, for example, can strongly be fixed to substrates modified with SA or one of its derivatives [173, 174]. 1-Ethyl-3-[3-dimethylaminopropyl]carbodiimide hydrochloride/*N*-hydroxysuccinimide (EDC/NHS) coupling, on the other hand, enables the attachment of NH_2 -modified aptamers onto COOH coated substrates [174]. It has to be kept in mind that when immobilizing DNA, part of its flexibility gets lost. This can possibly hamper aptamer-target interaction. However, introducing a linker in between label and aptamer can to a great extent reduce this risk. Linkers can comprise different modular components such as an alkyl group, an oligo-ethylene glycol unit and/or an oligonucleotide spacer [171].

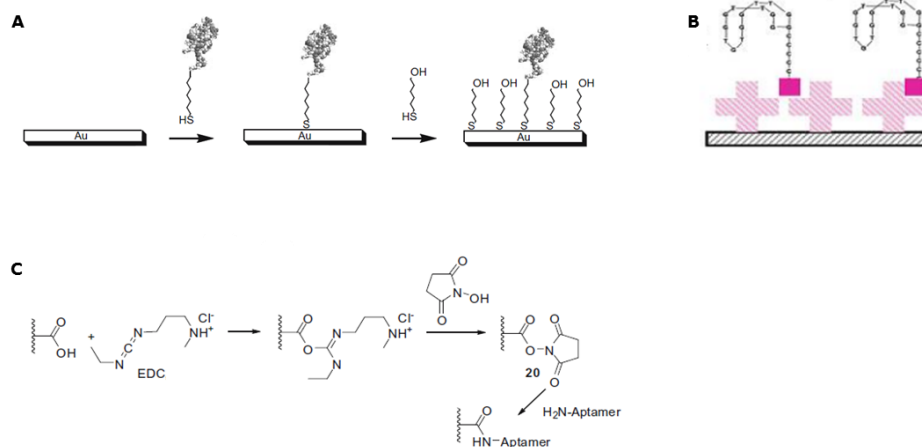


Figure 32: Examples of different DNA immobilization procedures. (A) Formation of a SAM by thiol-alkane modified aptamers; (B) Attachment of biotinylated aptamers on a SA-coated surface and (C) Immobilization of NH₂-modified aptamers on a COOH surface via EDC/NHS coupling [79, 171].

When immobilizing aptamer on an ELISA well plate, the most straightforward approach to detect target binding is via a sandwich design. The immobilized aptamer then functions as capture molecule and a second type of aptamer or an antibody acts as detection molecule [175]. Since the sandwich design requires dual binding sites of target, it is difficult to apply when studying the interaction between aptamers and small molecules. Aptamers often completely encapsulate small target molecules by generating a specific binding pocket into their 3D structure. This leaves no epitope free, so a sandwich cannot be made. Moreover, small molecules often only bear few functional groups which can act as potential epitope [10]. When analysing the interaction with small molecules, a competition assay is a more preferred strategy. Competition of an unknown amount of analyte and a fixed amount of labeled reference analyte for binding to immobilized receptor molecules generates a signal which is indirectly proportional to the concentration of analyte [176].

When immobilizing aptamers on more sophisticated solid matrices such as NCD or gold, electronic and opto-electronic binding assays can be developed. These assays make use of intrinsic characteristics of the compounds to be tested, such as electrical charge, MW, size versus charge ratio and conformational alterations. Changes in these characteristics can be detected via different signal generation platforms such as impedance spectroscopy [177, 178], electric field-effect based devices [179], SPR technology [180], quartz crystal microbalance (QCM) [181], atomic force microscopy (AFM) [182] and the recently developed monitoring of R_{th} [183]. These techniques generate detailed information about the interaction of target and aptamer (affinity and kinetics data), often in real-time and without labeling.

NH₂-labeled aptamers can covalently be immobilized onto COOH-modified boron-doped NCD samples. The interaction with target free in solution can then be measured via impedance spectroscopy and R_{th} monitoring. Impedance spectroscopy involves measuring the response (current and its phase) of an electrochemical system to an applied oscillating potential as a function of the frequency. The speed of electron transfer is one of the parameters responding to changes on an electrode surface [178]. Binding of target with immobilized aptamer can result in an altered electron transfer because of two reasons. The bound target can elicit a spatial blocking effect resulting in a decreased electron transfer. Alternatively, a decrease or increase in electron transfer can be attributed to a partial change of aptamer conformation after target binding causing more or less movement of electrons to the electrode surface [184]. The change in electron transfer is expected to be more pronounced at low frequencies because there the impedance is dominated by events in the molecular layer while at higher frequencies impedance is more sensitive to the composition of the buffer solution than to the surface capacitance effects [185]. R_{th} monitoring implicates measuring in real-time the response (transfer of heat) at a solid-liquid interface after exposing the interface to a certain temperature. Transfer of heat is a recently discovered parameter responding to changes on an electrode surface. van Grinsven *et al.* (2012) [183] observed that there is a difference in R_{th} over NCD samples immobilized with dsDNA and ssDNA. dsDNA grafted onto NCD forms a kind of molecular brush (stiff rods) through which

heat is easily transferred. ssDNA coated onto NCD, on the other hand, tends to coil and in this way behaves more like a thermally insulating layer resulting in a decreased transfer of heat. Based on this phenomenon, when monitoring R_{th} upon DNA denaturation, they were able to detect and identify mismatched DNA strands, which is useful for single nucleotide polymorphism (SNP) detection. The technique has also proven to be versatile because since 2012 promising platforms have been developed by combining R_{th} monitoring with MIP target recognition for a.o. the detection of cancer cells and small molecules. Target binding to MIPs generally hampers the transition of heat. R_{th} results have also been obtained for the detection of the peanut allergen Ara h1 via interaction with aptamers [186]. However, the use of aptamers in this kind of set-up is still in its infancy and demands further research.

Biotin-labeled aptamers can covalently be coated onto SA-modified gold sensor chips. Interaction of aptamers and target on these chips can subsequently be measured based on the SPR principle. Changes in MW on the chip elicit alterations in refractive index afterwards translated into a signal. Since the MW of free aptamer is lower than that of aptamer-target complex, target binding can be detected. By using very sensitive instrumentation, weight changes as low as 100 Da can be detected. However, for small molecules such as E2, the generated response will be very limited [180].

For this chapter, several binding assays were tested on a limited amount of aptamer sequences to check their applicability. The most promising type of binding assay was ultimately used to test six selected aptamers of SELEX A and 2 aptamers obtained by SELEX B, as described in Chapter 2.

4.2 Materials and Methods

4.2.1 Materials

DNA was purchased from IDT. E2 Sepharose® 6B affinity chromatography beads and Dexamethasone Sepharose® 6B Novel Immobilized Steroid Beads were supplied by Polysciences Inc. Blocking solutions BSA and marvel and tween 20 were obtained by Sigma Aldrich. Synthetic blocker NB3025 was purchased from NOF corporation. Sonicated salmon sperm ssDNA, SA-HRP and HRP substrate were received from Life Technologies. An iMark™ microplate reader was obtained from Bio Rad (Temse, Belgium). A lightcycler® 1.5 carousel and 1x SYBR mix were derived from Roche. Reacti-Bind™ NeutrAvidin™ coated well plates were supplied by Thermo Fischer Scientific Inc. (Waltham, USA). Steroid hormones and a human E2 ELISA kit were obtained from Sigma Aldrich. EDC and NHS were bought from Perbio Science (Erembodegem, Belgium). NCD samples and an impedimetric/heat-transfer measurement set-up were kindly provided by IMO (Diepenbeek, Belgium). A Biacore T200 SPR system and SPR sensor chips were supplied by GE Healthcare (Uppsala, Sweden). All buffers were homemade.

4.2.2 Enzyme-linked oligonucleotide assay

A 1 h incubation of E2 or dexamethasone sepharose beads (blocked with 1% BSA, 1% marvel, 4% synthetic blocker NB3025 and an excess of sonicated salmon sperm ssDNA) in the presence of 10^8 oligonucleotides (random DNA or aptamer) in 10 mM HEPES at RT was followed by 7 washing steps (3 x with TBS and 4 x with MQ). Subsequently, detection of bound oligonucleotides occurred via interaction of a 5'-biotin label (together with a 5 T linker tagged to the applied oligonucleotides) with SA-HRP in 1x PBS + 0.05% tween 20. After triple washing (2 x with 1x PBS + 0.5% tween 20 and 1 x with 1x PBS), HRP substrate

was added and chemiluminescence was measured at 450 nm in a microplate reader (Figure 33).

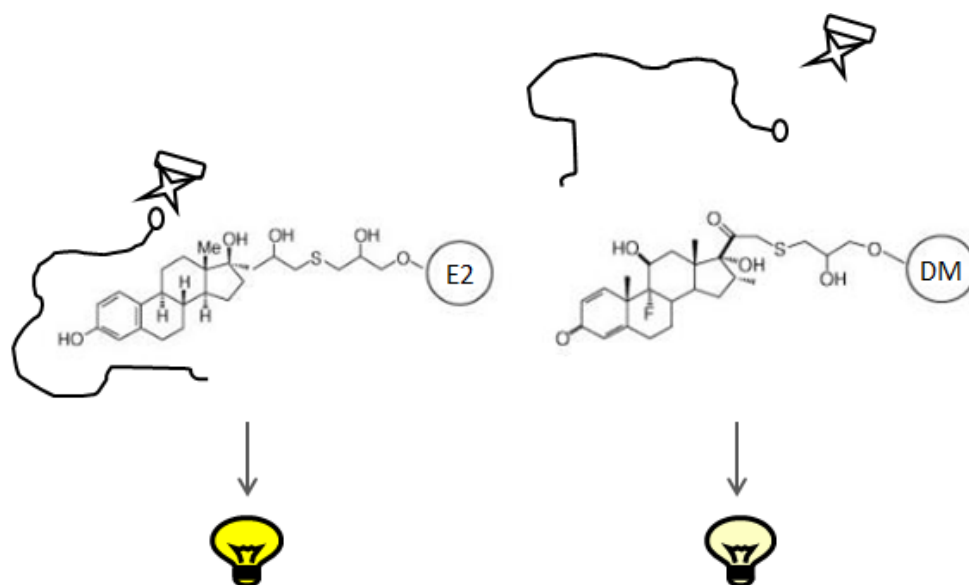


Figure 33: Schematic overview of an ELONA set-up with SA-HRP detection. A fixed amount of biotin tagged aptamers or random DNA was incubated with E2 sepharose beads (left) or dexamethasone sepharose beads (right). Bound DNA was visualized using streptavidin-HRP detection and absorbance was measured at 450 nm.

4.2.3 Quantitative real-time PCR binding assay

E2 or dexamethasone sepharose beads (blocked with 1% BSA, 1% marvel, 4% synthetic blocker NB3025 and an excess of sonicated salmon sperm ssDNA) were incubated with 10^8 oligonucleotides (random DNA or aptamer) in 10 mM HEPES for 1 h at RT. After 7 washing steps (3 x with TBS and 4 x with MQ), the bound oligonucleotides were eluted by incubating the beads-DNA complex in TE buffer + 3 M urea, pH 8 at 80°C for 5 min. Extraction and purification were followed by qRT-PCR (as previously described in section 3.2) to quantify the amount of bound DNA.

4.2.4 Competitive enzyme-linked oligonucleotide assay

Competitive ELONA consisted of 2 steps (Figure 34). In a first step (Figure 34, left), oligonucleotides (random DNA or aptamer) were immobilized onto a Reacti-Bind™ NeutrAvidin™ coated well plate by incubating 10^{13} biotin-tagged oligonucleotides (including a 5T linker) dissolved in 100 μ l 1x TBS + 0.1% BSA + 0.05% tween 20 for 2 h at RT. The aptamers were enlarged using 5 T's at the 5' biotin binding site to give them more flexibility for target-binding. After triple washing with 1x TBS + 0.1% BSA + 0.05% tween 20, 50 μ M E2 dissolved in 100 mM Tris-HCl, 200 mM NaCl, 25 mM KCl, 10 mM MgCl₂, 5% ethanol, pH 8.0 was applied for 1 h at RT. Triple washing was followed by a 10 min elution step with 40 mM Tris-HCl, 10 mM EDTA, 3.5 mM urea, 0.02% Tween 20, pH 8.0 at 80°C. In a second step (Figure 34, right), the eluted fraction from step 1 was incubated for 2 h at RT with 50 μ M HRP-tagged E2 for competitive binding to an anti-E2 antibody immobilized on an ELISA well plate. HRP-tagged E2, anti-E2 antibody and the ELISA well plate were part of a commercially available human E2 ELISA kit. After 4 washing steps with washing buffer included in the kit, HRP substrate made visualization possible. Chemiluminescence was measured at 450 nm in a microplate reader.

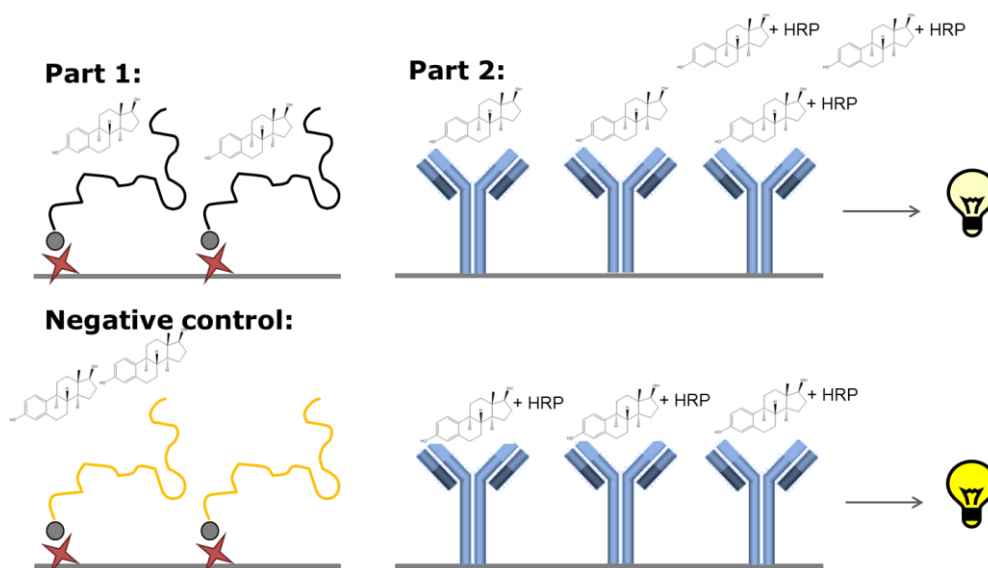


Figure 34: Schematic overview of a two-step competitive ELONA. In a first step, immobilized E2-binding aptamers were exposed to a fixed concentration of E2. After exposure, the bound E2 molecules were eluted and used in the next step. In this step, these E2 molecules went in competition with a fixed amount of HRP-labeled E2 molecules for binding to E2-antibodies. Absorbance was measured at 450 nm. In the negative control condition, aptamers were replaced by random DNA in the first step.

4.2.5 Sensor set-up impedimetric and heat-transfer resistance measurements

The set-up is described in detail by van Grinsven *et al.* (2012) [183]. The most important features are repeated here. The set-up (Figure 35) comprises a flow cell (FC) with an inner volume of 110 μl . Liquids are exchanged with a syringe-driven flow system which automatically injects buffers and reagents in solution. Two thermocouples monitor the temperature of a copper backside contact (T_1) and the temperature of the liquid in the center of the FC (T_2). The heat flow is generated with a power resistor (22 Ω) glued onto the copper block with heat conductive paste. To regulate T_1 , the thermocouple signal is led to a data acquisition unit and from there processed into a PID controller. The calculated output voltage is sent via a second controller to a power operational amplifier

and fed into the power resistor. Sampling of T_1 and T_2 and the voltage values is done at a rate of one measurement per second.

The central element through which the heat is transferred, is a silicon chip covered with a thin layer of NCD. The NCD sample has to be mounted on the backside of a copper block via conductive silver paste. The frontside of the sample is exposed to applied buffer or reagent in the FC with a contact area of 28 mm^2 , sealed by an O-ring.

For impedimetric measurements, two electrodes are present. An NCD working electrode is sealed with the O-ring. It is pressed with the silicon backside on the copper lid. A gold counter electrode is present at a distance of 1.7 mm from the surface of the working electrode. Impedance is measured by applying a fixed AC potential of 10 mV. The response of this potential is an AC current. The impedance is measured for 31 frequencies, equidistant on a logarithmic scale, in a frequency range of 100 Hz to 100 kHz. The duration of a complete frequency sweep is 5.7 s.

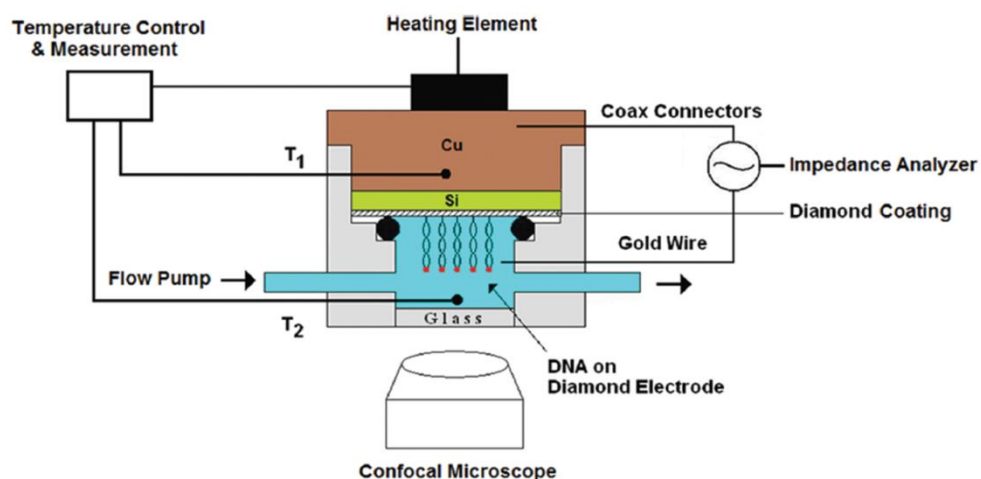


Figure 35: Schematic lay-out of a sensor cell allowing for thermal, impedimetric and optical monitoring [183].

Impedimetric measurement

NH₂-tagged aptamers were covalently immobilized on a COOH-functionalized NCD surface via EDC/NHS coupling. The aptamers were enlarged using 5 T's at the 5' NH₂ binding site to give them more flexibility for target-binding. The NCD sample was incubated 30 min at RT with a 50 µl reaction mixture of 25 mg/ml EDC and NHS in 25 mM 2-(N-morpholino)ethanesulfonic acid (MES) buffer pH 6. After rinsing the sample in 25 mM MES pH 6, 300 pmol of NH₂-tagged aptamer in 100 mM MES pH 5.5 was incubated for 2 h at 4°C. Subsequently, triple washing in 1x PBS was followed by blocking the remaining activated COOH groups via 200 mM ethanolamine in a carbonate buffer pH 9.6 for 1 h. Non-reacted aptamers and ethanolamine were removed by washing the sample in 2x saline-sodium citrate (SSC) buffer + 0.5% SDS for 30 min at RT.

FC injections were programmed as 3 ml injections at a 0.25 ml/min flow rate followed by a 30 min stabilization period. The first injection was preceded by a stabilization period of 40 min. Real-time impedance curves from aptamer-functionalized NCD samples were recorded continuously, both during stabilization and injection periods.

Heat-transfer resistance measurement

NH₂-tagged aptamers were immobilized on a COOH-functionalized NCD surface via EDC/NHS coupling as described before. The heat-transfer device was operated in a temperature-stabilized environment at 19.3°C (± 1°C). Therefore, a higher temperature was needed to ensure significant heat-transfer over the interface. T₁ was set at 37°C. The FC injections were programmed as 3 ml injections at a 0.25 ml/min flow rate followed by a 30 min stabilization period. The first injection was preceded by a stabilization period of 40 min. Next to T₁, T₂ was monitored, both during injection and stabilization, at a rate of one measurement per second. R_{th} was calculated according to the following formula: $R_{th} = (T_1 - T_2) / P$ with T₁ = internal temperature (°C) of the solid phase copper block, T₂ = temperature (°C) measured in the liquid phase FC and P = electrical heating power (W) needed to maintain T₁.

4.2.6 Surface plasmon resonance measurement

SA sensor chips were immobilized by a standard immobilization procedure with filtered 1x HBS-EP⁺ (10 mM HEPES, 500 mM NaCl, 3 mM EDTA and 0,05% v/v surfactant P20) as running buffer. Using SA-biotin coupling, FC 1 and 3 were immobilized with biotinylated random DNA as a reference and FC 2 and 4 with biotinylated aptamer. Both the random DNA and the aptamers were enlarged using 5 T's at the 5' biotin binding site to give them more flexibility for target-binding.

To determine the binding affinity of the selected aptamers, different concentrations of E2 ranging from 0.1 µg/ml to 50 µg/ml were passed over the immobilized FCs via a standard kinetics/affinity procedure with filtered 1x PBS + 10% ethanol as running buffer. Sensorgrams, depicting the response in function of the time, were double referenced. This includes subtraction of blanks (buffer without E2) from the datasets once the contributions from the reference FC are subtracted ($[FC\ 2 - FC\ 1]_{conc\ x} - [FC\ 2 - FC\ 1]_{buffer}$; $[FC\ 4 - FC\ 3]_{conc\ x} - [FC\ 4 - FC\ 3]_{buffer}$). The concentration that led to half the maximum response was defined as the K_D of the aptamer.

To define the epitope specificity of the selected aptamers, fixed concentrations of E2 and six additional steroids (Figure 36) were injected over the immobilized FCs via a standard binding procedure with filtered 1x PBS + 10% ethanol as running buffer. Sensorgrams were double referenced. Subsequently, binding responses were corrected for MW and normalized with respect to the MW adapted response of E2, which was set at 100%. Negative values were set at zero.

All reactions were conducted in triplicate at 25°C.

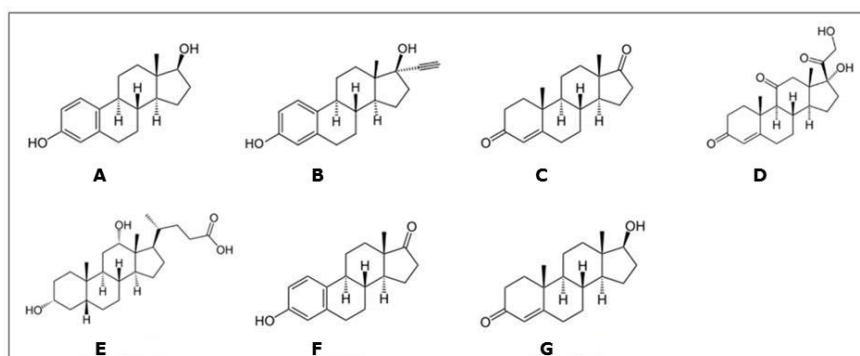


Figure 36: Chemical structure of steroid hormones used for testing epitope specificity of E2 aptamers by means of SPR. (A) E2 (272 Da); (B) α -ethinylestradiol (296 Da); (C) androstenedione (286 Da); cortisone (360 Da); (E) deoxycholic acid (393 Da); (F) estrone (270 Da) and (G) testosterone (288 Da).

4.3 Results

4.3.1 Enzyme-linked oligonucleotide assay

In order to get a general idea about the binding capacity of selected aptamers for E2, an ELONA assay mimicking the SELEX set-up was tested. When focusing on Apta 5A, there was a differential response (Table 7). As was expected, Apta 5A showed a higher interaction (higher OD_{450nm}) with E2 sepharose beads when compared to dexamethasone sepharose beads. However, unexpectedly, the same differential response was seen for random DNA.

Table 7: ELONA assay with SA-HRP detection*.

oligonucleotide	target	OD_{450nm}
Apta 5A	E2 sepharose beads	1.04
Apta 5A	dexamethasone sepharose beads	0.110
random DNA	E2 sepharose beads	0.950
random DNA	dexamethasone sepharose beads	0.100

* OD values measured at 450 nm for oligonucleotides bound on E2 or dexamethasone sepharose beads (n = 2).

Apta 5A: sequence see Table 4 Chapter 2.

Random DNA: 5'-agcagcacagaggtcagttcgctgtaaggtggtcggtgtggcgagtgtgtaggagagattgccta tgcgtgctaccgtgaa-3'.

4.3.2 Quantitative real-time PCR binding assay

As an alternative to ELONA, the SELEX set-up was mimicked but now the amount of bound oligonucleotides was quantified by means of qRT-PCR instead of via enzymatic signal generation. For this type of assay, a differential response was visible when checking the interaction of three different aptamers with E2 sepharose beads when compared to dexamethasone sepharose beads (Table 8). The aptamers showed a higher binding capacity towards E2 sepharose beads (lower C_t) than to dexamethasone beads. Moreover, this differential response disappeared when the interaction of random DNA towards the two types of beads was checked.

Table 8: qRT-PCR binding assay*.

oligonucleotide	target	C_t
Apta 5A	E2 sepharose beads	18.9
Apta 5A	dexamethasone sepharose beads	23.5
Apta 6A	E2 sepharose beads	15.6
Apta 6A	dexamethasone sepharose beads	20.6
Apta 9A	E2 sepharose beads	16.9
Apta 9A	dexamethasone sepharose beads	21.4
random DNA	E2 sepharose beads	25.3
random DNA	dexamethasone sepharose beads	25.9

* C_t values were calculated by qRT-PCR for oligonucleotides bound on E2 or dexamethasone sepharose beads (n=2).

Apta 5A, 6A and 9A: sequences see Table 4 Chapter 2.

Random DNA: 5'-agcagcacagaggtcagttcgctgtaaggtggtcgggtgtggcgagtggttaggagagattgccta tgcgtgtaccgtgaa-3'.

4.3.3 Competitive enzyme-linked oligonucleotide assay

A two-step competitive ELONA was tested as a first type of binding assay where not the target itself, but the aptamer was immobilized. Random DNA resulted in a higher optical signal in the second step when compared to the optical signal generated by Apta 5A (Figure 37). This was consistent with our expectations since random DNA is not able to capture E2 in the first step of the experiment which leads to little or no competition with HRP-tagged E2 in the next step.

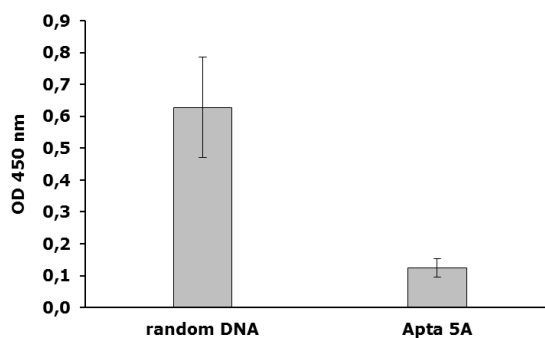


Figure 37: Competitive ELONA. In a first step, E2 was captured by aptamer or random DNA (control condition). In a second step, the captured E2 had to compete with a fixed concentration of labeled E2 for binding to an E2 antibody. Plot shows mean OD values at 450 nm with indicated standard deviations ($n = 3$).

Apta 5A: sequence see Table 4 Chapter 2.

Random DNA: 5'-agcagcacagaggtcagttcgctgtaaggtgggtcggtgtggcgagtggttaggagagattgcctatgctgtctaccgtgaa-3'.

4.3.4 Impedimetric and heat-transfer measurement

Impedimetric monitoring was tested as a tool to calculate the binding affinities of selected aptamers for E2. Therefore, after a 40 minute stabilization period, immobilized Apta 5A was incubated with 50 μ M E2 in 1x PBS + 10% ethanol in the impedimetric measurement set-up. An injection period of 12 min was followed by a stabilization period of 30 min. The binding of E2 to Apta 5A did not occur or had no measurable effect on the impedance over the NCD sample and this for all tested frequencies. The impedimetric signals of both stabilization period 1 and 2 were comparable. Introducing a second injection period, now only injecting 1x PBS + 10% ethanol to remove a possible excess of non-bound E2, was followed by a third stabilization period. Also in this stabilization period, the impedimetric signal stayed unaltered.

Figure 38 shows impedance in function of time at a frequency of 100 Hz. In general, a long time span to initially stabilize the signal and a non-smooth curve can be detected.

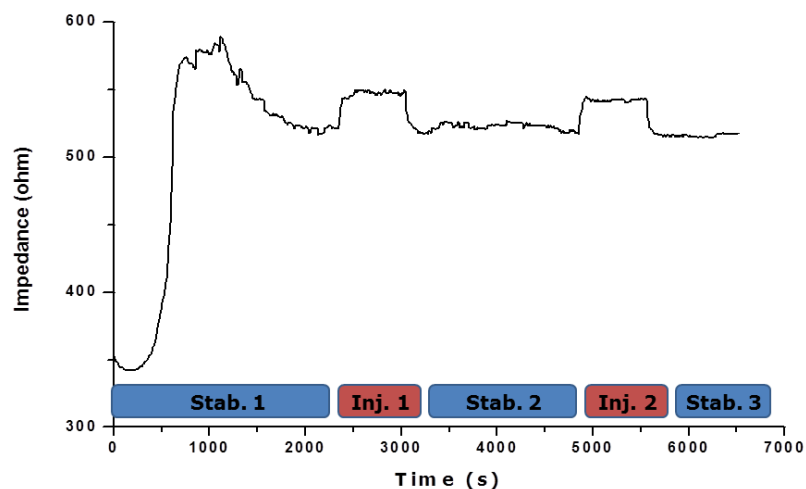


Figure 38: Impedimetric profile of Apta 5A-E2 interaction. NCD sample coated with Apta5A via EDC/NHS coupling was exposed to a fixed concentration of E2. Apta 5A: sequence see Table 4 Chapter 2. Impedance was measured at 100 Hz and 37°C. (Stab. 1) Stabilization in 1x PBS + 10% ethanol; (Inj. 1) Injection of 50 μ M E2 in 1x PBS with 10% ethanol with an injection rate of 0.25 ml/min; (Stab. 2) Stabilization in 50 μ M E2 in 1x PBS with 10% ethanol; (Inj. 2) Injection of 1x PBS + 10% ethanol with an injection rate of 0.25 ml/min and (Stab. 3) Stabilization in 1x PBS + 10% ethanol.

Additionally, R_{th} monitoring was tested as a tool to calculate the binding affinities of selected aptamers for E2. Therefore, after a 40 minute stabilization period, immobilized Apta 5A was incubated with 50 μ M E2 in 1x PBS + 10% ethanol in the heat-transfer set-up. An injection period of 12 min was followed by a stabilization period of 30 min. As shown in Figure 39, the binding of E2 to Apta 5A did not occur or had no measurable effect on the heat-transfer over the NCD sample. The R_{th} signals of both stabilization period 1 and 2 were comparable. Introducing a second injection period, now only injecting 1x PBS + 10% ethanol to remove a possible excess of non-bound E2, was followed by a third stabilization period. Also in this stabilization period, the R_{th} signal stayed unaltered.

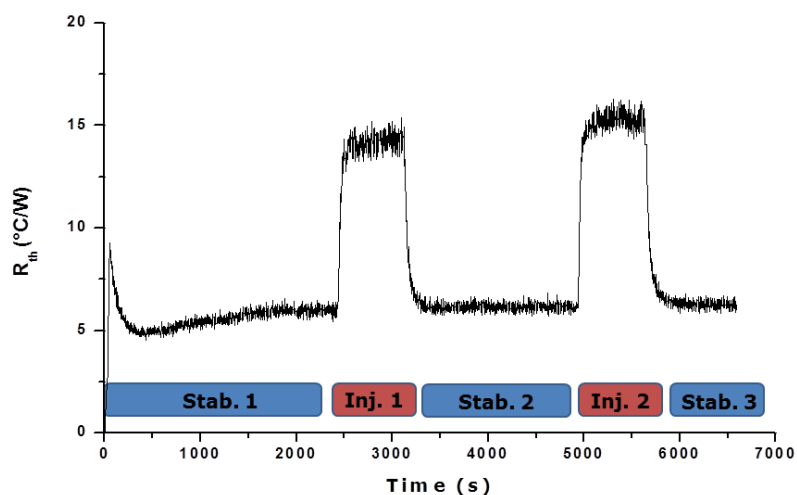


Figure 39: Heat-transfer profile of Apta 5A-E2 interaction. NCD sample coated with Apta5A via EDC/NHS coupling was exposed to a fixed concentration of E2. Apta 5A: sequence see Table 4 Chapter 2. Heat-transfer was measured with T_1 set at 37°C. (Stab. 1) Stabilization in 1x PBS + 10% ethanol; (Inj. 1) Injection of 50 μ M E2 in 1x PBS with 10% ethanol with an injection rate of 0.25 ml/min; (Stab. 2) Stabilization in 50 μ M E2 in 1x PBS with 10% ethanol; (Inj. 2) Injection of 1x PBS + 10% ethanol with an injection rate of 0.25 ml/min and (Stab. 3) Stabilization in 1x PBS + 10% ethanol.

4.3.5 Surface plasmon resonance measurement

Ultimately, a binding assay based on the SPR principle was tested and trial experiments with immobilized aptamer and E2 free in solution showed good results. Therefore, binding characteristics of several E2 aptamers were examined towards different concentrations of E2. An example of a sensorgram is given in Figure 40. Since the sensorgrams had not sufficient curvature and approximated a square-wave pulse (indicating rapid association and dissociation), kinetic information was not sufficient enough for reliable evaluation (Figure 41A). Therefore, only an affinity constant K_D could be defined (Figure 41B) [187].

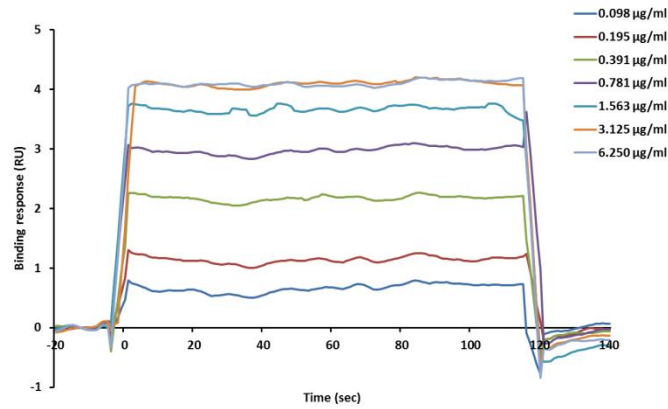


Figure 40: Double referenced sensorgram obtained by SPR methodology showing a fast association and dissociation of Apta 1B interacting with different concentrations of E2.

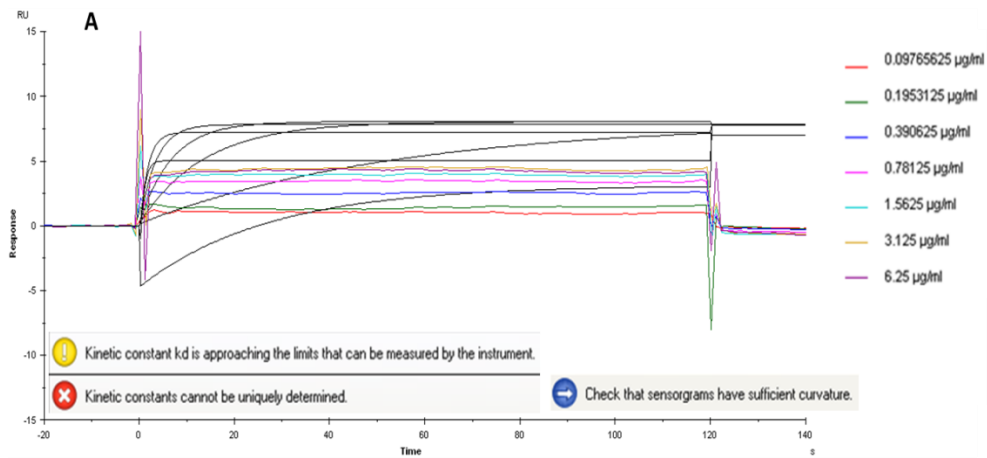


Figure 41A: Kinetics results obtained by SPR methodology for Aptamer 1B. The results for kinetics are displayed as fitted curves overlaid in black on the experimental data. To fit, a predefined 1:1 model was used. Warnings are given by the software.

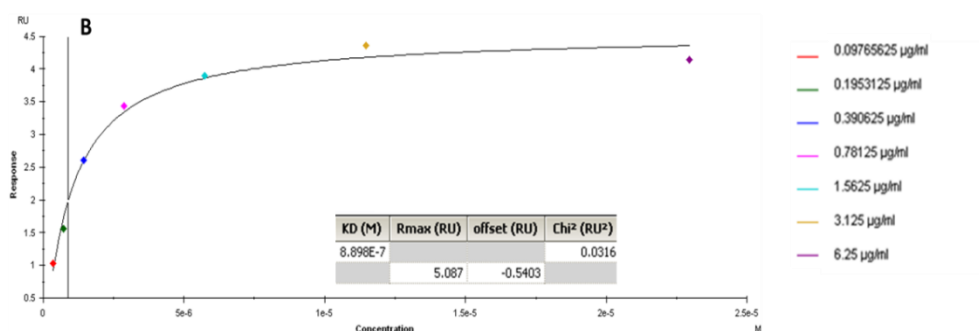


Figure 41A: Affinity results obtained by SPR methodology for Apta 1B. The reported K_D value is marked on the plot as a vertical line. K_D , R_{max} , offset and Chi^2 are given by the software.

Apta 1B: sequence see Table 4 Chapter 2.

Random DNA: agcagcacagaggtcagttcgctgtaaggtggtcggtgtggcgagtggttaggagagattgcacctatgctgtaccgtgaa-3'.

The K_D values of the six different ssDNA aptamers of SELEX A were in the range of 27 – 124 μM (Table 9). Among them, the K_D of Apta 8A (124 μM) was remarkably higher than the other aptamers. Therefore, this aptamer was not further analyzed. The binding affinities of the two aptamers from SELEX B were 10 to 100 times higher than those of SELEX A, which is represented by their K_D values of 0.9 and 6 μM (Table 9). In addition to the calculated K_D values for all aptamers, also Chi^2 and R_{max} are given in Table 9. Chi^2 forms an indicator of how closely fitted curves (which are applied to determine the K_D value) agree with the experimental data. Ideally, Chi^2 is lower than 10% of R_{max} . R_{max} is the maximum analyte binding capacity of the surface, expressed in RU.

Table 9: K_D values of selected E2 aptamers as determined by SPR methodology, linked to Chi^2 and R_{max} of a 1:1 model fit.

Clone ID	K_D value (μM)	Chi^2	R_{max} (RU)
Apta 5A	27.0	0.681	9.77
Apta 6A	36.0	0.274	7.97
Apta 8A	124	0.0391	3.07
Apta 9A	52.0	1.18	16.0
Apta 11A	51.0	0.0777	15.1
Apta 13A	63.0	2.72	25.8
Apta 1B	0.900	0.0316	5.09
Apta 19B	6.00	0.0125	2.32

Apta 5A, 6A, 8A, 9A, 11A, 13A, 1B and 19B: sequences see Table 4 Chapter 2.

Random DNA: 5'-agcagcacagaggtcagttcgctgtaaggtggtcggtgtggcgagtggttaggagagattgcacctatgctgtaccgtgaa-3'

In order to assess the specificity of the selected aptamers and to elucidate the most important interacting functional groups of E2 with each of these aptamers, six steroid hormones (α -ethinylestradiol, androstenedione, cortisone, deoxycholic acid, estrone and testosterone) were selected based on their structural similarity to E2. By means of SPR methodology, binding characteristics of each aptamer towards these hormones were examined. Results showed that the aptamers of SELEX A behave differently regarding the tested steroids in comparison to those of SELEX B. The 5 aptamers of SELEX A showed various binding patterns (Figure 42). Besides E2, they were all able to bind α -ethinylestradiol and testosterone to a greater or lesser degree. Regarding other steroids, however, aptamer-target interaction was dependent on the binding characteristics of the particular aptamer. Apta 6A showed a clear distinction between binding steroids E2, α -ethinylestradiol and testosterone and non-binding steroids androstenedione, cortisone, deoxycholic acid and estrone. The other aptamers of SELEX A were able to bind E2, α -ethinylestradiol and testosterone. Their binding responses towards other steroids, however, differed dependent on the particular aptamer.

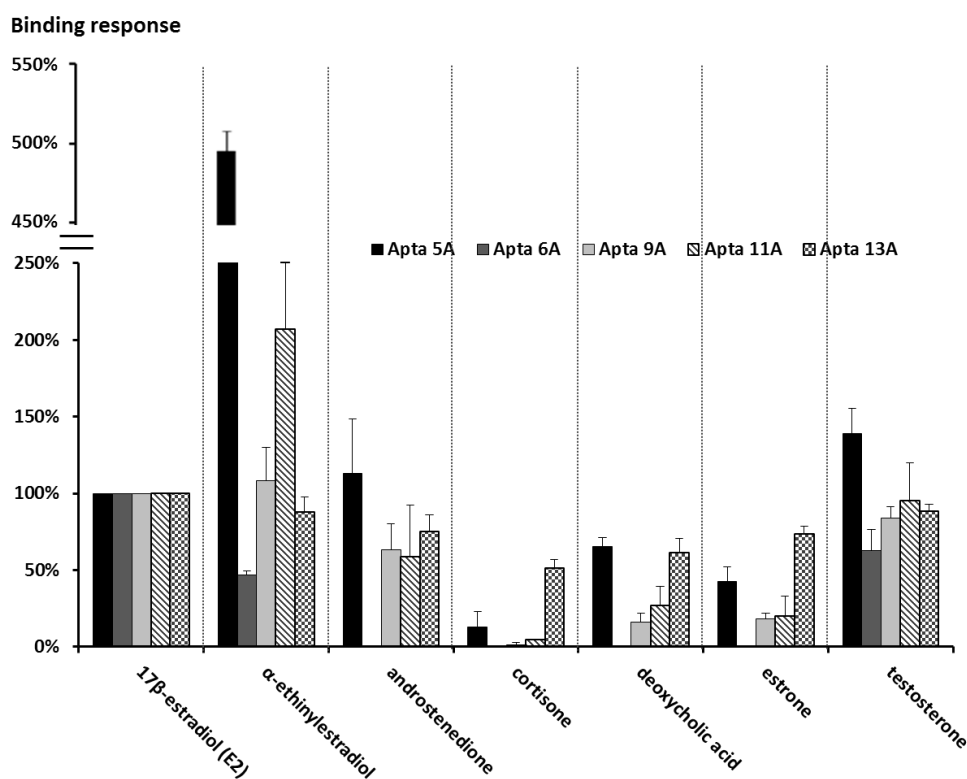


Figure 42: Binding responses of selected E2 aptamers of SELEX A towards several steroid hormones determined by SPR methodology. The average binding responses are presented as a percentage of the E2 binding response (which was set at 100%) \pm standard deviation (N = 3).

Apta 5A, 6A, 8A, 9A, 11A and 13A: sequences see Table 4 Chapter 2.

Random DNA: 5'-agcagcacagaggtcagttcgctgtaaggtggtcggtgtggcgagtgtgtaggagagattgccct atgctgtctaccgtgaa-3'.

Conversely, both aptamers of SELEX B were similar in their binding pattern (Figure 43). Both were binding E2 as well as α -ethinylestradiol and estrone. They were not able to bind androstenedione, cortisone, deoxycholic acid and testosterone. Small differences in binding responses towards the three binding steroids could be seen. α -ethinylestradiol showed a slightly higher binding response and estrone a lower binding response compared with E2.

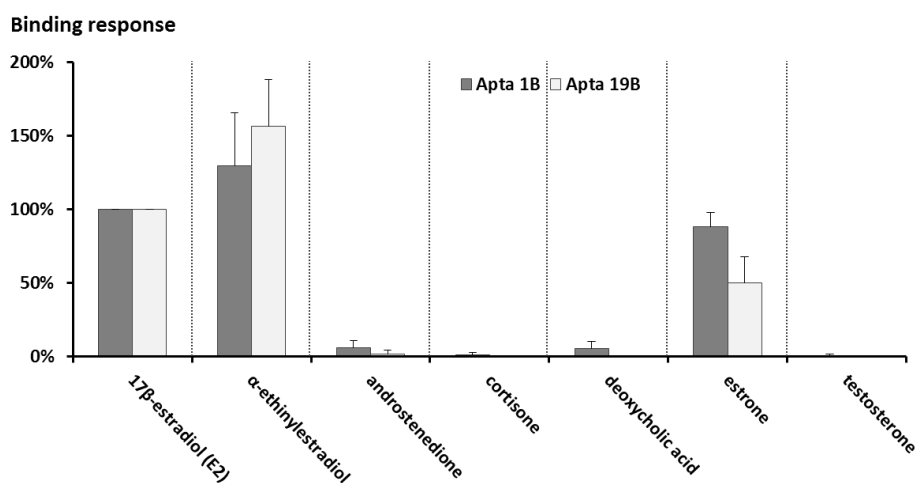


Figure 43: Binding responses of selected E2 aptamers of SELEX B towards several steroid hormones determined by SPR methodology. The average binding responses are presented as a percentage of the E2 binding response (which was set at 100%) \pm standard deviation (N = 3).

Apta 1B and 19B: sequences see Table 4 Chapter 2.

Random DNA: 5'-agcagcacagaggtcagttcgctgtaaggtggtcgggtgtggcgagtggttaggagagattgccctatgctgtctaccgtgaa-3'.

4.4 Discussion

Detailed characterization of selected aptamers is of crucial importance for their ultimate application efficiency. During this dissertation, several types of binding assays were tested making use of a limited amount of selected E2-binding aptamers. A first group of assays mimicked the original selection design. A second group of binding assays showed more resemblance with potential future aptasensing. Ultimately, the most promising type of binding assay was used to characterize several selected E2-binding aptamers.

The ELONA assay with immobilized target and SA-HRP signal generation suffered from high noise. The binding response of aptamer towards E2 sepharose beads was 9.45 x higher than its binding response towards dexamethasone beads. However, a comparable binding pattern was seen for random DNA, with a binding response which was 9.5 x higher for E2 beads than for dexamethasone beads. Therefore, it is not clear if the response of aptamer onto E2 beads is caused by specific aptamer-target interaction or has to be considered as a false positive result due to non-specific DNA interactions and/or cross-talk effects of signal generators with E2 sepharose beads.

The qRT-PCR binding assay, which is based on the same principle as the ELONA assay but with a different read-out system, suffered from less noise. This assay showed a higher binding level of aptamer on E2 sepharose beads than on dexamethasone sepharose beads, for all three tested aptamers. Moreover, this differential binding pattern was not present when comparing the interaction of random DNA with the two types of beads. The latter suggests that the high noise of random DNA onto E2 sepharose beads as seen via ELONA was mainly due to cross-talk between SA-HRP labels with this type of beads. However, qRT-PCR showed a substantial amount of aptamer binding to the control beads. This can potentially be attributed to the high sensitivity of this read-out technique, visualizing even the slightest amount of remaining oligonucleotide sequences. Increasing the stringency of washing steps with 0.5% dextran sulfate resulted in the loss of both specific and aspecific interaction.

The qRT-PCR binding assay seems a promising tool to get a first idea about the binding capacity of aptamers to their target. However, for full characterization of aptamers, this technique has too many drawbacks. It is a labor-intensive, time-consuming method, not suitable for high-throughput screening. It tests the capacity of aptamers to bind immobilized target which differs from target in its native state. And moreover, calculation of affinity and kinetic values is almost impossible. Therefore, this technique was not used to test all aptamers selected by SELEX A and B.

The first assay with immobilized aptamer which was tested, was a two-step competitive ELISA. We chose for a two-step assay, since we did not know if our aptamers are able to interact with enzyme-linked E2. By splitting up the assay in two parts, the potential problem of lower affinities for enzyme-modified E2 is circumvented. After optimization of assay buffer, the assay offered promising results for one aptamer. However, the assay did not offer the same positive results for other aptamers which were tested. Because of the labor-intensive character of this assay and the lack of reproducibility, we did not continue to work with this type of assay.

More sophisticated binding assays requiring specialized instrumentation which were tested were impedimetric and R_{th} monitoring. Therefore, aptamer was immobilized onto an NCD surface and binding of target was registered by monitoring the change in impedance and R_{th} over the surface. Via these techniques, we were not able to visualize the interaction between aptamer and target. A possible explanation for this absent binding response lies in the fact that the applied target is very small and has a MW of only 272 Da. Therefore, changes in impedance and R_{th} can hardly be elicited via a spatial blocking effect induced by E2 itself. Changes solely can come from conformational alterations of the aptamer after target-binding. These changes are aptamer dependent and can, for some aptamers, be very limited or even absent. Aptamer selection strategies generally produce well-folded aptamers that do not show a conformation-switching architecture [188]. Regarding R_{th} , it is also possible that E2 binding locally affects the insulating layer on the surface but is not effecting R_{th} in general since heat can still escape due to gaps in between the different immobilized aptamers. Whereas denatured DNA can be seen as one blanket of ssDNA on the NCD surface, E2-aptamer complexes can be seen as multiple mini-blankets on dedicated spots spread over the surface [183]. Moreover, aptamer-target interaction is a dynamic process and not an on/off phenomenon which makes a drastic influence on the insulating layer on the surface rather unlikely. Research about the use of aptamers in an R_{th} set-up is still in its infancy and needs further attention to clarify its applicability. Recently, Peeters *et al.* (2015) were the first one to show R_{th} based detection of protein (Ara h 1) making use of aptamer-type receptors and results indicated detection limits in the lower nM

range [186]. Impedimetric monitoring, on the other hand, already showed its potency to characterize aptamers targeting proteins such as IgE [189] and thrombin [190] and small molecules such as anatoxin-a [191] and progesterone [184]. However, it is unclear if this technique is general applicable to all kind of aptamers or is limited to aptamers with a conformation-switching architecture.

Later on, we switched from impedimetric and R_{th} monitoring to monitoring based on the SPR principle. This technique turned out to be a useful tool to test our E2 aptamers and was therefore applied for the characterization of 6 aptamers obtained by SELEX A and 2 aptamers selected during SELEX B.

All selected aptamers showed affinities in the low μM range as determined by SPR methodology (Table 9). In general, K_D values of aptamers for small molecules such as diclofenac, tryptophan and ATP are typically in the high nM to low μM range [192], which is markedly higher than aptamers for proteins and peptides such as thrombin and IgE [193]. Moreover, aptamers for hydrophobic molecules typically show lower affinities than aptamers for hydrophilic molecules, since hydrophobic molecules are less attractive for strongly hydrophilic ssDNA [194]. E2 is a hydrophobic compound containing two polar groups [129]. Therefore, detecting K_D values in the low μM range in this study was reasonable. The higher affinities of the aptamers of SELEX B in comparison with SELEX A are due to the more stringent selection character of SELEX B.

Ultimately, both sets of selected E2-binding aptamers have shown to be oriented towards different functional groups of E2. Their binding behavior towards several steroids was different during measurement by SPR methodology (Figure 42 and 43). The 5 tested aptamers of SELEX A showed various binding patterns. Besides E2, they were all able to bind α -ethinylestradiol and testosterone. Regarding other steroids, however, aptamer-target interaction was dependent on the binding characteristics of the particular aptamer. Apta 6A showed a clear distinction between binding steroids E2, α -ethinylestradiol and testosterone and non-binding steroids androstenedione, cortisone, deoxycholic acid and estrone. Therefore, the epitope for this aptamer could be defined as the upper part of the B, C and D ring of the cyclopentanoperhydrophenanthrene ring system of

steroids (Figure 44a). This epitope is present on the binding steroids and absent on the non-binding steroids. The other aptamers of SELEX A were also able to bind E2, α -ethinylestradiol and testosterone. Their binding responses towards other steroids, however, were different dependent on the particular aptamer. Various binding behaviors suggest that these aptamers are all oriented towards slightly different epitopes of E2. Based on our current information, the epitopes of these aptamers cannot be defined. Epitope heterogeneity may be caused by the large structural difference between E2 and dexamethasone, the countermolecule used during SELEX A. Conversely, both aptamers of SELEX B were similar to each other in binding pattern. Both were binding E2 as well as α -ethinylestradiol and estrone. They were not able to bind androstenedione, cortisone, deoxycholic acid and testosterone. These results indicate that both aptamers are directed towards the hydroxylated aromatic A ring (Figure 44b). Small differences in binding responses towards the three binding steroids could be seen. α -ethinylestradiol showed a slightly higher binding response and estrone a lower binding response compared with E2. This is probably due to structural differences surrounding the defined epitope which a.o. leads to different torsion angles between the A ring and rings B, C and D as well as to different charge distributions over the entire molecules [129]. This suggests that not only a specific epitope, but also the area surrounding an epitope is crucial for aptamer-target interaction.

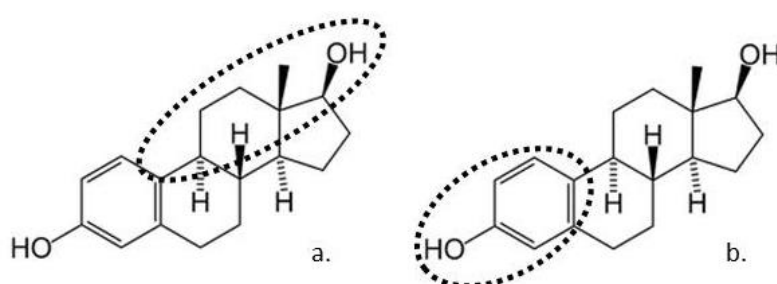


Figure 44: Schematic illustration of the chemical structure of E2 with the most crucial epitopes for binding of Apta 6A (a) and Apta 1B / Apta 19B (b).

4.5 Conclusion and future perspectives

To the best of our knowledge, this study is the first one to select aptamer sets against different functional groups of E2.

Several types of binding assays were tested prior to E2 aptamer characterization in order to explore their applicability. Binding assays mimicking the original SELEX design, thus making use of E2 sepharose beads, suffered from high noise. This noise was due to non-specific interactions of signal generators or DNA with the immobilization matrix. When immobilizing aptamers instead of target, target-aptamer interaction could not efficiently be detected via a two-step competitive ELONA, impedimetric and R_{th} monitoring. SPR analysis, on the other hand, turned out to be a promising tool to characterize the E2 aptamers and was therefore applied for further analysis.

Since aptamer-E2 interaction was characterized by a very fast association and dissociation, kinetic analysis revealing both association (k_a) and dissociation (k_d) constants could not be performed. However, affinity analysis and calculation of affinity constants (K_D) was possible. Both selected aptamer sets displayed affinities in the low μM range. Moreover, specificity studies revealed epitope specificity as was intended.

Although it was possible to detect E2-aptamer interaction by means of the highly sensitive Biacore T200, signal generation was limited. In this set-up, the magnitude of the signal is directly correlated to the change in mass after binding and since binding of the low MW molecule E2 only adds 272 Da per bound molecule, the generated response is restricted and really on the edge of what can be measured. If in future these aptamers will be used for in-field monitoring, higher signal generation is desired.

In view of increasing signals generated by aptamer-small molecule interaction, the principle of TISD will be explored in the next chapter. This comprises hybridization of aptamers with (partially) complimentary oligonucleotides. After incubation of this complex with target, the complex is disrupted and aptamer-target interaction takes place. Instead of monitoring aptamer-target interaction,

the transition of dsDNA to ssDNA will be monitored. This transition leads to significant detectable changes independent of the nature of the target [195].

5

Enhancement of signal generation via TISD

Since direct detection of aptamer-small molecule interaction often leads to limited signal generation, exploring alternative detection approaches seems appropriate. These approaches are preferably not dependent on the nature of the target itself, so that they can be used for all kinds of targets. In this chapter, we will explore the potential of the TISD strategy. Aptamers can switch from a duplex structure with a complementary strand to a complex structure with target. They can switch from duplex to complex upon target addition and measuring this switch may yield a significant signal change.

5.1 Introduction

In conventional aptasensors, aptamer-target interaction is often monitored based on changes in mass or electrical properties upon target binding at the mercy of the target and its characteristics. Conventional aptasensors however stumble when it comes to the detection of small molecules. Signal generation is limited, as demonstrated in Chapter 4 of this dissertation, since small molecules do not carry a significant size, weight or charge [195].

Aptasensors making use of a target induced strand displacement (TISD) strategy introduce a new freedom in small molecule detection, acting independently of a target's nature. An aptamer is hybridized with a (partially) complementary oligonucleotide strand and subsequently, aptamer-target interaction leads to the dissociation of this oligonucleotide duplex. Monitoring the transition from ds to ss oligonucleotides makes large signal generation possible, also for small molecules [195]. This approach can be used for both DNA and RNA aptamers, in solution and on surfaces. Although many studies use this principle for the detection of ATP [196], this method has also been used to detect other small molecules such as theophylline [197], histidine [198], ochratoxin A (OTA) [199], guanosine triphosphate (GTP) [200] and arginine [201].

An excellent selectivity is one of the advantages of this type of aptasensing. High selectivity arises not only from the specificity of the aptamer itself, but also

from the additional stringency due to the competition between the oligonucleotide duplex and the aptamer-target complex [202].

Aptasensing based on TISD can further be classified into a signal-off, a signal-on and a label-free mode [203].

In signal-off mode, the presence of target is determined from signal suppression. Wu *et al.* (2007) designed a signal-off assay for adenosine detection. Ferrocene labeled aptamers were confined near an electrode surface through hybridization with a thiolated complementary sequence which was immobilized onto a gold electrode. In the absence of adenosine, the redox tag gave strong electrochemical signals (redox current). The introduction of adenosine resulted in the dissociation of the ferrocene labeled aptamers from the electrode surface and the electrochemical signal decreased. Adenosine could be quantified over a concentration range of 0.1 to 10 μM . This range was 10 times wider than when these aptamers were used in other set-ups. The detection limit was 500-fold lower than the literature value obtained using a label-free and reagentless aptamer-based sensor and more than 3 orders of magnitude lower than the detection limit using a colorimetric method based on gold nanoparticle aggregation [204].

In signal-on mode, aptamer-target interaction leads to signal enhancement. Han *et al.* (2009) reported a signal-on strategy for ATP detection. Unlabeled ATP aptamer sequences were hybridized with their complementary sequences which were immobilized onto a gold electrode. Incubation of this dsDNA with ATP resulted in the dissociation of aptamer-target complexes from the electrode. Subsequently, the remaining immobilized ss complementary sequences were further hybridized with a third sequence, a ferrocene labeled sequence, resulting in the emergence of an electrochemical signal. The detection range was from 10 to 100 μM , which is comparable to what was obtained by using this aptamer in a different kind of set-up [205].

In order to avoid complicated labeling procedures potentially reducing the aptamer's bioaffinity, increasingly attractive attention has been focused on the development of a label-free mode. Via a faradaic impedance spectroscopy assay based on target-induced aptamer displacement, Peng *et al.* (2009) detected

lysozyme. A duplex of lysozyme binding aptamer and partial complementary DNA was tethered on the surface of a gold electrode. Introducing lysozyme induced the displacement of the aptamer from the complex on the electrode into solution, decreasing the electron transfer resistance of the sensor. This assay had a detection limit of 70 pM, which is much lower than the previously reported value of 36.0 nM [206]. Das *et al.* (2012) recently suggested to mask the initial charge of aptamers by hybridizing them with partially complementary peptide nucleic acids (PNA) tagged with positively charged amino acids. When the target of interest displaced the neutralizing PNA, a shift in charge was the result. This set-up enabled the researchers to detect a whole panel of molecules ranging from DNA and RNA to cocaine, ATP and thrombin [195]. Shukoor *et al.* (2012) functionalized two aptamer-modified AuNPs with complementary strands of DNA, each aptamer recognizing only one of two proteins, either PDGF or VEGF. Color change from red (dispersed AuNP's) to purple (aggregated AuNP's) occurred only when both protein targets are recognized [207].

At first sight, the strategy of aptasensing by means of TISD seems easy to generalize for any aptamer without in-depth knowledge about the nature of both aptamer and target. However, this assumption of simplicity is not fully consistent with reality. Especially the choice of the complementary strand is not as simple as first could be thought. Only when the target of interest binds the aptamer more strongly, rapidly and robustly than the complementary strand binds the aptamer, strand displacement and thus target detection can be achieved [195].

The purpose of our work described in this chapter was to develop a label-free and sensitive aptasensor based on a TISD strategy with the aim of increasing signal generation when detecting small molecules. At first, the usefulness of two sensing platforms (R_{th} monitoring and SPR based detection) for monitoring the transition of ds to ssDNA was investigated. Secondly, we tried to incorporate one of our own aptamers in a TISD set-up making use of our SPR sensing platform. Thirdly, we tried to translate TISD experiments performed by other researchers to our SPR sensing platform by using their aptamers.

5.2 Materials and Methods

5.2.1 Materials

DNA was bought from IDT. EDC and NHS were obtained from Perbio Science. E2, thrombin, adenosine, ATP and SA were supplied by Sigma Aldrich. The R_{th} device and NCD samples were kindly provided by IMO and a Biacore T200 SPR device and sensor chips were bought from GE Healthcare. All buffers were home-made.

5.2.2 Transition of dsDNA to ssDNA via thermal denaturation in an R_{th} set-up

In a first step, 300 pmol NH_2 -tagged probe DNA (Table 10) was covalently linked on a COOH-functionalized NCD surface via EDC/NHS coupling as described in section 4.2.5.

A second step was comprised of hybridization of target DNA (Table 10) to the immobilized probe DNA, by incubating the DNA-modified NCD sample for 2 hours at 30°C with 1200 pmol of target DNA in 10x PCR buffer. To remove excess of target DNA, a 30 min washing step in 2x SSC + 0.5% SDS was followed by two 5 min washing steps in 0.2x SSC.

Table 10: Probe and target DNA used for thermal denaturation in an R_{th} set-up.

	Sequence (5' → 3')
Probe DNA	/5AmMC6/TGAGTCCAACCACACCA
Target DNA	TGGTGTGGTTGGACTCA

A third step included R_{th} monitoring during thermal denaturation of dsDNA into a heat-transfer device. Therefore, during the measurement, T1 was increased

from 25°C to 75°C with a heating rate of 1°C/min and cooled back to 35°C at the same rate by reducing the heating power. The heating/cooling run was repeated once. R_{th} was calculated according to the following formula: $R_{th} = (T_1 - T_2) / P$ with T_1 = internal temperature (°C) of the solid phase copper block, T_2 = temperature (°C) measured in the liquid phase FC and P = electrical heating power (W) needed to maintain T_1 .

5.2.3 Transition of dsDNA to ssDNA via chemical denaturation in an SPR set-up

At first, 200 pmol biotin-tagged probe DNA (Table 11) was covalently linked on an SA chip via a standard immobilization procedure (SA-biotin coupling procedure) with filtered 1x HBS-EP⁺ (10 mM HEPES, 500 mM NaCl, 3 mM EDTA and 0.05% v/v surfactant P20) as running buffer.

Secondly, 800 pmol target DNA (Table 11) was hybridized to the immobilized probe DNA via a manual run with filtered 10 mM HEPES + 5 mM Ca²⁺ as running buffer. Target DNA was injected for 480 sec with a flow rate of 10 µl/min. To remove excess of target DNA, hybridization was followed by a 300 sec washing step with 10 mM HEPES + 5 mM Ca²⁺.

Table 11: Probe and target DNA used for chemical denaturation in an SPR set-up.

	Sequence (5' → 3')
Probe DNA	/5Biosg/TTTTT TTCACGGTAGCACGCATAGGTCAAATTCGGCTTGGTCAGGCCAAATTTAGTTCGACATAAGAAGCTGA CCTCTGTGCTGCT
Target DNA	AGCAGCACAGAGGTCAGTTCTTATGTGCGAACTAAATTTGGCCTGACCAAGCCGAATTTGACCTATGC GTGCTACCGTGAA

Chemical denaturation of dsDNA was elicited by 9 successive injections (60 or 120 sec; flow rate 10 µl/min) with increasing concentrations of NaOH (1 mM; 2 mM; 3 mM; 4 mM and 10 mM).

5.2.4 Transition of dsDNA to ssDNA via target induced strand displacement in an SPR set-up

SA chips (Figure 45) were immobilized with biotin-tagged probe DNA as described in section 5.2.3. C1 chips (Figure 45) were immobilized with NH₂-tagged probe DNA or SA via a standard immobilization procedure (covalent EDC/NHS coupling) with filtered 1x HBS-N buffer (10 mM HEPES, 150 mM NaCl) as running buffer. Biotin-labeled DNA was attached to immobilized SA performing a manual run with 1x HBS-EP⁺ + 350 mM NaCl as running buffer via an injection of 1800 sec with a flow rate of 10 μ L/min.

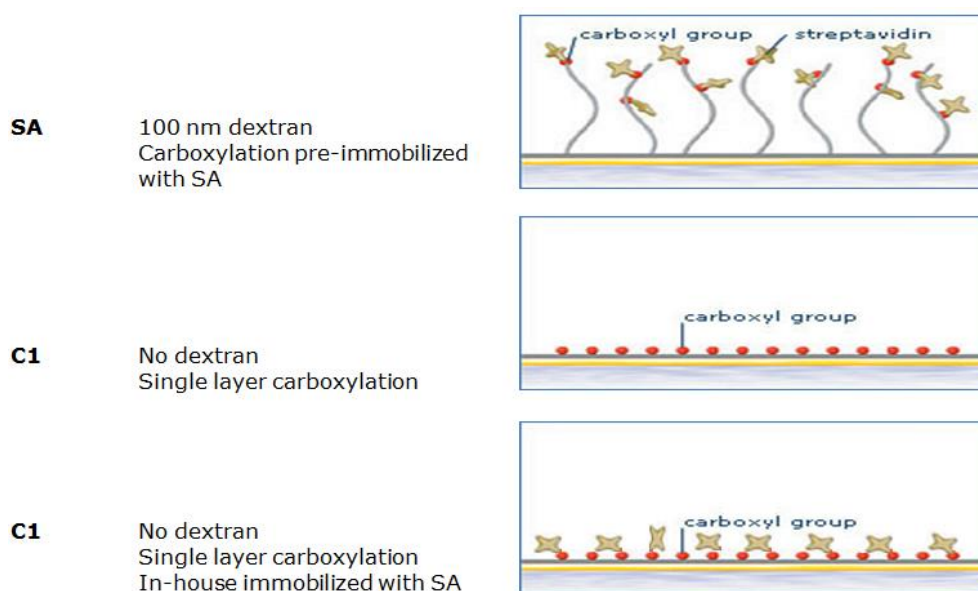


Figure 45: Overview of SPR chips used to test TISD [46].

Aptamer was hybridized to the immobilized probe DNA as described before. All hybridizations were performed under the same conditions (identical buffer and temperature).

Ultimately, to induce strand displacement, dsDNA was exposed to a high concentration of target via an injection of 1800 sec with a flow rate of 10 μ L/min.

The buffer used as running buffer and to dissolve target was dependent on the tested aptamer (Table 12).

Table 12: Applied buffers and target concentrations for TISD experiments.

Aptamer	Applied buffer	Applied target concentration
Apta 13A	1x PBS + 10% alcohol	63 μ M E2
Apta Das	1x PBS	8.2 nM thrombin
Apta Wu	1x PBS + 0.3 M NaCl	10 μ M adenosine
Apta Han	10 mM HEPES + 50 mM NaClO ₄	1 mM ATP
Apta Yang	20 mM Tris + 1 M NaCl + 10 mM MgCl ₂	63 μ M E2

Figure 46 represents the intended TISD SPR set-up and results which were to be expected.

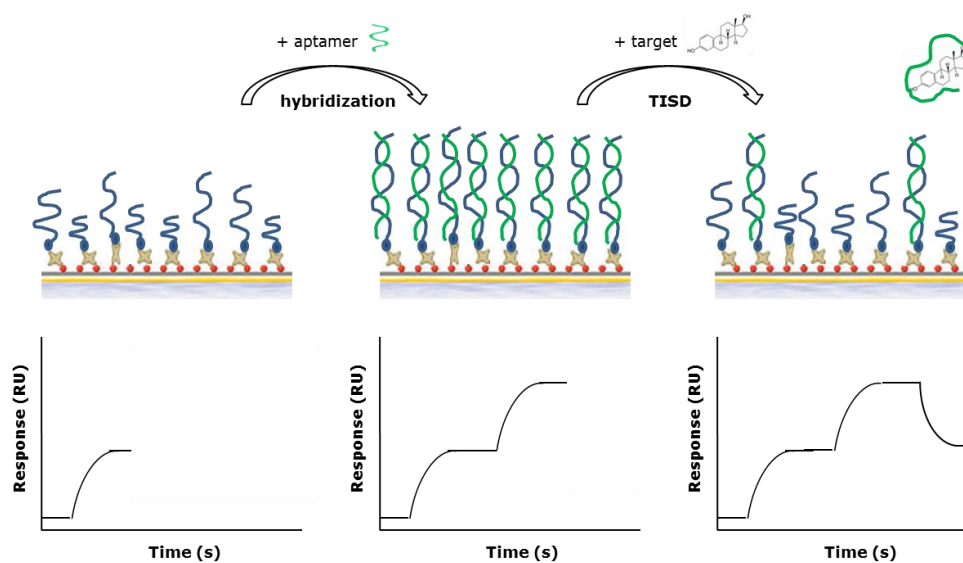


Figure 46: Schematic representation of a TISD experiment in an SPR set-up (up) in combination with results which can be expected (down).

5.3 Results

5.3.1 Transition of dsDNA to ssDNA via thermal denaturation in an R_{th} set-up

Figure 47 shows the behavior of dsDNA upon thermal denaturation in an R_{th} set-up. In the beginning of the measurement, an R_{th} of 7.8 °C/W was found. The R_{th} started to increase around 46°C and reached a new equilibrium R_{th} value of 9.2 °C/W at and above 55°C. The midpoint of the transition was found at 49.3°C (blue curve). During a second heating run, an almost T1 independent R_{th} value of 9.1 °C/W was observed (black curve).

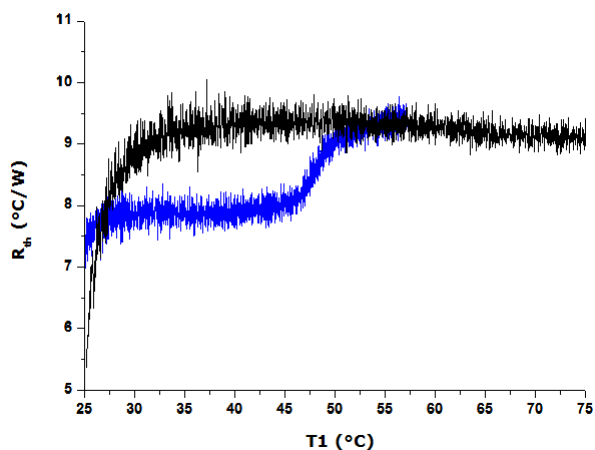


Figure 47: R_{th} in function of temperature T1 during thermal denaturation of dsDNA (blue curve) compared to ssDNA (black curve).

5.3.2 Transition of dsDNA to ssDNA via chemical denaturation in an SPR set-up

Figure 48 shows the behavior of dsDNA upon chemical denaturation with NaOH in an SPR set-up. After conditioning the surface, biotinylated DNA was immobilized to a binding response of 708 RU (Figure 48a). In a second step, immobilized probe DNA got hybridized with its target DNA and non-hybridized

complementary strands were washed away. Hybridization resulted in a response of 407 RU (Figure 48b). Successive steps with increasing concentrations of NaOH led to a total decrease of 487 RU corresponding to the removal of all hybridized strands (Figure 48c).

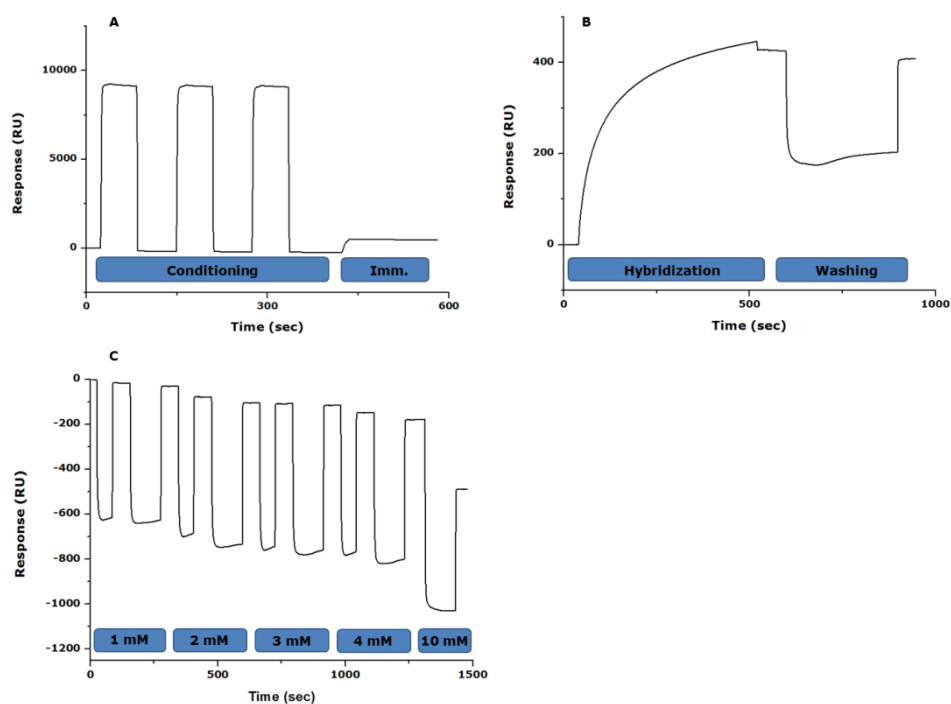


Figure 48: SPR sensorgrams of DNA immobilization, hybridization and chemical denaturation. (A) 3 successive conditioning steps were followed by immobilization of biotinylated probe DNA; (B) Hybridization of immobilized probe DNA with target DNA was followed by a removal of non-hybridized strands and (C) dsDNA was denatured by increasing concentrations of NaOH and complementary strands were removed under flow.

5.3.3 Transition of dsDNA to ssDNA via target induced strand displacement

Firstly, it was tested by means of SPR if one of our own aptamers, Apta 13A, can be integrated in a TISD set-up.

Several strands (partially) complementary to Apta 13A were designed. One DNA strand (FM) was fully complementary to Apta 13A. Four strands (MM1, MM2, MM3 and MM4) had the same length as Apta 13A, but several mismatches were introduced. Two strands (MM5 and MM6) were shorter than Apta 13A and possessed different mismatches. OligoAnalyzer 3.1 revealed ΔG 's for the DNA hybrids ranging from -156.47 kcal/mol to -8.29 kcal/mol (Table 13).

Table 13: Hetero-dimer analysis of Apta 13A/complementary strand hybrids*.

	Max. ΔG (kcal/mol)
Apta 13A + FM AGCAGCACAGAGGTCAGTTCTTATGTCGAACTAAATTTGGCCTGACCAAGCCGAATTTGACCTATGCGTGCTACCGTGAA TCGTCGTCTCCAGTCAAGAATACAGCTTGATTTAAACCGGACTGTTGCGCTTAAACTGGATACGCACGATGGCACTT	-156.47
Apta 13A + MM1 AGCAGCACAGAGGTCAGTTCTTATGTCGAACTAAATTTGGCCTGACCAAGCCGAATTTGACCTATGCGTGCTACCGTGAA :: :::: TCCTCGTCTCCACTCAACAATACACCTTCATTTAAACCGGACTGTTGCGCTTAAACTCGATACCCACCATGCCACTT	-15.240
Apta 13A + MM2 AGCAGCACAGAGGTCAGTTCTTATGTCGAACTAAATTTGGCCTGACCAAGCCGAATTTGACCTATGCGTGCTACCGTGAA :: :::: TCCTCGTCTCCACTCAAGTATACACCTTGAATTTAAACCGGACTGTTGCGCTTAAACAGGATACCCAGGATGCCACTT	-13.330
Apta 13A + MM3 AGCAGCACAGAGGTCAGTTCTTATGTCGAACTAAATTTGGCCTGACCAAGCCGAATTTGACCTATGCGTGCTACCGTGAA :: :::: TCCTCGTCTCCACTCAACAARAACACCTTCATTTAAACCGGACTGTTGCGCTTATACTCGATACCCACCATGCCACTT	-9.1800
Apta 13A + MM4 AGCAGCACAGAGGTCAGTTCTTATGTCGAACTAAATTTGGCCTGACCAAGCCGAATTTGACCTATGCGTGCTACCGTGAA :: :::: TCCTCGTCTCCACTCAACAARAACACCTTCATTTAAACCGGACTGTTGCGCTTATAGTGCATACCCACCATGCCACTT	-9.1800
Apta 13A + MM5 AGCAGCACAGAGGTCAGTTCTTATGTCGAACTAAATTTGGCCTGACCAAGCCGAATTTGACCTATGCGTGCTACCGTGAA TCGTCGTCTCCAGAGTTGAATACAGCAACTAAATAACC	-27.440
Apta 13A + MM6 AGCAGCACAGAGGTCAGTTCTTATGTCGAACTAAATTTGGCCTGACCAAGCCGAATTTGACCTATGCGTGCTACCGTGAA : : : : : TCCTCGTCTCGCAGAGTTGAATAGAGCAACTAAATAACC	-8.2900

* Most stable hybrid complexes formed by Apta 13A (upper sequence) and partially complementary DNA (lower sequence). ΔG values were calculated via OligoAnalyzer 3.1. The ΔG was calculated by taking into account the longest consecutive set of complementary bases (solid lines). Additionally complementary bases (dotted lines) for that dimer structure did not impact calculated ΔG values. However, these complementary bases do influence the actual ΔG . All complementary strands possessed a biotin label and a 5T linker at the 3' end (omitted in the table) not showing any overlap with Apta 13A.

Complementary strands, biotin-labeled and extended with 5 T oligonucleotides at the 3' end, were effectively immobilized onto separate FC's of SA chips. Hybridization of Apta 13A with immobilized strands was successful for FM, MM1, MM2, MM3, MM4 and MM5. Hybridization of Apta 13A with MM6 failed. TISD was tested for all formed hybrid complexes, but failed in all conditions. Exposure of the hybrid duplexes to a high concentration of E2 did not result in the break-down of the hybrid duplex. No drop in SPR signal was visible (Table 14).

Table 14: Immobilization of complementary DNA, hybridization with Apta 13A and TISD in an SPR set-up.

	Immobilization response (RU)	Hybridization response (RU)	TISD
FM	1523	1176	✗
MM1	1520	906.8	✗
MM2	1530	951.8	✗
MM3	1492	903.3	✗
MM4	882.9	504.5	✗
MM5	1482	1132	✗
MM6	1077	5.800	NA

✗ = not present; NA = not applicable

Secondly, four aptamers [38, 195, 204, 205] described in literature which were proven to function in a TISD set-up, were tested by means of SPR.

For three aptamers [195, 204, 205], the original set-up was comprised of the immobilization of an oligonucleotide hybrid duplex and monitoring break-down of the duplex after target exposure via an electrochemical read-out system. We tried to translate their set-up to our SPR set-up. Aptamers were applied as such. Complementary DNA was adapted to a limited extent for immobilization purposes (Table 15). Unfortunately, we were not able to prove the suitability of these aptamers for TISD by means of SPR measurements (data not shown).

Table 15: Sequences described in literature proven to be useful for TISD.

DNA strand	Target	Sequence
Apta Das	thrombin	5'-GGTTGGTGTGGTTGG-3'
Compl Das (PNA)		5'-KKKKKCGACAGCAAKKKKK/3BioTEG/-3'
Apta Wu	adenosine	5'-AGAGAACCTGGGGGAGTATTGCGGAGGAAGGT-3'
Compl Wu		5'-CCCAGGTTCTCT/3BioTEG/-3'
Apta Han	ATP	5'-ACCTGGGGGAGTATTGCGGAGGAAGGT-3'
Compl Han		5'-CTTCTCCGCAATACTCCCCAGGT/3BioTEG/-3'

The fourth aptamer [38] has proven its worth for TISD in solution. Fluorophore labeled aptamer (Apta Yang + F) and quencher tagged complementary strand (Compl Yang + Q) hybridize (Table 16). The hybridization duplex gets disrupted when target is introduced resulting in an increased fluorescence signal. Initially, we tried to reproduce the original experiment in exactly the same way and this turned out to be successful. A concentration dependent increase in fluorescence could be detected when exposing aptamer-complementary strand to target E2. In the absence of E2, the fluorescence signal of the aptamer/complementary strand was only 8% of the maximum fluorescence signaling capability (as compared to the solution where the quencher tagged complementary strand was omitted). 200 μM E2, on the other hand, was able to produce 46.5 % of the maximum fluorescence signaling capacity (Figure 49).

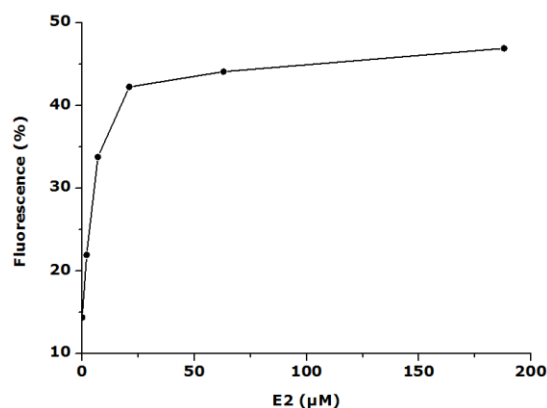


Figure 49: A TISD experiment in solution. Fluorescently labeled aptamer and quencher tagged complementary DNA were exposed to different concentrations of E2. Fluorescence is expressed relative to the fluorescence of fluorescently labeled aptamer in the absence of quencher tagged complementary strand.

In a next step, we tried to translate the set-up performed in solution into an SPR set-up, characterized by immobilization of complementary strand, hybridization with aptamer and capturing/removal of aptamer by the introduction of target. The influence of different parameters was tested (Table 16).

Initially, biotin-labeled probe DNA (Compl Yang + 10T) was immobilized onto an SA chip, which has a 3D structure because of the presence of a dextran layer. Later, we switched to a flat C1 chip. Direct immobilization of NH₂-labeled probe DNA turned out to be impossible. Immobilization of SA onto the flat C1 chip, on the other hand, enabled us to immobilize biotin-labeled aptamer onto this kind of chip. Subsequently, aptamer (Apta Yang) was efficiently hybridized to the immobilized probe DNA. However, neither on an SA chip nor on a SA coated C1 chip, we were able to show TISD (data not shown).

Next, we tested different linker lengths. Biotin-labeled probe DNA extended with 10, 15, 20, 30 or 40 T's was immobilized on an SA coated C1 chip. Subsequent hybridization with aptamer (Apta Yang) and exposure to E2, however, did not result in TISD (data not shown). Additionally, immobilized probe DNA was hybridized with fluorescently labeled aptamer (Apta Yang + F). However, also here, TISD could not be proven (data not shown).

Table 16: Aptamer/complementary strand duplex described in literature proven to be useful for TISD + adaptations to the complementary strand.

DNA strand	Sequence
Apta Yang	5'-CTCTCGGGACGACATGGATTTTCCATCAACGAAGTGCCTCCGTCCTCCG-3'
Apta Yang + F	5'-/56-FAM/ CTCTCGGGACGACATGGATTTTCCATCAACGAAGTGCCTCCGTCCTCCG-3'
Compl Yang + Q	5'-GTCGTCCCGAGAG/3Dab/-3'
Compl Yang + 10T	5'-GTCGTCCCGAGAG(10T)/3Bio/-3'
Compl Yang + 15T	5'-GTCGTCCCGAGAG(15T)/3Bio/-3'
Compl Yang + 20T	5'-GTCGTCCCGAGAG(20T)/3Bio/-3'
Compl Yang + 30T	5'-GTCGTCCCGAGAG(30T)/3Bio/-3'
Compl Yang + 40T	5'-GTCGTCCCGAGAG(40T)/3Bio/-3'

5.4 Discussion

Small molecules such as E2 are difficult to identify by conventional detection techniques since their small size, low MW and lack of charge often lead to limited signal generation. TISD introduces a new freedom in small molecule detection. It takes advantage of the universal ability of aptamers to adopt two different structures: a duplex structure with a complementary strand and a complex structure with target. It is shown that an aptamer can switch structure from duplex to complex upon target addition yielding a significant signal change relatively independent of the nature of the target. TISD is expected to offer excellent selectivity, not only because of the high specificity of the applied aptamer, but also from the additional stringency due to competition between the duplex and the aptamer structure [195, 202].

Monitoring TISD requires a proper sensing platform. In house, two techniques are available which can monitor the transition from dsDNA towards ssDNA, R_{th} monitoring and SPR based detection. These techniques can thus be applied to detect the break-up of the duplex structure once target binds the aptamer. The degree of break-up of duplex structure is thereby correlated to the concentration of target.

Denaturation of dsDNA immobilized onto an NCD sample leads to an increase in R_{th} , as was previously discovered by van Grinsven *et al.* (2012) [183]. Immobilized dsDNA acts as stiff rods through which heat is easily transferred. Immobilized ssDNA, on the other hand, tends to curl and then forms an insulating layer which hampers heat-transfer. Thermal denaturation of prototype dsDNA led to an increase in R_{th} value by approximately 1.4 °C. This corresponded to a 15% increase in R_{th} which is a substantial effect since the layer of DNA molecules on the diamond electrodes is only a miniscule component (fragment length corresponds to 20 nm) as compared to the total heat-transfer path with a distance of almost 3 mm between the two thermocouples. The rise in R_{th} can vary dependent on the length of the used oligonucleotides. In general, the absolute R_{th} change upon denaturation slightly decreases with increasing oligonucleotide lengths, due to an increased initial R_{th}

value of dsDNA. When using dsDNA fragments of 150 bp or more, there will be no change upon denaturation anymore. A possible explanation is that the longer the dsDNA becomes, the more it approaches the persistence length of dsDNA and tends to bend instead of remain upright. This will hamper the heat-transfer through the spaces in between the immobilized dsDNA fragments, resulting in a lowered resolution between dsDNA and ssDNA, illustrated by a decreased absolute R_{th} change upon denaturation [208]. However, the size of most aptamers and their corresponding complementary strands stays within the detection range. Denaturation of dsDNA on a gold chip leads to a significant drop in SPR induced response. This was previously demonstrated by Delport *et al.* (2012) [209]. By making use of an FO-SPR sensor platform, with silica nanobead signal amplification, they performed high resolution DNA melting curve analysis inside a standard PCR thermocycler. They characterized both the hybridization and melting events between DNA immobilized on the sensor surface and DNA probes on silica nanoparticles. The magnitude of the response is related to the total mass of removed DNA strands. For our research, denaturation of prototype DNA led to a decrease of 487 RU, which can be defined as a substantial decrease.

As previously described in literature [183, 208] and as shown via pilot experiments, both R_{th} monitoring and SPR measurements generate clear signals when dsDNA is transformed into ssDNA. This makes these detection techniques ideal tools to monitor TISD. For practical reasons (e.g. availability of the sensing platform and sensorchips), TISD was further explored by making use of SPR technology.

One of the major challenges in the design of a TISD set-up is the fine-tuning of the complementary strand. Many complementary strands have to be tested before a suitable signaling system can be established. Both the length and the composition of the sequence have to be considered. The longer the complementary strand and the higher the level of nucleotide complementarity, the higher the stability of the duplex structure. A highly stable duplex structure is suggested to be unfavorable for TISD since the affinity of the aptamer for its target has to exceed the affinity of the aptamer for its complementary strand in

order to get released after target interaction. On the other hand, extremely unstable duplex structures are also unfavorable because of the risk of breakdown of the duplex structure in the absence of target. Often shortened complementary strands with few mismatches are applied. Apparently, a shorter complementary strand has less effect on the aptamer's spatial folding resulting in a higher recognition affinity, better selectivity and a faster hybridization/dehybridization rate, which are all required for optimal functioning of the strand displacement principle [206, 210].

Firstly, we tried to integrate one of our own aptamers, Apta 13A, in a TISD set-up. We designed several complementary strands for it, ranging in length and amount of mismatches. Subsequently, we immobilized these complementary strands on separate FCs of SPR gold chips, hybridized them with Apta 13A and tried to induce strand displacement via exposure to a high concentration of target E2. However, for none of the conditions, TISD could be seen. It is possible that the complementary strands (partially) block the binding site of the aptamer reducing the affinity of the aptamer for its target. This is because the aptamer-target complex is not directly formed between the target and the free target-binding site but rather between the target and the aptamer that is partially occupied by complementary strands. For high-affinity aptamers such as some protein binding aptamers, the strong binding interaction between the aptamer and the target competes favorably with the oligonucleotide duplex structure. As a result, the use of complementary strands has a negligible effect on the affinity of the aptamer. However, with a 'relatively' low-affinity aptamer such as Apta 13A ($K_D = 63 \mu\text{M}$), the relatively weak target-aptamer interaction probably does not compete favorably with the complementary strand/aptamer interaction which impedes TISD [50].

Secondly, we tested four aptamers which are described in literature to be used for TISD. In this way, we could use the complementary strands which they optimized and applied.

We started with three aptamers [195, 204, 205] which were originally incorporated in a heterogeneous set-up with one of the two oligonucleotide

strands immobilized on a solid support matrix. Monitoring of TISD by these researchers occurred via electrochemical read-out systems. We tried to translate this set-up to our SPR read-out system. Unfortunately, we were not able to successfully show TISD. No break-down of duplex structures could be detected. How is this possible? We tried to work under conditions similar to the original experimental conditions (e.g. buffers and temperature). Except for the read-out system, only the solid support matrix differed between our and their experiments. Maybe, this matrix contributes to the success of the experiment. The answer to the question why translation was unsuccessful is open and further investigation is required.

Subsequently, we tested one aptamer [38] which was originally used in a homogeneous set-up where both aptamer and complementary strand stayed in solution. Duplex formation by fluorescently labeled aptamer and quencher tagged complementary strand was counteracted by addition of target E2, resulting in an increased fluorescent signal. Identical imitation of the original experiment, strand displacement in solution, was successful. Translation to strand displacement on a solid surface (SPR gold chip), however, did not work. Here, the question must be asked why it works in solution but not when one of the participating strands is fixed onto a surface. One possible explanation is that there is a certain degree of steric hindrance when the duplex structure is immobilized making it more difficult for the target to interact with that structure. To reduce the risk of steric hindrance, we switched from the commercially available 3D structured SA chip to the flat C1 chip which we coated with SA ourselves. Additionally, we tested different linker lengths attached to the immobilized complementary strands. The linker exposes the complex structure above the surface in order to promote accessibility of target to the aptamer binding site. Often, a string of T nt is used as a linker. The number of T nt varies widely, which is also the case for linker designs in the literature for DNA hybridization studies on surfaces [171]. These adaptations, however, did not yield satisfying results. Another explanation for the failed translation of the original experiment is that originally, strands were labeled with a fluorescent label or a quencher. The possibility exists that the combination of both labels destabilizes the duplex structure, facilitating strand displacement. During one of

the SPR based experiments, we therefore hybridized fluorescently labeled aptamer instead of unlabeled aptamer to immobilized complementary DNA (although we did not need the label as such). However, we were not capable of applying quencher labeled complementary strands in this set-up because quencher labeling is not compatible with immobilization of DNA on the sensor chip. Unfortunately, the fluorescent label alone did not elicit enough destabilization of the duplex structure to facilitate TISD.

One can think of further destabilizing the oligonucleotide duplex structure by playing with buffer conditions (e.g. decreased ion concentration) or increasing the experimental temperature. Nutiu *et al.* (2002) [50] reported a structure-switching signaling aptamer constructed with a long complementary strand that solely works at elevated temperatures (such as 37°C), whereas complementary strands of the same size that block fewer nt in the aptamer domain lead to successful results at much lower temperatures (as low as 15°C). They also found that a lower Mg²⁺ concentration supports lower temperature sensing. However, changing buffer and temperature conditions may be favorable for destabilization of the duplex structures, it not always favors aptamer-target interaction. Aptamers often only work under specific, predefined conditions and changing these conditions potentially negatively influences their binding capacity.

To overcome problems with post-SELEX integration of aptamers in a TISD set-up, one can use the power of the so called capture-SELEX. This kind of SELEX permits the selection of aptamers that are encoded with a duplex-to-complex switching capability and are therefore extremely suitable for TISD experiments. A capture-SELEX provides an alternative approach by immobilizing the oligonucleotide library to a solid matrix instead of the target. This is done via hybridization between a fixed sequence of the library and a complementary capture oligo that is immobilized onto a surface. The selection concept is based on the release of those oligonucleotides from the library which show a higher affinity for the applied target than for the capture probe. In a later stage the capture probe can be applied, together with the selected aptamers, to set-up TISD experiments. The fact that this procedure eliminates the need for target immobilization offers an additional advantage, especially in cases where small

molecules with only few or no suitable functional groups serve as aptamer target. Based on this capture-SELEX, aptamers against kanamycin [211] and four different steroid hormones [38] were selected as described in literature.

5.5 Conclusion

The results in this chapter clearly indicate that the theory behind TISD is rather simple, but that bringing this theory into practice is a huge challenge. Although two sensing platforms are available at our research institute which can be powerful tools to monitor TISD, we were not able to establish a successful TISD set-up. Apparently, finding a suitable complementary strand was a major bottleneck in setting up these experiments. To overcome the problems we encountered, selection of aptamers by means of capture-SELEX can offer a solution. By means of this SELEX, only aptamers which are inherently encoded to make the switch from an oligonucleotide duplex structure to an aptamer-target complex are selected.

Although we were not yet capable of setting up a TISD set-up, we still believe in the power of this detection method. We are convinced that it can pave the way to highly sensitive aptasensing.

6

General discussion, conclusion and future perspectives

Since the discovery of aptamers in 1990, the field of aptamer research has progressed rapidly. Aptamers promise a bounty of applications; regarding their use as a diagnostic and therapeutic tool, as a biosensing probe and in the development of new drugs, drug delivery systems,... In this work, aptamers are studied as a probe in the construction of a biosensor for the detection of the small molecule E2 and its analogues. E2 (analogues) often end up in the environment where they act as EDCs. Monitoring the presence of EDCs is recommended because of the adverse health effects they can elicit on wildlife and human. Currently used detection techniques such as MS suffer from several drawbacks. A cross-reactive aptasensor offers a promising alternative.

In the introductory chapter, three major milestones of this research were defined in order to take the first steps to an ultimate goal. This ultimate goal entails the development of a cross-reactive aptasensor for the detection and identification of E2 and its analogues in environmental samples. Results related to the defined milestones will be discussed in the final chapter of this dissertation. Furthermore, some future recommendations and perspectives will be put forward.

6.1 General discussion

Aim 1: Selection of aptamers directed towards different epitopes of E2

The selection of two series of E2-binding aptamers, both oriented towards different functional groups of E2, is described in Chapter 2.

Selection of epitope specific aptamers is possible by means of several approaches, as is described in the introduction of Chapter 2 [104]. We chose to switch between positive and counter selection steps, whereby in the end all selected aptamers are expected to be oriented towards an epitope which is present on the target molecule but absent on the counter molecule. This approach is highly suitable when working with small targets. An alternative approach could be the withdrawal of certain target-bound sequences via

competitive elution by ligands which bind a similar target epitope. Several aptamers which are selected in this way have epitope specificity for an epitope which is present on the target molecule but absent on the competitor. However, still a substantial amount of selected aptamers show affinity for other epitopes present on the target molecule. The selection progress is thus expected to be slower via this approach when compared to the former approach. The three other proposed methods which were described in Chapter 2 are more suitable for larger targets such as proteins and are, according to us, not feasible when working with small molecules.

A lot of effort was put in optimizing the selection process before final SELEX implementation. We thereby strongly focused on library design and amplification. It is known that the heterogeneous character of a SELEX library can lead to excess formation of by-products, eventually resulting in the loss of potential high affinity and specificity aptamers and even in the failure of aptamer selection. The dynamics of product and by-product formation strongly depends on the design of the library and its corresponding primers [122]. The libraries were therefore designed in a way to avoid by-product formation as much as possible. However, since the composition of the inner part is unknown and different for all sequences, complete avoidance of by-product formation is not feasible. By-products which were formed, were removed via size separation on gel. This allowed us to successfully finish two SELEX procedures without significant disturbance of by-products.

After optimization, two independent SELEX procedures were performed. Both procedures used E2 as a target during positive selection steps. The difference lied in the applied molecule during counter selection steps. During SELEX A, dexamethasone was used. This molecule has the same core structure as E2, but expresses several different functional groups. During SELEX B, on the other hand, nortestosterone was used. The resemblance between E2 and nortestosterone is high. The only difference is that E2 has a hydroxylated aromatized A ring whereas nortestosterone has an A ring with a ketone group on it. To completely purge the selection pool from non-specific binding oligonucleotides and oligonucleotides specifically binding unwanted epitopes, counter selection steps outnumbered positive selection steps. Additional

adjustments which were made to avoid selection of non-specific binders were comprised of the addition of non-specific DNA and changing the timing of amplification. Non-amplifiable aspecific DNA blocks non-specific binding spaces. In this way, non-specific target binders will not be selected during positive selection steps and target specific oligonucleotides will not get lost during counter selection steps. However, the amount of non-specific DNA which is added cannot be too high in order to avoid problems during PCR and GE purification. Each selection round comprised several counter selection steps with in between one positive selection step before amplification in order not to over-amplify the present non-specific binders.

SELEX A resulted in a heterogeneous pool of sequences, all unique in composition, but approximately half of them showing a common motif of 8 nt. Independent of the presence of the motif, many sequences were able to form a similar three-way junction structure. This structure was earlier described by Kato *et al.* (2000) [4] as an important structure for the binding of cholic acid aptamers. SELEX B, on the other hand, resulted in the clear enrichment of 2 sequences. Both tended to form G-quadruplex structures. G quadruplex structures are often formed by aptamers, as is described in literature [137-139]. The difference in degree of enrichment is potentially related to the nature of the applied counter molecule. Dexamethasone is structurally very different from E2. This leaves several epitopes on E2 free for aptamer binding allowing various aptamers to bind. Nortestosterone, on the other hand, is structurally more similar to E2, leaving only the hydroxylated aromatized A ring available for aptamer binding. This allows only few sequences to bind.

A newly developed technique to monitor the SELEX process and its efficiency, rMCA, is described in Chapter 3.

Both direct measurements of SELEX progression (in terms of affinity of the ssDNA pool for the target) and indirect measurements (in terms of intrinsic characteristics of the ssDNA pool independent of the target) have been described in literature [142, 144, 145, 148, 152]. Since direct measurements of SELEX pool affinities are prone to several limitations and need a target-specific approach, we focused on the development of an indirect monitoring system.

ssDNA selection pool diversity and enrichment were monitored by performing a rMCA after every selection round. Enriched SELEX libraries tend to remelt at a higher temperature when compared to more random SELEX libraries. This method is proven to be reproducible and irrespective of target characteristics and SELEX design. Its usefulness was demonstrated for three SELEX designs (bead based, plate based and CE SELEX) and three targets (E2, CRP and peptide X).

SELEX A showed a slowly, gradually arising enrichment with still a large amount of random DNA present upon termination of the selection procedure, as was reflected by a large remelting peak at low temperature and a small remelting peak at higher temperature. SELEX B, on the other hand, showed strong enrichment with a clear remelting peak at higher temperature. These findings were later confirmed by sequencing results of both SELEX pools.

Generally spoken, we can say that our first aim is met. Two series of aptamers towards E2 were successfully selected out of random DNA libraries. Moreover, for SELEX optimization and monitoring, the newly developed tool rMCA appeared of great help.

Aim 2: Characterization of selected E2 aptamers regarding affinity and epitope specificity

Characterization of the selected E2-binding aptamers in terms of affinity and epitope specificity is dealt with in Chapter 4.

Characterization of small molecule binding aptamers is a huge challenge since direct detection of target binding often results in restricted signal generation. This is due to the target's small size, low MW and often lack of charge.

Binding assays similar to the original selection set-up were tested, but did not show potential for efficient screening of the E2-binding aptamers. They mainly suffered from high noise due to non-specific interactions of signal generators or DNA with the immobilization surface. When immobilizing aptamer instead of target, several read-out platforms such as impedance and R_{th} monitoring turned

out not be able to detect target binding. SPR, on the other hand, appeared to be sensitive enough to detect E2 and its analogues. We were in the possibility of detecting small molecule binding since we have in our lab the latest new version of SPR device, the Biacore T200 from GE Healthcare. This device has a detection limit of 100 Da so that even molecules with a very low MW can be detected.

All tested E2-binding aptamers showed affinities in the low μM range, which is in agreement with expectations for small molecule binding aptamers. Additionally, epitope specificity was confirmed. Aptamers obtained by SELEX A showed different binding patterns towards several E2 analogues, reflecting their epitope heterogeneity. Both aptamers of SELEX B, on the other hand, showed similar binding patterns meaning that they are both directed towards the same epitope.

Although achieving the second goal was challenging, we were able to fully characterize the selected E2-binding aptamers in terms of affinity and epitope specificity. This characterization proved the success of the previous aptamer selection. Our aptamers turned out to have an acceptable affinity in combination with intended epitope specificity.

Aim 3: Integration of E2 aptamers as recognition element in a sensor set-up suitable for lab-on-chip screening

In order to integrate the E2 aptamers in a lab-on-chip sensor, different conditions have to be fulfilled. It requires a compact and cost effective, array-type sensor set-up which accurately and reproducibly translates aptamer-target interaction in a clear and detectable signal. During the final stage of this project, the focus was put on generating a 'clear' signal. Since direct detection of aptamer-target interaction only generates small signals, an attempt was made to enhance signal generation by applying TISD. This is described in Chapter 5.

Although the aim has been addressed in detail, it has not been fulfilled. We have two sensing platforms which are ideal to monitor TISD (SPR sensing platform and R_{th} set-up), but we were not able to successfully incorporate one of our own

aptamers, nor several aptamers out of literature into a TISD set-up. The theory behind TISD looks simple. Its translation into practice proved to be challenging.

6.2 Concluding remarks and future perspectives

In this dissertation, epitope specific aptamer selection for the small molecule E2 was described, as well as the characterization of these aptamers in terms of affinity and epitope specificity. Subsequently, the principle of TISD was explored in order to amplify signal generation.

The ultimate, future, goal is to integrate these aptamers in a kind of cross-reactive array making use of TISD strategy in order to achieve perfect classification of individual E2 (analogues), as visualized in Figure 50.

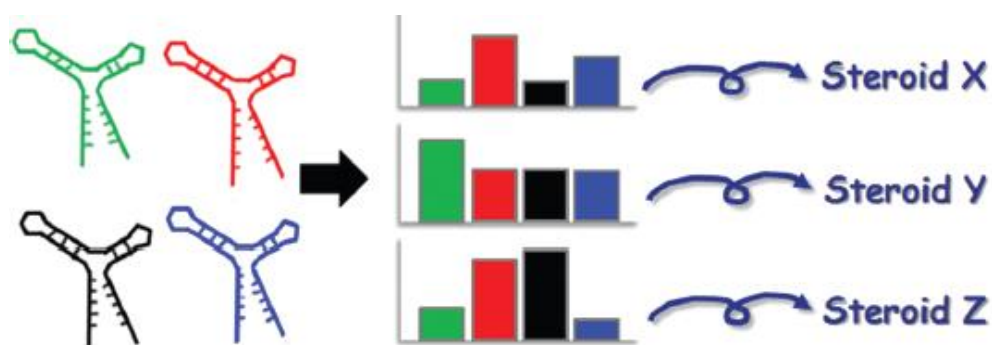


Figure 50: Visual display of target identification by means of a cross-reactive aptasensor. Various aptamers, all directed towards different epitopes of E2, are integrated in a cross-reactive sensor. Classification of individual steroids becomes possible since every steroid shows its own, specific binding pattern towards the respective aptamers [38].

An ideal sensing device meets various criteria. It comprises receptor molecules that are easy to obtain and show good target affinity and specificity. Signal generation should be clear, which is possible by combining the right sensing principle and read-out platform. Additionally, the sensor has to be compact and

cost-effective in order to make the transfer from a laboratory environment to the 'real world' possible. Does the cross-reactive aptasensor array making use of TISD strategy, as we envision it, meet these criteria?

Firstly, can E2-binding aptamers compete with other available receptor molecules for E2 detection?

One of the biggest advantages of aptamers compared to antibodies is related to their *in vitro* selection process occurring independent of animals or cell lines. Next to the ethical benefits, the *in vitro* selection process also implies that selection conditions can be adjusted taking into account future applications, whereas antibodies often only work under more standard conditions [2, 10, 21]. MIPs, on the other hand, are also synthesized in an *in vitro* way. But they are burdened with the limitation that they exhibit a better performance in organic rather than in aqueous medium, although molecular imprinting under aqueous conditions is feasible [212].

Often, aptamer selection is presented in literature as a rather straightforward procedure which is easy to apply for all kind of targets. However, in reality, aptamer selection is still a highly target specific process and certainly not routine, especially when working with small molecules as target.

A major complication when working with small molecules arises from the need to immobilize the target on a solid support matrix for easy and efficient partitioning of target-bound and non-bound sequences. For this research, commercially available sepharose beads linked to E2 were applied. However, these beads have some disadvantages. Chemical modification of the target is required. Thus, library is exposed to chemically modified E2, rather than the desired unmodified E2. This increases the likelihood of selecting sequences which display binding properties towards the sepharose beads and/or the linker arm, whether or not in combination with E2. Despite counter selection steps, carry-over of such sequences is hard to avoid [213]. Any aptamer affinity derived from (partial) binding to the support matrix or from chemical modifications will reduce the functionality of the aptamer in the intended applications where unmodified, free target has to be detected. Binding assays showed that the selected E2 aptamers are able to bind free, unmodified E2 despite the use of immobilized E2 during

the selection procedure. However, the extent to which their affinity is affected, is difficult to estimate. Potentially, higher affinities would be achieved when the selection procedure made use of free E2. An additional drawback of sepharose beads is that they are very 'sticky', which increases the risk of non-specific binding. Other beads like magnetic beads exhibit these problems less. The risk for non-specific interactions can be reduced significantly via aptamer selection in solution by means of CE SELEX. CE SELEX is normally believed to be only suitable for selecting aptamers for large proteins since it requires aptamers to undergo a mobility shift upon target binding. However, few researchers reported CE SELEX for smaller targets such as neuropeptide Y (4272 Da) [214] and N-methyl mesoporphyrin (580 Da) [215]. In the case of small molecule targets, the mobility of the complex differs only minimally from the non-binding sequences, which results in an only partial separation of bound and unbound sequences. However, since nucleic acids can be exponentially amplified by PCR, satisfactory enrichment can be achieved, even if only a small portion of the complex can be collected [215].

Another challenge of aptamer selection comprises the choice of proper binding conditions to be applied during the SELEX process. These conditions should be specifically crafted for the target in hand. However, practical considerations also play a role in this decision making. E2 is a relatively lipophilic molecule when compared to other endogenous steroid hormones [216]. A buffer with a solvent (such as DMSO or ethanol) is therefore often applied during the selection procedure. However, aptamers show a large dependence on the applied selection conditions. When solvents are absent in the ultimate application, aptamer functionality can be strongly compromised. Any deviation from the original selection buffer requires a re-assay of function. To circumvent dependence of an aptamer on one specific buffer, one can switch between different buffers in the course of the selection process. Also temperature and incubation time can be changed during the selection procedure. Only oligonucleotides which can bind the target under all these conditions, will survive the selection process.

Over the years, significant progress was made in automating the SELEX procedure to reduce some of the handling, cost and duration of the selection

process. The first automated SELEX process was developed by Cox and Ellington (1998) [217] based on a Biomek 200 pipetting robot which they used for the selection of lysozyme binding aptamers. It only comprised a partial automation since only pipetting, and not the whole SELEX process, was automatically operated in their system. Later, Eulberg *et al.* (2005) [218] modified the automated SELEX process. An Amp 4200E robotic workstation was coupled to an ultrafiltration system, a fluorescence detector and a semi-quantitative PCR device. Using this robot, these researchers identified RNA aptamers to the mirror-image configuration of the neuropeptide 'substance P'. An upgraded version of the automated SELEX process was developed using a microfluidic system, enabling a start-to-finish SELEX including transcription, selection, RT-PCR and partitioning [219]. The automated SELEX system can be a good tool to establish standard SELEX protocols in order to make aptamer selection accessible for a broader public.

The binding affinity of the selected E2 aptamers is comparable to that of MIPs imprinted for E2, as is described in literature [220]. Initially, the affinity of antibodies for E2 was rather moderate. E2 is unable to cause an immunogenic reaction. Therefore, it needs to be coupled to an immunogenic protein like BSA for antibody selection purposes. Consequently, the antibody has often a weaker affinity for the free steroid than for the immunogen [221]. However, more recently developed E2 antibodies show much higher affinity after applying mutagenesis and/or phage display [222]. Their affinity can transcend that of aptamers.

To bridge the diversity gap between antibodies and aptamers and to further improve aptamer affinity, modified aptamer sequences can be used. In the past, modifications were introduced post-SELEX [223]. Nowadays, SELEX procedures are performed with libraries comprising nt which are already modified [224]. Several modifications are fully compatible with the enzymatic steps of the selection procedure and allow for PCR amplification from modified templates [225]. Other modifications are not fully PCR-compatible, but can still be incorporated by primer extension methods, allowing (linear) production from unmodified templates. The C5 position on thymine (and uracil) nucleobases is the most suitable site for modifications, since modifications at these sites are

most often still accepted by polymerases [224]. Altogether, modified nt strongly increase the chemical variation of aptamer building blocks, which are then not constrained anymore to the limited properties of natural nucleic acids. Although these developments broaden the range of potential targets and potentially improve aptamer affinity and stability, the limited availability and the required chemical knowledge on the synthesis of such modified nt, pose a huge challenge for their widespread availability in the near future.

Regarding epitope specificity, aptamers are ideal receptor molecules when compared to antibodies and MIPs. Thanks to the combination of positive and counter selection steps, aptamers can really be directed to a specific, predefined epitope. Both antibodies and MIPS, on the other hand, can reach good overall specificity.

Due to the highly specific nature of aptamer performance, mimicking experiments which are described in literature is difficult. Often crucial details about aptamer performance are omitted when they are published. Cho *et al.* (2009) [226] proposed standards for aptamer research and documentation in literature. Experiments have to be described in sufficient detail in order to allow reproduction of experiments. Otherwise, experiments cannot be reproduced independently.

Secondly, is the strategy of TISD in combination with SPR or R_{th} monitoring ideal to sense small molecules such as E2?

SPR and R_{th} based measurements are supposed to be ideal read-out platforms to monitor TISD since both tools generate clear signals when dsDNA is transformed into ssDNA. For SPR, DNA denaturation occurring on a gold sensor chip leads to a drop in signal since a substantial mass is removed from the surface [209]. For R_{th} , DNA denaturation on an NCD sample leads to an increase in signal because of the higher insulating capacity of ssDNA when compared to dsDNA [183].

However, setting up a successful TISD experiment is challenging. The design of a suitable complementary strand for the initial duplex formation with an aptamer is depending on several external factors e.g. in solution the system will behave

differently than on a sensor surface. In order to gather more information about the requirements for complementary strand design, further research is needed. Additionally, the fact that DNA is immobilized onto a surface may impede strand displacement due to steric hindrance. Performing strand displacement in solution, eg by working with fluorescent and quenching labels, would potentially be a solution for that. Selecting aptamers by means of capture-SELEX probably also increases the chance of obtaining aptamers which are suitable to incorporate in a TISD set-up.

Thirdly, can a compact and cost-effective SPR/ R_{th} sensor be built so that translation to in-field detection of E2 (analogues) is possible?

In-field detection based on SPR technology and R_{th} monitoring is possible, but different adaptations to the standard devices are required.

A conventional SPR device is a suitable tool for monitoring aptamer-target interaction in a laboratory environment. In-field, however, such a device cannot be applied because of its size and high cost. Currently, lots of effort is put in the development of miniaturized and more affordable devices making use of the SPR measuring principle. The Portuguese company Biosurfit recently launched the spinit® system. This small footprint device (\pm 4 kg; 215 x 236 x 306 mm) integrates microfluidic elements and a surface with capture molecules in a disposable, plastic DVD-like disc. Immunoassays (e.g. CRP detection) can be performed with SPR detection, using a polarized laser beam focused on detection spots and a phototransistor for detecting the resonance of light. Operation occurs by a simple rotation protocol using a standard DVD drive [227]. Regarding the costs, a conventional SPR device can also be replaced by a FO-SPR sensor. Tran *et al.* (2013) [32] used a home-built FO-SPR platform for the detection of the peanut allergen Ara h1 protein in both buffer and food matrix samples.

Using the R_{th} set-up outside the lab is possible, but also here some adaptations to the current set-up have to be made. The set-up is already cost effective when compared to a conventional SPR device. However, miniaturization of the device

is needed. A first step would comprise miniaturization of the sensing electrodes. Diamond-based electrodes on glass substrates with a diameter below 100 μm have been described in literature [228]. Furthermore, diamond nanowires with a thickness below 10 nm have been documented [229]. The functionalization of these micro- and nanostructures with receptor molecules can be achieved by means of dip-pen nanolithography [230]. So miniaturization seems possible, but still needs to be done.

The first steps have been taken towards the construction of a cross-reactive aptasensor in order to identify E2 analogues. Epitope specific E2 aptamers have successfully been selected. Using these aptamers for the direct detection of E2 (analogues) is shown to be feasible by means of standard SPR technology. However, a number of steps still have to be taken before final in-field application of these aptamers is possible. In order to increase signal generation, which a.o. would improve detection sensitivity, indirect detection of E2 (analogues) is recommended. A possible indirect method is based on TISD strategy, coupled to an SPR or R_{th} read-out system. This strategy needs further investigation in order to apply it, but seems very promising.

List of references

1. Ellington, A. and J. Szostak, *In vitro selection of RNA molecules that bind specific ligands*. Nature, 1990. **346**(6287): p. 818-22.
2. Šmuc, T., I.-Y. Ahn, and H. Ulrich, *Nucleic acid aptamers as high affinity ligands in biotechnology and biosensorics*. Journal of Pharmaceutical and Biomedical Analysis, 2013. **81-82**(0): p. 210-217.
3. Joeng, C.B., et al., *ssDNA aptamers that recognize diclofenac and 2-anilinophenylacetic acid*. Bioorganic & Medicinal Chemistry, 2009. **17**(15): p. 5380-5387.
4. Kato, T., et al., *In vitro selection of DNA aptamers which bind to cholic acid*. Biochimica et Biophysica Acta (BBA) - Gene Structure and Expression, 2000. **1493**(1-2): p. 12-18.
5. Tombelli, S., et al., *Aptamer-based biosensors for the detection of HIV-1 Tat protein*. Bioelectrochemistry, 2005. **67**(2): p. 135-141.
6. Wang, M., et al., *C-reactive protein (CRP) aptamer binds to monomeric but not pentameric form of CRP*. Analytical and Bioanalytical Chemistry, 2011. **401**(4): p. 1309-1318.
7. Dwivedi, H., R.D. Smiley, and L.-A. Jaykus, *Selection and characterization of DNA aptamers with binding selectivity to Campylobacter jejuni using whole-cell SELEX*. Applied Microbiology and Biotechnology, 2010. **87**(6): p. 2323-2334.
8. Ohuchi, S., *Cell-SELEX Technology*. BioResearch Open Access, 2012. **1**(6): p. 265-272.
9. Peyrin, E., *Nucleic acid aptamer molecular recognition principles and application in liquid chromatography and capillary electrophoresis*. Journal of Separation Science, 2009. **32**(10): p. 1531-1536.
10. Stoltenburg, R., C. Reinemann, and B. Strehlitz, *SELEX—A (r)evolutionary method to generate high-affinity nucleic acid ligands*. Biomolecular Engineering, 2007. **24**(4): p. 381-403.
11. Szeitner, Z., et al., *Is less more? Lessons from aptamer selection strategies*. Journal of Pharmaceutical and Biomedical Analysis, (0).
12. Tada, S., et al., *In vitro selection of a photoresponsive peptide aptamer to glutathione-immobilized microbeads*. Journal of Bioscience and Bioengineering, (0).
13. Baines, I.C. and P. Colas, *Peptide aptamers as guides for small-molecule drug discovery*. Drug Discovery Today, 2006. **11**(7-8): p. 334-341.
14. Tuerk, C. and L. Gold, *Systematic evolution of ligands by exponential enrichment: RNA ligands to bacteriophage T4 DNA polymerase*. Science, 1990. **249**(4968): p. 505-10.
15. Potyrailo, R., et al., *Adapting selected nucleic acid ligands (aptamers) to biosensors*. Analytical Chemistry, 1998. **70**(16): p. 3419-25.
16. Ng, E.W.M., et al., *Pegaptanib, a targeted anti-VEGF aptamer for ocular vascular disease*. Nat Rev Drug Discov, 2006. **5**(2): p. 123-132.
17. Santosh, B. and P.K. Yadava, *Nucleic Acid Aptamers: Research Tools in Disease Diagnostics and Therapeutics*. BioMed Research International, 2014. **2014**: p. 13.

18. Berezovski, M.V., et al., *Aptamer-Facilitated Biomarker Discovery (AptaBiD)*. Journal of the American Chemical Society, 2008. **130**(28): p. 9137-9143.
19. Information, N.C.f.B. 2015 [cited 2015 25 March]; Available from: <http://www.ncbi.nlm.nih.gov/pubmed/?term=aptamers>.
20. SomaLogic.inc. 2015 [cited 2015 25 March]; Available from: <http://www.somallogic.com/Technology/SOMAmers-basic-info.aspx>.
21. Song, K.-M., S. Lee, and C. Ban, *Aptamers and Their Biological Applications*. Sensors, 2012. **12**(1): p. 612-631.
22. Frauendorf, C. and A. Jäschke, *Detection of small organic analytes by fluorescing molecular switches*. Bioorganic & Medicinal Chemistry, 2001. **9**(10): p. 2521-2524.
23. Michaud, M., et al., *A DNA Aptamer as a New Target-Specific Chiral Selector for HPLC*. Journal of the American Chemical Society, 2003. **125**(28): p. 8672-8679.
24. Kuwahara, M. and N. Sugimoto, *Molecular Evolution of Functional Nucleic Acids with Chemical Modifications*. Molecules, 2010. **15**(8): p. 5423-5444.
25. Radom, F., et al., *Aptamers: Molecules of great potential*. Biotechnology Advances, 2013. **31**(8): p. 1260-1274.
26. Hianik, T., et al., *Influence of ionic strength, pH and aptamer configuration for binding affinity to thrombin*. Bioelectrochemistry, 2007. **70**(1): p. 127-133.
27. Kiani, Z., et al., *In vitro selection and characterization of deoxyribonucleic acid aptamers for digoxin*. Analytica Chimica Acta, 2012. **748**(0): p. 67-72.
28. Zhou, N., et al., *Selection and identification of streptomycin-specific single-stranded DNA aptamers and the application in the detection of streptomycin in honey*. Talanta, 2013. **108**(0): p. 109-116.
29. Vianini, E., M. Palumbo, and B. Gatto, *In vitro selection of DNA aptamers that bind l-tyrosinamide*. Bioorganic & Medicinal Chemistry, 2001. **9**(10): p. 2543-2548.
30. Bianchini, M., et al., *Specific oligobodies against ERK-2 that recognize both the native and the denatured state of the protein*. Journal of Immunological Methods, 2001. **252**(1-2): p. 191-197.
31. Rhie, A., et al., *Characterization of 2'-Fluoro-RNA Aptamers That Bind Preferentially to Disease-associated Conformations of Prion Protein and Inhibit Conversion*. Journal of Biological Chemistry, 2003. **278**(41): p. 39697-39705.
32. Tran, D.T., et al., *Selection of aptamers against Ara h 1 protein for FO-SPR biosensing of peanut allergens in food matrices*. Biosensors and Bioelectronics, 2013. **43**(0): p. 245-251.
33. Gyllensten, U.B. and H.A. Erlich, *Generation of single-stranded DNA by the polymerase chain reaction and its application to direct sequencing of the HLA-DQA locus*. Proceedings of the National Academy of Sciences, 1988. **85**(20): p. 7652-7656.
34. Espelund, M., R.A.P. Stacy, and K.S. Jakobsen, *A simple method for generating single-stranded DNA probes labeled to high activities*. Nucleic Acids Research, 1990. **18**(20): p. 6157-6158.

-
35. Avci-Adali, M., et al., *Upgrading SELEX Technology by Using Lambda Exonuclease Digestion for Single-Stranded DNA Generation*. *Molecules*, 2009. **15**(1): p. 1-11.
 36. Vanbrabant, J., et al., *reMelting curve analysis as a tool for enrichment monitoring in the SELEX process*. *Analyst*, 2014. **139**(3): p. 589-595.
 37. Mehta, P.K., et al., *Detection of potential microbial antigens by immuno-PCR (PCR-amplified immunoassay)*. *Journal of Medical Microbiology*, 2014. **63**(Pt 5): p. 627-641.
 38. Yang, K.-A., et al., *Optimizing Cross-reactivity with Evolutionary Search for Sensors*. *Journal of the American Chemical Society*, 2011. **134**(3): p. 1642-1647.
 39. Kusser, W., *Chemically modified nucleic acid aptamers for in vitro selections: evolving evolution*. *Reviews in Molecular Biotechnology*, 2000. **74**(1): p. 27-38.
 40. Kong, H.Y. and J. Byun, *Nucleic Acid Aptamers: New Methods for Selection, Stabilization, and Application in Biomedical Science*. *Biomolecules and Therapeutics*, 2013. **21**(6): p. 423-434.
 41. Klussman, ed. *The aptamer handbook. Functional oligonucleotides and their applications*. 2006, Wiley-VCH Verlag GmbH & Co. KGaA: Weinheim. 490.
 42. Zuker, M., *Mfold web server for nucleic acid folding and hybridization prediction*. *Nucleic Acids Research*, 2003. **31**(13): p. 3406-3415.
 43. Kikin, O., L. D'Antonio, and P.S. Bagga, *QGRS Mapper: a web-based server for predicting G-quadruplexes in nucleotide sequences*. *Nucleic Acids Research*, 2006. **34**(suppl 2): p. W676-W682.
 44. Forster, C., et al., *Comparative crystallization and preliminary X-ray diffraction studies of locked nucleic acid and RNA stems of a tenascin C-binding aptamer*. *Acta Crystallogr Sect F Struct Biol Cryst Commun*, 2006. **62**(Pt 7): p. 665-8.
 45. Ranpura, H., D. Bialonska, and P.H. Bolton, *Finding and characterizing the complexes of drug like molecules with quadruplex DNA: combined use of an enhanced hydroxyl radical cleavage protocol and NMR*. *PLoS One*, 2014. **9**(4): p. e96218.
 46. Healthcare, G. 2015 [cited 2015 25 March]; Available from: <https://www.biocore.com/lifesciences/products/Consumables/guide/index.html>.
 47. Zhou, J., M. Battig, and Y. Wang, *Aptamer-based molecular recognition for biosensor development*. *Analytical and Bioanalytical Chemistry*, 2010. **398**(6): p. 2471-2480.
 48. Stojanovic, M.N., P. de Prada, and D.W. Landry, *Catalytic Molecular Beacons*. *ChemBioChem*, 2001. **2**(6): p. 411-415.
 49. Tan, W., et al., *Molecular Beacons: A Novel DNA Probe for Nucleic Acid and Protein Studies*. *Chemistry – A European Journal*, 2000. **6**(7): p. 1107-1111.
 50. Nutiu, R. and Y. Li, *Structure-Switching Signaling Aptamers*. *Journal of the American Chemical Society*, 2003. **125**(16): p. 4771-4778.
 51. Nagatoishi, S., et al., *Fluorescence energy transfer probes based on the guanine quadruplex formation for the fluorometric detection of potassium ion*. *Analytica Chimica Acta*, 2007. **581**(1): p. 125-131.
 52. Liu, J., Z. Cao, and Y. Lu, *Functional Nucleic Acid Sensors*. *Chemical Reviews*, 2009. **109**(5): p. 1948-1998.
-

-
53. Fang, X., et al., *Molecular aptamer for real-time oncoprotein platelet-derived growth factor monitoring by fluorescence anisotropy*. Anal Chem, 2001. **73**(23): p. 5752-7.
 54. Amalgaam. *Interaction analysis in solution*. 2014 [cited 2014; Available from: http://www.amalgaam.co.jp/support/application/fluc_deux_trypsinized_protein.html].
 55. Book, B., J. Chen, and J. Irudayaraj, *Quantification of receptor targeting aptamer binding characteristics using single-molecule spectroscopy*. Biotechnology and Bioengineering, 2011. **108**(5): p. 1222-1227.
 56. Spectroscopy, P.I.f.T.K. *Fluorescence polarisation*. 2014 [cited 2014; Available from: <http://www.hi-techsci.com/techniques/anisotropy/>].
 57. Jin, Y., J. Bai, and H. Li, *Label-free protein recognition using aptamer-based fluorescence assay*. Analyst, 2010. **135**(7): p. 1731-1735.
 58. Martín, M.E., et al., *DNA Aptamers Selectively Target <italics>Leishmania infantum</italics> H2A Protein*. PLoS ONE, 2013. **8**(10): p. e78886.
 59. Narendran, K., et al., *Demonstration and Optimization of Multiple Aptamer- Demonstration and Optimization of Multiple Aptamer-ELISA "ELASA" Assays with Novel DNA ELISA "ELASA" Assays with Novel DNA Aptamers*. Poster presented at TIDES 2012, Las Vegas NV May 21-23, 2012.
 60. Fischer, N.O., T.M. Tarasow, and J.B.H. Tok, *Protein detection via direct enzymatic amplification of short DNA aptamers*. Analytical Biochemistry, 2008. **373**(1): p. 121-128.
 61. Liao, S., et al., *Aptamer-Based Sensitive Detection of Target Molecules via RT-PCR Signal Amplification*. Bioconjugate Chemistry, 2010. **21**(12): p. 2183-2189.
 62. Patching, S.G., *Surface plasmon resonance spectroscopy for characterisation of membrane protein-ligand interactions and its potential for drug discovery*. Biochimica et Biophysica Acta (BBA) - Biomembranes, 2014. **1838**(1, Part A): p. 43-55.
 63. Biacore, *Sensor surface handbook*. 2014.
 64. Ashley, J. and S.F.Y. Li, *An aptamer based surface plasmon resonance biosensor for the detection of bovine catalase in milk*. Biosensors and Bioelectronics, 2013. **48**(0): p. 126-131.
 65. Deng, B., et al., *Aptamer binding assays for proteins: The thrombin example—A review*. Analytica Chimica Acta, 2014. **837**(0): p. 1-15.
 66. Mir, M., M. Vreeke, and I. Katakis, *Different strategies to develop an electrochemical thrombin aptasensor*. Electrochemistry Communications, 2006. **8**(3): p. 505-511.
 67. Polsky, R., et al., *Nucleic Acid-Functionalized Pt Nanoparticles: Catalytic Labels for the Amplified Electrochemical Detection of Biomolecules*. Analytical Chemistry, 2006. **78**(7): p. 2268-2271.
 68. Xiao, Y., et al., *Label-Free Electronic Detection of Thrombin in Blood Serum by Using an Aptamer-Based Sensor*. Angewandte Chemie International Edition, 2005. **44**(34): p. 5456-5459.
 69. Huang, Y.C., et al., *Immobilized DNA Switches as Electronic Sensors for Picomolar Detection of Plasma Proteins*. Journal of the American Chemical Society, 2008. **130**(25): p. 8023-8029.
 70. Turner, A., I. Karube, and W. GS, *Biosensors: Fundamentals and Applications*. 1987, Oxford: Oxford Science publication.
-

-
71. Scheller, F.W., et al., *Research and development in biosensors*. Current Opinion in Biotechnology, 2001. **12**(1): p. 35-40.
 72. Umali, A.P. and E.V. Anslyn, *A general approach to differential sensing using synthetic molecular receptors*. Curr Opin Chem Biol, 2010. **14**(6): p. 685-92.
 73. Albert, K.L., N.; Schauer, C.; Sotzing, G.; Stitzal, S.; Vaid, T.; Walt, D., *Cross-Reactive Chemical Sensor Arrays*. Chem. Rev., 2000 **100**: p. 2595–2626.
 74. Wan, Y., et al., *Surface-immobilized aptamers for cancer cell isolation and microscopic cytology*. Cancer Res, 2010. **70**(22): p. 9371-80.
 75. Zhang, P., et al., *Using an RNA aptamer probe for flow cytometry detection of CD30-expressing lymphoma cells*. Lab Invest, 2009. **89**(12): p. 1423-32.
 76. Zhang, J., et al., *Fast determination of the tetracyclines in milk samples by the aptamer biosensor*. Analyst, 2010. **135**(10): p. 2706-2710.
 77. Tang, Z., et al., *Generating Aptamers for Recognition of Virus-Infected Cells*. Clinical Chemistry, 2009. **55**(4): p. 813-822.
 78. Baird, G.S., *Where Are All the Aptamers?* American Journal of Clinical Pathology, 2010. **134**(4): p. 529-531.
 79. Baldrich, E., A. Restrepo, and C.K. O'Sullivan, *Aptasensor Development: Elucidation of Critical Parameters for Optimal Aptamer Performance*. Analytical Chemistry, 2004. **76**(23): p. 7053-7063.
 80. Tapiero, H., G.N. Ba, and K.D. Tew, *Estrogens and environmental estrogens*. Biomed Pharmacother, 2002. **56**(1): p. 36-44.
 81. Miller, W.L. and R.J. Auchus, *The molecular biology, biochemistry, and physiology of human steroidogenesis and its disorders*. Endocr Rev, 2011. **32**(1): p. 81-151.
 82. White, B.A. and S.P. Porterfield, *Endocrine and reproductive physiology*. 4th edition ed. 2013: Elsevier.
 83. Heldring, N., et al., *Estrogen receptors: how do they signal and what are their targets*. Physiol Rev, 2007. **87**(3): p. 905-31.
 84. Chighizola, C. and P.L. Meroni, *The role of environmental estrogens and autoimmunity*. Autoimmun Rev, 2012. **11**(6-7): p. A493-501.
 85. Writer, J.H., et al., *Fate of 4-nonylphenol and 17beta-estradiol in the Redwood River of Minnesota*. Environ Sci Technol, 2012. **46**(2): p. 860-8.
 86. Chang, H.S., et al., *The methods of identification, analysis, and removal of endocrine disrupting compounds (EDCs) in water*. J Hazard Mater, 2009. **172**(1): p. 1-12.
 87. Jobling, S., et al., *Predicted exposures to steroid estrogens in U.K. rivers correlate with widespread sexual disruption in wild fish populations*. Environ Health Perspect, 2006. **114 Suppl 1**: p. 32-9.
 88. Rosenfeldt, E.J. and K.G. Linden, *Degradation of endocrine disrupting chemicals bisphenol A, ethinyl estradiol, and estradiol during UV photolysis and advanced oxidation processes*. Environ Sci Technol, 2004. **38**(20): p. 5476-83.
 89. Lai, K.M., et al., *Binding of Waterborne Steroid Estrogens to Solid Phases in River and Estuarine Systems*. Environmental Science & Technology, 2000. **34**(18): p. 3890-3894.
-

-
90. Writer, J.H., et al., *Biodegradation and attenuation of steroidal hormones and alkylphenols by stream biofilms and sediments*. Environ Sci Technol, 2011. **45**(10): p. 4370-6.
 91. Nohynek, G.J., et al., *Endocrine disruption: Fact or urban legend?* Toxicology Letters, 2013. **223**(3): p. 295-305.
 92. Sumpter, J.P. and A.C. Johnson, *10th Anniversary Perspective: Reflections on endocrine disruption in the aquatic environment: from known knowns to unknown unknowns (and many things in between)*. J Environ Monit, 2008. **10**(12): p. 1476-85.
 93. Tashiro, Y., et al., *Livestock wastes as a source of estrogens and their effects on wildlife of Manko tidal flat, Okinawa*. Mar Pollut Bull, 2003. **47**(1-6): p. 143-7.
 94. Ingerslev F., V.E.a.H.-S.B., *Pharmaceuticals and personal care products - A source of endocrine disruption in the environment?* Pure Appl. Chem., 2003. **75**(11-12): p. 1881-1893.
 95. Sonneveld, E., et al., *Development of Androgen- and Estrogen-Responsive Bioassays, Members of a Panel of Human Cell Line-Based Highly Selective Steroid-Responsive Bioassays*. Toxicological Sciences, 2005. **83**(1): p. 136-148.
 96. Yadav, S.K., et al., *A review on determination of steroids in biological samples exploiting nanobio-electroanalytical methods*. Analytica Chimica Acta, 2013. **762**(0): p. 14-24.
 97. McKeague, M. and M.C. DeRosa, *Challenges and Opportunities for Small Molecule Aptamer Development*. Journal of Nucleic Acids, 2012. **2012**: p. 20.
 98. Miyashita, M., et al., *Surface plasmon resonance-based immunoassay for 17 β -estradiol and its application to the measurement of estrogen receptor-binding activity*. Analytical and Bioanalytical Chemistry, 2005. **381**(3): p. 667-673.
 99. Xu, Z.X., et al., *The biomimetic immunoassay based on molecularly imprinted polymer: a comprehensive review of recent progress and future prospects*. J Food Sci, 2011. **76**(2): p. R69-75.
 100. Jayasena, S.D., *Aptamers: An Emerging Class of Molecules That Rival Antibodies in Diagnostics*. Clinical Chemistry, 1999. **45**(9): p. 1628-1650.
 101. Nery, A.A., C. Wrenger, and H. Ulrich, *Recognition of biomarkers and cell-specific molecular signatures: Aptamers as capture agents*. Journal of Separation Science, 2009. **32**(10): p. 1523-1530.
 102. Kim, Y.S., et al., *Electrochemical detection of 17 β -estradiol using DNA aptamer immobilized gold electrode chip*. Biosens Bioelectron, 2007. **22**(11): p. 2525-31.
 103. Alsager, O.A., et al., *Small molecule detection in solution via the size contraction response of aptamer functionalized nanoparticles*. Biosensors and Bioelectronics, 2014. **57**(0): p. 262-268.
 104. Kulbachinskiy, A.V., *Methods for selection of aptamers to protein targets*. Biochemistry (Mosc), 2007. **72**(13): p. 1505-18.
 105. Rockey, W.M., et al., *Rational truncation of an RNA aptamer to prostate-specific membrane antigen using computational structural modeling*. Nucleic Acid Ther, 2011. **21**(5): p. 299-314.
-

106. Han, S.R., J. Yu, and S.W. Lee, *In vitro selection of RNA aptamers that selectively bind danofloxacin*. *Biochem Biophys Res Commun*, 2014. **448**(4): p. 397-402.
107. Thiel, W.H., et al., *Nucleotide Bias Observed with a Short SELEX RNA Aptamer Library*. *Nucleic Acid Therapeutics*, 2011. **21**(4): p. 253-263.
108. Ozer, A., J.M. Pagano, and J.T. Lis, *New Technologies Provide Quantum Changes in the Scale, Speed, and Success of SELEX Methods and Aptamer Characterization*. *Mol Ther Nucleic Acids*, 2014. **3**: p. e183.
109. Luo, X., et al., *Computational approaches toward the design of pools for the in vitro selection of complex aptamers*. *RNA*, 2010. **16**(11): p. 2252-2262.
110. Ouellet, E., et al., *A simple method for eliminating fixed-region interference of aptamer binding during SELEX*. *Biotechnology and Bioengineering*, 2014. **111**(11): p. 2265-2279.
111. Pan, W., et al., *Primer-Free Aptamer Selection Using A Random DNA Library*. 2010(41): p. e2039.
112. Pan, W., P. Xin, and G.A. Clawson, *Minimal primer and primer-free SELEX protocols for selection of aptamers from random DNA libraries*. *Biotechniques*, 2008. **44**(3): p. 351-60.
113. Cowperthwaite, M.C. and A.D. Ellington, *Bioinformatic analysis of the contribution of primer sequences to aptamer structures*. *J Mol Evol*, 2008. **67**(1): p. 95-102.
114. Lee, S., et al., *A cross-contamination-free SELEX platform for a multi-target selection strategy*. *BioChip Journal*, 2013. **7**(1): p. 38-45.
115. Nieuwlandt, D., *In Vitro Selection of Functional Nucleic Acid Sequences*. *Curr. Issues Mol. Biol.* , 2000. **2**(1): p. 9-16.
116. Wilson, C. and J.W. Szostak, *Isolation of a fluorophore-specific DNA aptamer with weak redox activity*. *Chem Biol*, 1998. **5**(11): p. 609-17.
117. Gopinath, S.C., *Methods developed for SELEX*. *Anal Bioanal Chem*, 2007. **387**(1): p. 171-82.
118. Stoltenburg, R., C. Reinemann, and B. Strehlitz, *FluMag-SELEX as an advantageous method for DNA aptamer selection*. *Analytical and Bioanalytical Chemistry*, 2005. **383**(1): p. 83-91.
119. Geiger, A., et al., *RNA aptamers that bind L-arginine with sub-micromolar dissociation constants and high enantioselectivity*. *Nucleic Acids Res*, 1996. **24**(6): p. 1029-36.
120. Bridonneau, P., et al., *Site-directed selection of oligonucleotide antagonists by competitive elution*. *Antisense Nucleic Acid Drug Dev*, 1999. **9**(1): p. 1-11.
121. He, C.-Z., et al., *Single-primer-limited amplification: A method to generate random single-stranded DNA sub-library for aptamer selection*. *Analytical Biochemistry*, 2013. **440**(1): p. 63-70.
122. Musheev, M.U. and S.N. Krylov, *Selection of aptamers by systematic evolution of ligands by exponential enrichment: Addressing the polymerase chain reaction issue*. *Analytica Chimica Acta*, 2006. **564**(1): p. 91-96.
123. Tabarzad, M., et al., *Challenges to design and develop of DNA aptamers for protein targets. I. Optimization of asymmetric PCR for generation of a single stranded DNA library*. *Iran J Pharm Res*, 2014. **13**(Suppl): p. 133-41.

-
124. Shao, K., et al., *Emulsion PCR: a high efficient way of PCR amplification of random DNA libraries in aptamer selection*. PLoS One, 2011. **6**(9): p. e24910.
 125. Wakimoto, Y., J. Jiang, and H. Wakimoto, *Isolation of single-stranded DNA*. Curr Protoc Mol Biol, 2014. **107**: p. 2.15.1-9.
 126. Rychlik, W., *OLIGO 7 Primer Analysis Software (PCR Primer Design)*. Methods in Molecular Biology, 2007. **402**: p. 35-39.
 127. J, V., *Development of a suitable bioreceptor for C-reactive protein: Aptamer selection, validation and sensor development*. 2014, Hasselt University: Diepenbeek.
 128. Mehta, J., et al., *In vitro selection and characterization of DNA aptamers recognizing chloramphenicol*. Journal of Biotechnology, 2011. **155**(4): p. 361-369.
 129. Vaya, J.T., *S The Relation Between the Chemical Structure of Flavonoids and Their Estrogen-Like Activities*. Current Medicinal Chemistry, 2004. **11**(10): p. 1333-1343.
 130. Morris, K.N., et al., *High affinity ligands from in vitro selection: Complex targets*. Proceedings of the National Academy of Sciences, 1998. **95**(6): p. 2902-2907.
 131. Wu, J.S., et al., *Primer design using genetic algorithm*. Bioinformatics, 2004. **20**(11): p. 1710-7.
 132. Vallone, P.M. and J.M. Butler, *AutoDimer: a screening tool for primer-dimer and hairpin structures*. Biotechniques, 2004. **37**(2): p. 226-31.
 133. Chuang, L.Y., Y.H. Cheng, and C.H. Yang, *Specific primer design for the polymerase chain reaction*. Biotechnol Lett, 2013. **35**(10): p. 1541-9.
 134. Ridgwell, K., *Genetics tools: PCR and sequencing*. Vox Sang, 2004. **87 Suppl1**: p. 6-12.
 135. Tucker, W.S., KT; Tanner, JA, *G-quadruplex DNA aptamers and their ligands: structure, function and application*. Current Pharmaceutical Design, 2012. **18**(14).
 136. Salas, T.R., et al., *Human replication protein A unfolds telomeric G-quadruplexes*. Nucleic Acids Research, 2006. **34**(17): p. 4857-4865.
 137. De Rache, A., et al., *Elongated Thrombin Binding Aptamer: A G-Quadruplex Cation-Sensitive Conformational Switch*. Chemistry – A European Journal, 2012. **18**(14): p. 4392-4400.
 138. Fujita, H., et al., *Structural and Affinity Analyses of G-Quadruplex DNA Aptamers for Camptothecin Derivatives*. Pharmaceuticals, 2013. **6**(9): p. 1082-1093.
 139. Wu, J.W., C; Li, X; Song, Y; Wang, W; Li, C; Hu, J; Zhu, Z; Li, J; Zhang, W; Lu, Z; Yang, CJ, *Identification, characterization and application of a G-quadruplex structured DNA aptamer against cancer biomarker protein anterior gradient homolog 2*. PLoS One, 2012. **7**(9).
 140. Guschlbauer, W., J.-F. Chantot, and D. Thiele, *Four-Stranded Nucleic Acid Structures 25 Years Later: From Guanosine Gels to Telomer DNA*. Journal of Biomolecular Structure and Dynamics, 1990. **8**(3): p. 491-511.
 141. Schütze, T., et al., *Probing the SELEX process with next-generation sequencing*. PLoS One, 2011. **6**(12): p. e29604.
 142. Muller, J., et al., *Monitoring the progression of the in vitro selection of nucleic acid aptamers by denaturing high-performance liquid chromatography*. Anal Bioanal Chem, 2008. **390**(4): p. 1033-7.
-

-
143. Yoshida, W., et al., *Selection of DNA aptamers against insulin and construction of an aptameric enzyme subunit for insulin sensing*. Biosens Bioelectron, 2009. **24**(5): p. 1116-20.
 144. Wang, C., et al., *In vitro selection of high-affinity DNA aptamers for streptavidin*. Acta Biochim Biophys Sin (Shanghai), 2009. **41**(4): p. 335-40.
 145. Cao, X., et al., *Combining use of a panel of ssDNA aptamers in the detection of Staphylococcus aureus*. Nucleic Acids Res, 2009. **37**(14): p. 4621-8.
 146. Hwang, B. and S.W. Lee, *Improvement of RNA aptamer activity against myasthenic autoantibodies by extended sequence selection*. Biochem Biophys Res Commun, 2002. **290**(2): p. 656-62.
 147. Berezovski, M., et al., *Nonequilibrium capillary electrophoresis of equilibrium mixtures: a universal tool for development of aptamers*. J Am Chem Soc, 2005. **127**(9): p. 3165-71.
 148. Dausse, E., et al., *HAPIScreen, a method for high-throughput aptamer identification*. J Nanobiotechnology, 2011. **9**: p. 25.
 149. Tran, D.T., et al., *Selection and characterization of DNA aptamers for egg white lysozyme*. Molecules, 2010. **15**(3): p. 1127-40.
 150. Rowe, W., M. Platt, and P.J. Day, *Advances and perspectives in aptamer arrays*. Integr Biol (Camb), 2009. **1**(1): p. 53-8.
 151. Niazi, J.H., S.J. Lee, and M.B. Gu, *Single-stranded DNA aptamers specific for antibiotics tetracyclines*. Bioorg Med Chem, 2008. **16**(15): p. 7245-53.
 152. Charlton, J. and D. Smith, *Estimation of SELEX pool size by measurement of DNA renaturation rates*. Rna, 1999. **5**(10): p. 1326-32.
 153. Britten, R.J. and D.E. Kohne, *Repeated sequences in DNA. Hundreds of thousands of copies of DNA sequences have been incorporated into the genomes of higher organisms*. Science, 1968. **161**(3841): p. 529-40.
 154. Baum, P.D. and J.M. McCune, *Direct measurement of T-cell receptor repertoire diversity with AmpliCot*. Nat Methods, 2006. **3**(11): p. 895-901.
 155. Schutze, T., et al., *A calibrated diversity assay for nucleic acid libraries using DiStRO--a Diversity Standard of Random Oligonucleotides*. Nucleic Acids Res, 2010. **38**(4): p. e23.
 156. Wiegand, T.W., et al., *High-affinity oligonucleotide ligands to human IgE inhibit binding to Fc epsilon receptor I*. J Immunol, 1996. **157**(1): p. 221-30.
 157. Lamoureux, D., et al., *The efficacy of Cot-based gene enrichment in wheat (Triticum aestivum L.)*. Genome, 2005. **48**(6): p. 1120-6.
 158. Tsujimoto, M., K. Inoue, and S. Nojima, *Purification and characterization of human serum C-reactive protein*. J Biochem, 1983. **94**(5): p. 1367-73.
 159. O'Neil, M.J., *The Merck Index - An Encyclopedia of Chemicals, Drugs, and Biologicals*, M.C. Inc., Editor. 2006: Whitehouse Station, N.J., USA.
 160. Mencin, N., et al., *Optimization of SELEX: comparison of different methods for monitoring the progress of in vitro selection of aptamers*. J Pharm Biomed Anal, 2014. **91**: p. 151-9.
 161. Wang, Y., et al., *Screening of Single-Stranded DNA (ssDNA) Aptamers against a Zearalenone Monoclonal Antibody and Development of a*
-

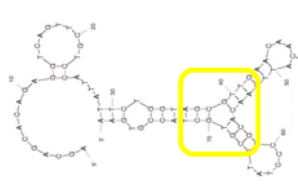
-
- ssDNA-Based Enzyme-Linked Oligonucleotide Assay for Determination of Zearalenone in Corn*. J Agric Food Chem, 2014.
162. Yan, X.R., et al., [Novel methods to detect cytokines by enzyme-linked oligonucleotide assay]. Sheng Wu Gong Cheng Xue Bao, 2004. **20**(5): p. 679-82.
163. Zhu, Z., et al., An aptamer based surface plasmon resonance biosensor for the detection of ochratoxin A in wine and peanut oil. Biosens Bioelectron, 2014. **65c**: p. 320-326.
164. Ashley, J. and S.F. Li, An aptamer based surface plasmon resonance biosensor for the detection of bovine catalase in milk. Biosens Bioelectron, 2013. **48**: p. 126-31.
165. Ashley, J. and S.F.Y. Li, Three-dimensional selection of leptin aptamers using capillary electrophoresis and implications for clone validation. Analytical Biochemistry, 2013. **434**(1): p. 146-152.
166. Jing, M. and M.T. Bowser, Methods for measuring aptamer-protein equilibria: A review. Analytica Chimica Acta, 2011. **686**(1-2): p. 9-18.
167. Khatkhatay, M.I. and M. Desai, A comparison of performances of four enzymes used in ELISA with special reference to beta-lactamase. J Immunoassay, 1999. **20**(3): p. 151-83.
168. Rotherham, L.S., et al., Selection and application of ssDNA aptamers to detect active TB from sputum samples. PLoS One, 2012. **7**(10): p. e46862.
169. Huber, D., et al., Effectiveness of natural and synthetic blocking reagents and their application for detecting food allergens in enzyme-linked immunosorbent assays. Anal Bioanal Chem, 2009. **394**(2): p. 539-48.
170. Terato, K., et al., Preventing intense false positive and negative reactions attributed to the principle of ELISA to re-investigate antibody studies in autoimmune diseases. J Immunol Methods, 2014. **407**: p. 15-25.
171. Balamurugan, S., et al., Surface immobilization methods for aptamer diagnostic applications. Anal Bioanal Chem, 2008. **390**(4): p. 1009-21.
172. Wang, R., et al., Immobilisation of DNA probes for the development of SPR-based sensing. Biosens Bioelectron, 2004. **20**(5): p. 967-74.
173. Suh, S.H. and L.A. Jaykus, Nucleic acid aptamers for capture and detection of *Listeria* spp. J Biotechnol, 2013. **167**(4): p. 454-61.
174. Hong, S.R., H.D. Jeong, and S. Hong, QCM DNA biosensor for the diagnosis of a fish pathogenic virus VHSV. Talanta, 2010. **82**(3): p. 899-903.
175. Fang, L., et al., A electrochemiluminescence aptasensor for detection of thrombin incorporating the capture aptamer labeled with gold nanoparticles immobilized onto the thio-silanized ITO electrode. Analytica Chimica Acta, 2008. **628**(1): p. 80-86.
176. Wang, S., et al., A direct competitive assay-based aptasensor for sensitive determination of tetracycline residue in Honey. Talanta, 2015. **131**(0): p. 562-569.
177. Rodriguez, M.C., A.N. Kawde, and J. Wang, Aptamer biosensor for label-free impedance spectroscopy detection of proteins based on recognition-induced switching of the surface charge. Chem Commun (Camb), 2005(34): p. 4267-9.
-

-
178. Xu, D., et al., *Label-free electrochemical detection for aptamer-based array electrodes*. *Anal Chem*, 2005. **77**(16): p. 5107-13.
 179. Goda, T. and Y. Miyahara, *A hairpin DNA aptamer coupled with groove binders as a smart switch for a field-effect transistor biosensor*. *Biosens Bioelectron*, 2012. **32**(1): p. 244-9.
 180. Lin, P.H., et al., *Studies of the binding mechanism between aptamers and thrombin by circular dichroism, surface plasmon resonance and isothermal titration calorimetry*. *Colloids Surf B Biointerfaces*, 2011. **88**(2): p. 552-8.
 181. Liss, M., et al., *An aptamer-based quartz crystal protein biosensor*. *Anal Chem*, 2002. **74**(17): p. 4488-95.
 182. Ivanov, Y.D., et al., *Atomic force microscopy fishing and mass spectrometry identification of gp120 on immobilized aptamers*. *Int J Nanomedicine*, 2014. **9**: p. 4659-70.
 183. van Grinsven, B., et al., *Heat-transfer resistance at solid-liquid interfaces: a tool for the detection of single-nucleotide polymorphisms in DNA*. *ACS Nano*, 2012. **6**(3): p. 2712-21.
 184. Contreras Jimenez, G., et al., *Aptamer-Based Label-Free Impedimetric Biosensor for Detection of Progesterone*. *Anal Chem*, 2015. **87**(2): p. 1075-1082.
 185. Lasseter, T.L., W. Cai, and R.J. Hamers, *Frequency-dependent electrical detection of protein binding events*. *Analyst*, 2004. **129**(1): p. 3-8.
 186. Peeters, M., et al., *Label-free Protein Detection Based on the Heat-Transfer Method-A Case Study with the Peanut Allergen Ara h 1 and Aptamer-Based Synthetic Receptors*. *ACS Appl Mater Interfaces*, 2015. **7**(19): p. 10316-23.
 187. Nguyen, B., F.A. Tanious, and W.D. Wilson, *Biosensor-surface plasmon resonance: Quantitative analysis of small molecule-nucleic acid interactions*. *Methods*, 2007. **42**(2): p. 150-161.
 188. White, R.J., A.A. Rowe, and K.W. Plaxco, *Re-engineering aptamers to support reagentless, self-reporting electrochemical sensors*. *Analyst*, 2010. **135**(3): p. 589-94.
 189. Tran, D.T., et al., *Nanocrystalline diamond impedimetric aptasensor for the label-free detection of human IgE*. *Biosens Bioelectron*, 2011. **26**(6): p. 2987-93.
 190. Xu, H., et al., *Label-free impedimetric thrombin sensor based on poly(pyrrole-nitilotriacetic acid)-aptamer film*. *Biosensors and Bioelectronics*, 2013. **41**(0): p. 90-95.
 191. Elshafey, R., M. Siaj, and M. Zourob, *DNA aptamers selection and characterization for development of label-free impedimetric aptasensor for neurotoxin anatoxin-a*. *Biosens Bioelectron*, 2015. **68c**: p. 295-302.
 192. McKeague, M. and M.C. DeRosa, *Challenges and Opportunities for Small Molecule Aptamer Development*. *Journal of Nucleic Acids*, 2012: p. 20.
 193. Stoltenburg, R.R., Christine; Strehlitz, Beate, *SELEX—A (r)evolutionary method to generate high-affinity nucleic acid ligands*. *Biomolecular engineering*, 2007. **24**: p. 381-403.
 194. Luzzi, E.M., M; Tombelli, S; Mascini, M, *New trends in affinity sensing: aptamers for ligand binding*. *Trends in Analytical Chemistry*, 2003. **22**(11): p. 810-818.
 195. Das, J., et al., *An ultrasensitive universal detector based on neutralizer displacement*. *Nat Chem*, 2012. **4**(8): p. 642-648.
-

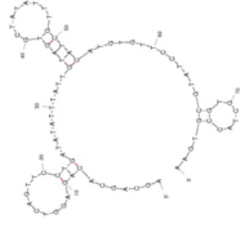
-
196. Rupcich, N., et al., *Entrapment of fluorescent signaling DNA aptamers in sol-gel-derived silica*. Anal Chem, 2005. **77**(14): p. 4300-7.
 197. Lau, P.S., B.K. Coombes, and Y. Li, *A general approach to the construction of structure-switching reporters from RNA aptamers*. Angew Chem Int Ed Engl, 2010. **49**(43): p. 7938-42.
 198. Liang, J., et al., *Electrochemical sensing of L-histidine based on structure-switching DNazymes and gold nanoparticle-graphene nanosheet composites*. Chem Commun (Camb), 2011. **47**(19): p. 5476-8.
 199. Chen, J., et al., *A simple and rapid biosensor for ochratoxin A based on a structure-switching signaling aptamer*. Food Control, 2012. **25**(2): p. 555-560.
 200. Nutiu, R. and Y. Li, *In vitro selection of structure-switching signaling aptamers*. Angew Chem Int Ed Engl, 2005. **44**(7): p. 1061-5.
 201. Null, E.L. and Y. Lu, *Rapid determination of enantiomeric ratio using fluorescent DNA or RNA aptamers*. Analyst, 2010. **135**(2): p. 419-22.
 202. Zuo, X., et al., *A Target-Responsive Electrochemical Aptamer Switch (TREAS) for Reagentless Detection of Nanomolar ATP*. Journal of the American Chemical Society, 2007. **129**(5): p. 1042-1043.
 203. Han, K., Z. Liang, and N. Zhou, *Design Strategies for Aptamer-Based Biosensors*. Sensors, 2010. **10**(5): p. 4541-4557.
 204. Wu, Z.-S., et al., *Reusable Electrochemical Sensing Platform for Highly Sensitive Detection of Small Molecules Based on Structure-Switching Signaling Aptamers*. Analytical Chemistry, 2007. **79**(7): p. 2933-2939.
 205. Han, K., et al., *Target induced dissociation (TID) strategy for the development of electrochemical aptamer-based biosensor*. Electrochemistry Communications, 2009. **11**(1): p. 157-160.
 206. Peng, Y., et al., *Label-free and sensitive faradic impedance aptasensor for the determination of lysozyme based on target-induced aptamer displacement*. Biosensors and Bioelectronics, 2009. **25**(1): p. 94-99.
 207. Shukoor, M.I., et al., *Aptamer-nanoparticle assembly for logic-based detection*. ACS Appl Mater Interfaces, 2012. **4**(6): p. 3007-11.
 208. Vanden Bon, N., et al., *Heat-transfer-based detection of SNPs in the PAH gene of PKU patients*. Int J Nanomedicine, 2014. **9**: p. 1629-40.
 209. Delport, F., et al., *Real-time monitoring of DNA hybridization and melting processes using a fiber optic sensor*. Nanotechnology, 2012. **23**(6): p. 065503.
 210. Tang, Z., et al., *Aptamer Switch Probe Based on Intramolecular Displacement*. Journal of the American Chemical Society, 2008. **130**(34): p. 11268-11269.
 211. Stoltenburg, R., N. Nikolaus, and B. Strehlitz, *Capture-SELEX: Selection of DNA Aptamers for Aminoglycoside Antibiotics*. J Anal Methods Chem, 2012. **2012**: p. 415697.
 212. Piletsky, S.A., N.W. Turner, and P. Laitenberger, *Molecularly imprinted polymers in clinical diagnostics--future potential and existing problems*. Med Eng Phys, 2006. **28**(10): p. 971-7.
 213. Schneider, D., Vanderslice, R and Gold, R, *Flow cell SELEX*. 1999: US.
 214. Mendonsa, S.D. and M.T. Bowser, *In vitro selection of aptamers with affinity for neuropeptide Y using capillary electrophoresis*. J Am Chem Soc, 2005. **127**(26): p. 9382-3.
-

-
215. Yang, J. and M.T. Bowser, *Capillary electrophoresis-SELEX selection of catalytic DNA aptamers for a small-molecule porphyrin target*. Anal Chem, 2013. **85**(3): p. 1525-30.
216. Anstead, G.M., K.E. Carlson, and J.A. Katzenellenbogen, *The estradiol pharmacophore: ligand structure-estrogen receptor binding affinity relationships and a model for the receptor binding site*. Steroids, 1997. **62**(3): p. 268-303.
217. Cox, J.C., P. Rudolph, and A.D. Ellington, *Automated RNA selection*. Biotechnol Prog, 1998. **14**(6): p. 845-50.
218. Eulberg, D., et al., *Development of an automated in vitro selection protocol to obtain RNA-based aptamers: identification of a biostable substance P antagonist*. Nucleic Acids Res, 2005. **33**(4): p. e45.
219. Hybarger, G., et al., *A microfluidic SELEX prototype*. Anal Bioanal Chem, 2006. **384**(1): p. 191-8.
220. Wei, S. and B. Mizaikoff, *Recent advances on noncovalent molecular imprints for affinity separations*. J Sep Sci, 2007. **30**(11): p. 1794-805.
221. Yoon, D.Y., et al., *Influence of the conjugation site on the specificity of monoclonal antibodies to progesterone and on the performance of direct enzyme immunoassay*. Biochem Mol Biol Int, 1993. **31**(3): p. 553-63.
222. Coulon, S., et al., *Improving the specificity of an anti-estradiol antibody by random mutagenesis and phage display*. Dis Markers, 2000. **16**(1-2): p. 33-5.
223. Eaton, B.E., et al., *Post-SELEX combinatorial optimization of aptamers*. Bioorg Med Chem, 1997. **5**(6): p. 1087-96.
224. Keefe, A.D. and S.T. Cload, *SELEX with modified nucleotides*. Curr Opin Chem Biol, 2008. **12**(4): p. 448-56.
225. Mayer, G., *The chemical biology of aptamers*. Angew Chem Int Ed Engl, 2009. **48**(15): p. 2672-89.
226. Cho, E.J., J.W. Lee, and A.D. Ellington, *Applications of aptamers as sensors*. Annu Rev Anal Chem (Palo Alto Calif), 2009. **2**: p. 241-64.
227. *Biosurfit solution*. 2015 [cited 2015 15/03]; Available from: <http://biosurfit.com/solution/#pipeline>.
228. Bonnauron, M., et al., *Transparent diamond-on-glass micro-electrode arrays for ex-vivo neuronal study*. physica status solidi (a), 2008. **205**(9): p. 2126-2129.
229. Yang, N., et al., *Vertically aligned diamond nanowires for DNA sensing*. Angew Chem Int Ed Engl, 2008. **47**(28): p. 5183-5.
230. Demers, L.M., et al., *Direct patterning of modified oligonucleotides on metals and insulators by dip-pen nanolithography*. Science, 2002. **296**(5574): p. 1836-8.

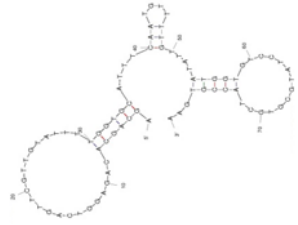
Appendix



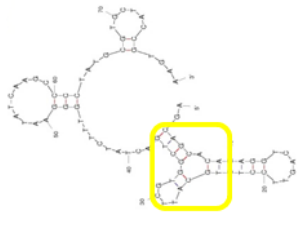
Apta 5A



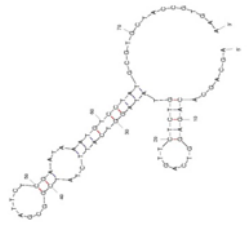
Apta 4A



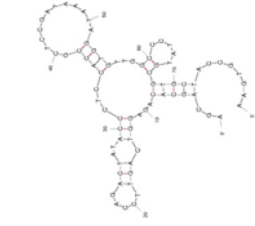
Apta 3A



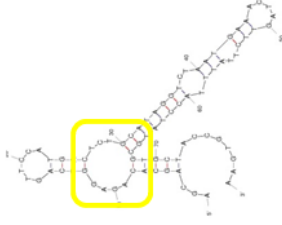
Apta 2A



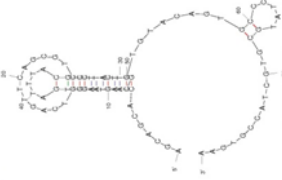
Apta 1A



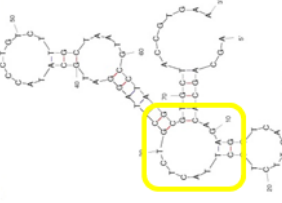
Apta 10A



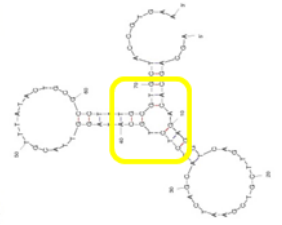
Apta 9A



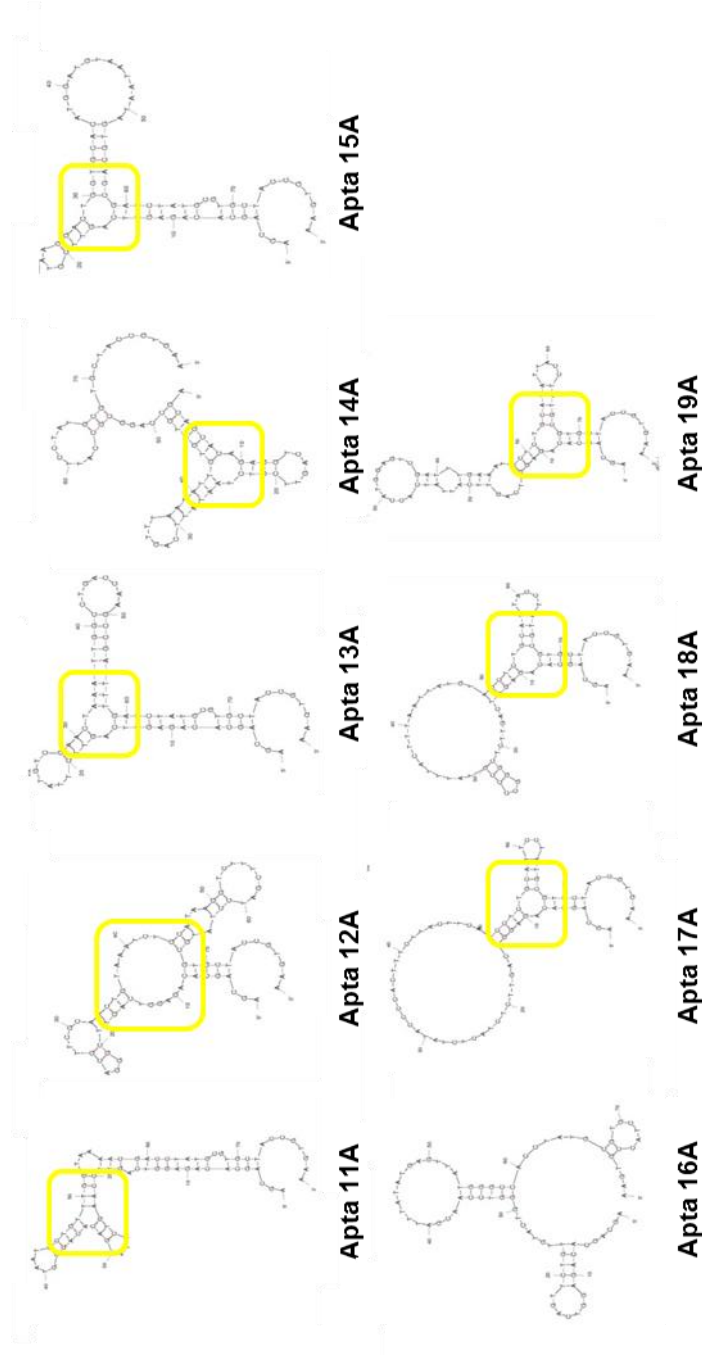
Apta 8A



Apta 7A



Apta 6A



Appendix Figure 1: Secondary structures of 19 selected E2-binding aptamers (SELEX A) predicted using Mfold software. Three-way-junction structures are highlighted by a squared box.

Curriculum vitae

Katrijn Vanschoenbeek werd geboren op 6 mei 1981 te Diest. In 1999 behaalde ze haar diploma Algemeen Secundair Onderwijs (ASO) in de studierichting Latijn-Wiskunde aan de Katholieke Centrumscholen Sint-Truiden (KCST) te Sint-Truiden. Hierna startte ze met haar opleiding Psychologie aan de Vrije Universiteit Brussel, waar zij in 2004 haar diploma licentiaat in de Klinische psychologie behaalde. Vervolgens volgde zij de opleiding Biomedische wetenschappen aan de Universiteit Hasselt (UH), waar zij in 2009 haar diploma master in de Klinisch moleculaire wetenschappen verkreeg. 2009 vormde tevens de start van haar doctoraat binnen de onderzoeksgroep Biosensoren onder leiding van Prof. dr. Luc Michiels aan het Biomedisch Onderzoeksinstituut (BIOMED) van de UH. Tijdens een periode van zes jaar deed ze onderzoek naar het gebruik van aptameren als middel voor de detectie van kleine moleculen. Haar doctoraatsthesis was getiteld: 'Aptamers as a tool to detect estrogens'. Daarnaast was ze als onderwijsassistente betrokken bij diverse onderwijsopdrachten binnen de Faculteit Geneeskunde en Levenswetenschappen van de UH. Daarnaast volgde ze diverse cursussen waaronder biosafety, good scientific conduct and labbook taking, omgaan met functiebeperkingen binnen het onderwijs, wetenschappelijk communiceren met een breed publiek en werken met een Biacore T200.

Publications

Vanschoenbeek K, Vanbrabant J, Hosseinkhani B, Vermeeren V and Michiels L (2015). Aptamers targeting different functional groups of 17 β -estradiol. J Steroid Biochem Mol Biol, 147: 10 – 6.

Vanbrabant J, Leirs K, Vanschoenbeek K, Lammertyn J and Michiels L (2014). reMelting curve analysis as a tool for enrichment monitoring in the SELEX process. Analyst, 139(3): 589-95.

Hosseinkhani B, Vanschoenbeek K, Struys T, Lambrichts I, van den Akker N, Molin D, Nelissen I, Hooyberghs J and Michiels L. Novel approaches in the biomarker-signature study of human endothelial cell derived-extracellular vesicles. *Journal of Extracellular Vesicles*. Submitted.

Dankwoord

Six years ago, I started my PhD project in the field of biosensing. It turned out to be a long battle against a small molecule. Luckily, I never fought alone. Numerous people contributed to the success of my PhD, each in their own way.

Luc. Bedankt om mij de kans te geven als doctoraatsstudente aan de slag te gaan. Jij introduceerde mij vol enthousiasme in de wondere wereld van de biosensoren. Dankzij jou kan ik nu ook perfect ganse wiskundige berekeningen maken zonder een rekenmachine ter hand te nemen. En dat je af en toe flexibel met gemaakte afspraken omspringt, tja, dat heeft me geleerd dat ook tijd een relatief gegeven is.

Co-promotor, leden van de jury en jury voorzitter. Bedankt voor jullie kritische blik en evaluatie van mijn werk. Jullie aandeel heeft mijn thesis zeker tot een hoger niveau getild.

People from the biosensor group. Thanks for your help and company in and outside the workplace:

Baharak. The first day we met, we felt a huge distance between each other. You remember? ;-) However, we were quickly able to bridge this distance and now I really appreciate you as a colleague and yes (!) also as a post-doc. Don't forget, you can text me in the middle of the night, that's no problem :-P

Evi. Jij bent mijn tofste buurmeisje, zowel op het werk als thuis. Dankzij jou ben ik bekend met het rijke aanbod dat de Quick te bieden heeft. En ook al zien we elkaar misschien niet zo vaak, ik weet je wel te vinden wanneer het nodig is ;-)

Jeroen. We hadden geregeld een andere visie en wetenschappelijke aanpak, maar onder ons tweetjes hebben we er toch voor gezorgd dat aptameren hun plaatsje hebben verworven binnen de onderzoeksgroep biosensoren!

Karolien. Jouw chaotische geest bracht leven in de brouwerij. Een drukke job combineren met drie kinderen, je moet het toch maar kunnen! En wat waren onze Amsterdam trip en Mexico reis toch onvergetelijke tijden.

Kaushik. Thanks to you I learned to appreciate Indian food. The smell stays strange, but the taste is good ;-). Success with your defense in the near future.

Lotte. Soms botste het wel eens tussen ons: 'Wie was nu weer verantwoordelijk voor het onderhoud van de SPR?'. Uiteindelijk konden we het toch nog goed met elkaar vinden. Vooral onze gesprekken over de zoektocht naar de ideale man zullen mij altijd bijblijven.

Natalie. Samen hebben we wat afgeklagd tijdens ons doctoraat: die techniek werkt niet, dat onderzoek 'sucks', persoon x werkt me tegen,... maar we hebben ook heel wat gelachen. Wie had ooit gedacht dat we beide de finish zouden bereiken? Daar mogen we best trots op zijn.

Revathy. I loved our daily chat and the way you updated me about the latest new versions of iPhone and iWatch. Oh, and before I forget, can I please borrow your lime green nail polish???

Sören. Bedankt voor de toffe babbels en het gezelschap tijdens mijn laatste maanden op BIOMED. Een man die oreo cheesecake kan maken, waar vind je die tegenwoordig nog ;-). Ik zal vaak aan je terugdenken, al was het maar omdat ik nog talloze films en series van jou op mijn hard disk heb staan.

Veronique. Je bent el eventjes weg, maar zeker nog niet vergeten. Jij maakte me wegwijs toen ik als doctoraatsstudente mijn eerste stappen in het labo zette en hielp me later met de 'optimalisatie' van mijn Engels voor diverse schrijfsels. Het besef dat het température is en niet tempérátüre, is echter nog steeds niet helemaal doorgedrongen ;-)

People from the other research groups of BIOMED. Thanks to share your experience with me. Sometimes it helps to see things from a different perspective. Een extra dankjewel gaat uit naar de *laboranten* voor het beantwoorden van al mijn domme en minder domme vragen, naar *Regine* voor het aanleveren van zuiver labomateriaal en naar *Rani* en *Veronique* voor de administratieve ondersteuning.

Leen. Met veel geduld leerde je mij de kneepjes van het vak wat betreft het lesgeven. Ik bewonder jouw nauwgezetheid en liefde voor het onderwijs. Ik hoop dat je als 'gepensioneerde' een leuke toekomst tegemoet gaat.

De steun die ik tijdens mijn doctoraat kreeg, kwam uiteraard niet enkel van mensen op de werkvloer. Ook talloze vrienden en familie hebben hun steentje bijgedragen. Daarom, een dikke merci voor jullie allemaal:

Anneleen, Astrid en Liesbet (VUB meisjes). Onze afspraakjes werden doorheen de jaren steeds beperkter, maar telkens is het een blij weerzien. Verhalen over trouwen en kindjes zijn een ver-van-mijn-bed-show... maar toch zou ik onze gesprekken voor geen geld van de wereld willen missen.

Anke, Katrien en Els (ladies of the UH). Na elke periode in je leven schieten enkele mensen over die deel blijven uitmaken van je leven. Jullie zijn de gelukkigen ;-). Anke, onze shopping dagen, filmuitjes en trip naar Londen hebben voor de broodnodige afleiding gezorgd gedurende de afgelopen jaren. Katrien en Els, frietjes en een goede babbel brengen ons samen. Wat is het elke keer toch weer gezellig!

Tijs. Bedankt voor je gezelschap gedurende de laatste maanden van mijn doctoraat. Het leven hoeft niet altijd saai te zijn :-P En zoals de paus al eerder zei: 'Bedankt voor die bloemen'.

Mijn *speelkameraadjes* van *ars ludendi* en *boardgaming inc.* Plato zei ooit: "Je komt meer van iemand te weten tijdens een uur spellen spelen dan in de loop van gesprekken gedurende een heel jaar". Ik denk dat we elkaar door en door kennen ;-)

Mijn wandel- en fietsmaatjes. De vele uurtjes die we al wandelend en fietsend doorbrengen, helpen me even alles te vergeten, waarvoor mijn oprechte dank. *Karl*, bedankt om de stilte der natuur af en toe te doorbreken met je uitleg over de werking van mijn versnellingen of het nut van de bij.

Roger. Speciaal voor jou, in het Nederlands, de herkomst van het woord aptameer. Aptus (Latijn): passen & Meros (Grieks): deeltje. Een aptameer is een stukje DNA dat past/bindt aan een deeltje. Net zoals twee puzzelstukjes die bijeen passen, of jij die bij Juliette past.

Katrijn. 'A friend from heaven, available on earth'. Bedankt om lief en leed met mij te delen. Laten we ons één doel voor ogen houden: ooit moeten we die vijf Japanse rondes halen!

Yoline en Yelle. Jullie glimlach en kinderlijk enthousiasme werken aanstekelijk. Ik wens jullie een mooie toekomst waarbij al jullie dromen mogen uitkomen.

Mama en papa. Bedankt voor de gezellige thuis, de vele presentjes, het lekkere eten (ook namens Winter), de interesse in mijn doctoraat en voor nog 101 andere dingen. Nooit zal ik kunnen terugdoen wat jullie allemaal voor mij gedaan hebben. Een eervolle vermelding in dit meesterwerk :-) is echter een eerste stap.

Because you never walk alone

Katrijn

